The Effect of Chemotherapy Treatment on Ribosomal RNA Integrity and Ribosomal Protein Composition in Ovarian Cancer Cells

by

Kyle Mispel-Beyer

A thesis submitted in partial fulfillment
of the requirements for the degree of
Master of Science (MSc) in Chemical Sciences

Faculty of Graduate Studies
Laurentian University
Sudbury, Ontario, Canada

THESIS DEFENCE COMMITTEE/COMITÉ DE SOUTENANCE DE THÈSE
Laurentian Université/Université Laurentienne
Faculty of Graduate Studies/Faculté des études supérieures

Title of Thesis Titre de la thèse	The Effect of Chemotherapy Treatment on Ribosomal RNA Integrity and Ribosomal Protein Composition in Ovarian Cancer Cells
Name of Candidate Nom du candidat	Mispel-Beyer, Kyle
Degree Diplôme	Master of Science
Department/Program Département/Programme	Chemical Sciences
Date of Defence Date de la soutenance	January 11, 2017

APPROVED/APPROUVÉ

Thesis Examiners/Examinateurs de thèse:

Dr. Carita Lannér
(Co-supervisor/Co-directeur(trice) de thèse)

Dr. Amadeo Parissenti
(Co-supervisor/Co-directeur(trice) de thèse)

Dr. Thomas Merritt
(Committee member/Membre du comité)

Approved for the Faculty of Graduate Studies
Approuvé pour la Faculté des études supérieures
Dr. David Lesbarrères
Monsieur David Lesbarrères
Dean, Faculty of Graduate Studies
Doyen, Faculté des études supérieures

Dr. Panagiotis Prinos
(External Examiner/Examinateur externe)

ACCESSIBILITY CLAUSE AND PERMISSION TO USE

Abstract

Recently we have demonstrated that several chemotherapy agents, of distinct mechanisms, promote highly reproducible ribosomal RNA (rRNA) degradation patterns, a phenomenon we call RNA disruption. These reproducible rRNA degradation bands have been observed in total RNA preparations from several cancer cell lines originating from various tissues. However, the effect of chemotherapeutic agents on ribosomal integrity and composition (including changes in rRNA and protein content) has not been examined. The purpose of the present study was to investigate the effect of docetaxel (DXL) chemotherapy treatment on ribosomal RNA and protein content in the A2780 ovarian carcinoma cell line. This involved isolation of ribosomes from untreated and DXL-treated A2780 cells using a differential centrifugation method. Differences in ribosomal RNA integrity and protein composition due to DXL treatment were determined using capillary gel electrophoresis (for rRNA), and 1D or 2D gel electrophoresis (for ribosomal proteins). Specific ribosomal proteins were detected by western blotting and quantified using densitometry. We report that DXL treatment of A2780 cells results in time-dependent degradation of rRNAs within isolated ribosomes, as well as changes in their relative protein composition. The DXL-induced changes in ribosome protein composition appeared to precede extensive rRNA degradation and were not observed in DXL-resistant A2780 cells.

Acknowledgments

I would like to take this small opportunity to thank several individuals for their help throughout my Master's degree and thesis. First, I would like to thank my supervisors Dr. Carita Lannér and Dr. Amadeo Parissenti, for their ongoing support, their dedication and helpful knowledge towards this research project over the past few years. I would also like to thank Rashmi Narendrula, fellow colleague and RNA Diagnostics employee for her help, advice and lab technique training during my years in the lab. Many thanks to Dr. Baoqing Guo for the experimental expertise and technical knowledge over the years. I would also like to take this opportunity to thank the Northern Ontario School of Medicine (NOSM), the Health Sciences North Research Institute (HSNRI) and RNA Diagnostics Inc. for providing the funding, opportunity and/or laboratory space necessary to carry on this project. Next I would also like to take the time to thanks the numerous other members of both the Parissenti and Lannér labs and many other colleagues for their critical knowledge, helpful feedback and encouragement to perform quality research and help me succeed in completing my thesis. Finally and most importantly, I would especially like to thank my family and my friends for their undying love and support. Without them, I would not have achieved this goal.

Table of Contents

List of Figures

1.0 Introduction

1.1 Ovarian Cancer, Complications and Treatment

1.1.1 Statistics Including Typical Patient Outcomes

Cancer poses one of the greatest threats to overall human health; it has now become the leading cause of death in Canada. In 2015, 196,900 new cases of cancer were diagnosed in Canada and 78,000 Canadians died of cancer[1]. This has driven a large increase in the efforts and funding being dedicated towards discovering cancer treatments, cures and improving care. With a total of 1 .6 million cancer cases (and just under 600 000 deaths) emerging per year in the United States, the U.S National Cancer Institute funding towards cancer research reached a total of 5 billion dollars[2]. Ovarian cancer is of great importance in the cancer research field because it is the most lethal gynecological cancer and the fifth leading cause of cancer death among women in the western world[3,4]. Worldwide, it is the eighth most common malignancy among women, resulting in more than 140 000 deaths[4]. The five year survival rate for advanced ovarian carcinoma is only 45%[2]. The high mortality rate can be attributed to the absence of symptoms early in the disease trajectory, resulting typically in a diagnosis of ovarian cancer at a very advanced stage[5]. The late diagnosis of ovarian cancer is one of the largest hurdles to overcome because there is a lack of effective screening procedures and early diagnosis methods[5]. Approximately 75% of patients with ovarian cancer present with tumour metastases, resulting in poor prognosis and high mortality[6]. The main reason that ovarian cancer progresses to such an advanced and lethal stage before detection is likely due to the fact that it is often isolated inside

the peritoneal cavity[7]. Additionally, early stage ovarian cancer may not cause many symptoms, or they may be vague and overlooked such as increasing pelvic pressure or pain, change in bowel habits such as diarrhea or constipation, or more frequent or urgent urination[8]. This also speaks to the lack of a sufficiently robust biomarker for early ovarian cancer detection[9], although Ca125 continues to be used in screening trials and for monitoring response to chemotherapy[9].

Another significant factor contributing to the lethality of ovarian cancer is drug resistance. This entails both the innate or primary resistance of the tumour to chemotherapy, along with acquired resistance after chemotherapeutic treatment[10]. Resistance frequently develops to all classes of drugs used in ovarian cancer[11] and has been attributed to distinct biochemical pathways depending upon the agent used. Single and dual agent resistance is documented, with distinct mechanisms occurring for each drug in single agent treatment and also different mechanisms during dual agent resistance[12]. Mechanisms of resistance to chemotherapy treatment in ovarian cancer have been attributed to: relative dose intensity playing a role in resistance to platinum complexes, induction of the membrane P-glycoprotein conferring resistance to taxanes and activation of DNA repair mechanisms. Avoiding drug-induced cell death mechanisms is also characteristic of resistance to platinating agents and to a lesser degree taxanes[13].

Ovarian cancers comprise a heterogeneous group of neoplastic diseases, with epithelial tumors as the most common ovarian cancer and also the most lethal gynecological malignancy. Based on histopathology and molecular genetic alterations, ovarian carcinomas are divided into five main subtypes [high-grade serous (70%), endometrioid (10%), clear-cell (10%), mucinous (3%), and low-grade serous carcinomas (<5%)][14]. The most common subtype of ovarian cancer, high grade serous carcinoma (HGSC), which accounts for up to 80% of ovarian cancer related

deaths almost always carries TP53 mutations[14]. A pathogenic model for ovarian cancer described by Bowtell et al.[15] proposes as primary events early p53 loss, followed by BRCA loss, leading to a deficiency in repair of double strand breaks (DSB) by homologous recombination. This triggers chromosomal instability (genetic chaos) and widespread gene copy number changes[16]; events that cause global changes in gene expression which facilitate tumor evolution[16].

1.1.2 Surgery and Chemotherapy Agents Used in Adjuvant and Neoadjuvant Settings in Ovarian Cancer

In North America, advanced stage ovarian tumours are most frequently treated by performing cytoreductive surgery initially, to remove the bulk of the mass of the tumor followed by adjuvant chemotherapy[17,18]. The current standard adjuvant regimen employs more than one cytotoxic chemotherapy agent, usually combining a platinating agent and a taxane[19]. The most common platinating agents encountered are cisplatin and carboplatin, with carboplatin demonstrating less nephrotoxicity and neurotoxicity, making it the drug of choice[20]. For taxanes, paclitaxel and docetaxel (DXL) are the sole agents used. In recent years, there has been a higher usage of DXL due to reduced cost (the drug has become off patent) and considerably less neuropathy. The hematologic toxicity of DXL is greater[21], although it can be relatively easily monitored and remediated by pegfilgrastim administration compared to the neuropathy induced by paclitaxel. This likely contributes to the popularity of DXL compared to paclitaxel. At present, adjuvant therapy is mainly dependent upon tumour stage and grade rather than type, although it is known that type I ovarian cancers (low grade serous cancer, clear cell, mucinous and endometrioid) do not respond well to current cytotoxic chemotherapy using platinating agents and taxanes[22]. This may change in the future with the development of new chemotherapeutic agents, targeted therapies and clinical trials[23]. Another aspect of treatment

under current debate is the efficacy of adjuvant versus neoadjuvant chemotherapy treatments in advanced stage ovarian HGSC[18,24]. In a small percentage of advanced stage tumours in North America, patients undergo neoadjuvant chemotherapy before de-bulking surgery. However, in Europe, neoadjuvant chemotherapy followed by interval de-bulking has shown promise, and is the standard of cancer care[17,25].

Over the past decade or so, there has been some small improvement in prognosis for ovarian cancer. During this time, the combination of carboplatin and paclitaxel/DXL has remained the standard first-line therapy. Response rates to this combination are in the region of 70%–80%, but the majority of these women subsequently relapse[9]. Despite a promising initial response to surgery and adjuvant chemotherapy, more than 50% of patients will fail to respond to chemotherapy and will develop a recurrent form of ovarian cancer, which is typically resistant to the previously administered chemotherapy agents[26]. This failure of the chemotherapeutic treatment in recurrent ovarian cancer is largely due to the evolution of resistance to the two classes of antineoplastic agents most commonly used to treat ovarian cancer: taxanes and platinating agents[27]. Resistance to both agents is not uncommon. Recent research into the resistance mechanisms of drug-resistant ovarian cancer has demonstrated that distinct gene expression changes take place as ovarian tumours or tumour cells acquire resistance to taxanes, carboplatin, or both drugs[12].

In some instances, particularly where primary de-bulking surgery is not suitable for ovarian cancer patients, neoadjuvant chemotherapy may be considered as a treatment option for patients suffering with advanced disease[28]. As well, in the case of recurrent disease for treatment of patients where surgery is not feasible or where platinum resistance is established, taxanes are the primary chemotherapeutic agent of choice[29].

1.1.3 Taxanes and Their Mechanism of Action

Taxanes are one of the most efficient and frequently used chemotherapy agents, applied in the treatment of a wide range of tumors and cancer settings. The first taxane to be isolated and purified for clinical usage was paclitaxel[29]. The two most commonly used taxanes encountered during ovarian cancer treatment are paclitaxel and DXL. Currently, in the clinic, taxanes are being used alone, following another drug regimen, or in combination with other drugs to treat several types of cancers[30]. DXL is active against several solid tumours including breast, gastric, ovarian and non-small cell lung cancer[31]. A recent ovarian cancer study showed that the addition of DXL (rather than paclitaxel) with the platinating agent resulted in an improved quality of life for the same length of progression free survival. This then identified DXL as an improved alternative for paclitaxel in ovarian cancer treatment[21,32]. Although other taxane derivatives exist, they are rarely used to treat cancer.

Paclitaxel is derived from the bark of the pacific yew tree (*Taxus brevifolia*), while DXL is a semi-synthetic derivative of the latter[31]. Both are known as mitotic inhibitors; they arrest the cell cycle of actively dividing cells [33]. Specifically, taxanes are cytotoxic drugs (meaning toxic to cells) that interfere with microtubule depolymerisation, causing cell cycle arrest in mitosis and followed by cell death via apoptosis[34]. However, apoptotic cell death is not the only type of cell death reported to occur following taxane exposure in cancer cells. It is also reported that taxanes induce multinucleation of cells followed by death via mitotic catastrophe[35].

Microtubules are important in retaining cell shape, allowing movement of organelles and facilitating cell division. Taxanes exhibit unique cytotoxic activity by stabilizing microtubules rather than destabilizing them, as vinca alkaloids do[36]. In particular they promote the assembly of microtubules but prevent their depolymerization, thus interfering with a number of normal

cellular functions that depend on the physiological balance between tubulin and microtubules[37]. This includes the ability of taxanes to block a phenomenon called treadmilling (a well-known process by which tubulin dimers added on to the microtubules at their plus ends are released from the minus ends)[38]. Blockage of treadmilling inhibits further progression in cell division and, hence, cell cycle progression. When taxanes bind to microtubules, which are polymers composed of α and β-tubulin, they bind tightly to β-tubulin monomers in the microtubules[36].

Preliminary research indicates that mainly the intrinsic (Bcl-2 mediated) apoptotic pathway is activated as a result of taxane chemotherapy treatment; however there may be alternate pathways to promote apoptosis or other cell death pathways [39]. Research reports that alternate apoptotic pathways, initiated through various distinct caspases are possible, and may be dependent on the cell type/line[40,41]. However, taxanes have also been shown to induce caspase-independent cell death pathways, both *in vitro* and *in vivo*, depending upon the dose, tumour microenvironment and cell type[40]. Several studies have also shown the involvement of autophagic cell death in taxane treatment of several types of cancers[42]. Cytokine and interleukin production have been reported in response to DXL and their relationship to the mechanism of action of DXL is still unclear[43]. Of increasing interest lately, is the cell signaling molecule TNF-α, or tumor necrosis factor alpha, involved in systemic inflammation and the initiation of apoptosis. A study investigating treatment of breast and ovarian cancer cell lines (MCF-7 and A2780 cells, respectively) with either paclitaxel or DXL reported dose-dependent increases in the production of sTNF-α, which may contribute to the cytotoxic effect of taxanes observed in cancer cell lines through the activation of TNFR1- (tumor necrosis factor receptor) -induced apoptosis[44]. TNF-α mediated apoptosis, bcl-2 mediated apoptosis and even VEGF down-

regulation (by production of reactive oxygen species) have all been proposed as downstream mechanisms of action for taxanes[44,45].

The most well-known and characterized of the taxanes is paclitaxel. Currently, however, the most promising anti-cancer taxane is the newer agent, DXL. This newer agent shows a comparable efficacy to paclitaxel, but it has significantly less and/or different types of toxicity. With respect to the binding of β-tubulin, DXL reportedly has an approximately 2-fold higher affinity for the β-tubulin binding site compared to paclitaxel[33]. Although DXL exhibits a more manageable toxicity profile than its counterpart, one of the recurrent problems associated with the use of these newer agents is the development of drug resistance; a problem encountered with all chemotherapeutic drugs used.

1.1.4 Pathways Associated with Resistance to Taxanes Agents *in vitro* and *in vivo*

Several important factors such as age, stage of disease and volume of residual disease after surgery affect the prognosis of a patient with ovarian cancer. One of the foremost factors that has limited the success of chemotherapy in ovarian cancer is the emergence of drug resistance in the tumor cell population, although host factors in the patient may be of similar of importance[46]. Treatment with taxane agents after surgery usually results in an initial high response rate; however, relapse usually occurs, accompanied with acquired drug resistance which often includes tumour metastases, contributing to chemotherapeutic treatment failure and death for the majority of patients[10]. The initial response rate may be high, due to the death of the highly vascularized portion of the tumour from chemotherapy, with relapse occurring due to a drug resistant tumour core remaining. This multi-faceted response of the tumor to the treatment course prompts us to believe that drug resistance in ovarian cancer is comprised of multiple

mechanisms. A large variety of *in vitro* and *in vivo* mechanisms of drug resistance have been identified. Of the mechanisms that have been characterized (mostly *in vitro*), frequently observed are: suppression of drug entry into tumour cells, active extrusion of drugs from cells, changes in P53 pathways, or even enzymatic drug inactivation among others[47, 48]. It is even possible for drug activity to be prevented by mutated genes or altered expression of proteins important in drug acting pathways. Defects associated with apoptosis, cellular senescence, cell cycle checkpoints and repair mechanisms have also been reported to contribute to drug resistance[48].

In the past 20-30 years of cancer research, studies have shown a tight-knit connection between the immune system, cytokines and cancer. Recent studies suggest that tumour necrosis factor alpha (TNFα) may be involved in taxane cytotoxicity and resistance. Accordingly, a study performed by Sprowl et al.[44] demonstrated that taxanes can promote dose-dependent TNF-α production in tumor cells at clinically relevant concentrations, which can contribute to taxane cytotoxicity. Moreover, the study provided evidence that defects in the TNF cytotoxicity pathway or activation of TNF-induced NF-κB-dependent survival genes may, in contrast, contribute to taxane resistance in tumor cells.

Some of the mechanisms involved in taxane resistance *in vitro and in vivo* have been identified, although, as is the case for other chemotherapy treatments, resistance to taxanes may be multifactorial and has yet to be fully understood. One of the proposed mechanisms of resistance to taxanes involves a direct 'suppression' of the mechanism of action of the drug; involving alterations in microtubule structures of the β-tubulin subunits. Kavallaris et al., reported increased expression of β-tubulin isotypes in DXL resistant cells lines and human tumours, which supports the importance of changes in specific β-tubulin gene expression in contributing to resistance[49]. A clinical study investigating the mechanism of resistance in non-

small cell lung cancer patients, identified the presence of missense mutations of the β-tubulin gene in tumour DNA isolated from patients, which conferred resistance to paclitaxel treatment[50]. Based on these studies, it seems that alterations in β-tubulin expression or mutations in the gene at the chromosomal level, can affect binding of taxanes to the β-tubulin subunit, allowing for some degree of resistance to taxane chemotherapy[51].

Since taxanes have been associated with induction of apoptosis, as previously mentioned, another mechanism of taxane resistance is the increased expression of anti-apoptotic genes. In a study investigating the sensitivity of MCF-7 breast cancer cells to taxanes, it was observed that over expression of the anti-apoptotic genes Bcl-xL and c-FLIP resulted in an increased survival of cancer cells to taxanes[52]. Bcl-xL inhibits the intrinsic pathway, and c-FLIP inhibits the extrinsic pathway of apoptosis. Therefore, the results from this study suggest that over-expression of these genes results in increased survival of cancer cells. However, there has been a lack of studies demonstrating a direct link to anti-apoptotic mechanisms in an *in vivo* setting. Survivin, which belongs to the inhibitor of apoptosis protein (IAP) family, is another anti-apoptotic protein which is highly expressed in some cancers, but is undetectable in normal adult tissue. Survivin has been shown to block both caspase-dependent and independent death pathways[53]. Increased survivin expression in ovarian cancer, as well as increased protein expression in tumours of advanced ovarian carcinoma patients have been significantly associated with resistance to the agent DXL[54,55].

Another common mechanism of taxane resistance identified in preclinical studies is the increased expression of certain types of efflux pumps, which prevent the chemotherapeutic drug from accumulating to cytotoxic levels in cancer cells[56]. P-GP (P-glycoprotein) or Abcb1, a product of multidrug resistance gene-1 (*MDR-1*), belongs to the ATP-binding cassette (ABC)

family of drug transporters located on the plasma membrane. These drug transporters are responsible for the ATP-dependent efflux of various chemotherapy drugs from tumour cells, including taxanes[57]. In cancer cells that are selected for survival in increasing concentrations of taxanes, *ABCB1* gene amplification is routinely observed as acquisition of resistance is achieved[12]. Armstrong et al. reported a significant increase in the expression of the *ABCB1* and *ABCB4* genes in A2780DXL cells, a DXL resistant ovarian cancer cell line that was generated by exposing cells to increasing doses of DXL[12]. Similar observations were made in paclitaxel-resistant SKOV-3 and OVCAR ovarian cancer cell lines, where upon the inhibition of ABCB1 expression paclitaxel sensitivity was restored[58]. P-glycoprotein expression has been associated in the clinic as a marker and prognostic indicator in advanced ovarian cancer[59]. An association between ABCB1 expression and resistance to chemotherapy was also established for ovarian cancer patients undergoing paclitaxel treatment, where the presence of a certain ABCB1 single nucleotide polymorphisms (SNP) resulted in chemo-resistance and shorter overall survival, although this might be linked to a different level of whole body clearance of paclitaxel overall[60].

P53 is a master regulator of ribosomal biogenesis and is a robust sensor of many types of nucleolar damage (as well as having the function of a genomic DNA damage sensor)[61]. Therefore, mutations and dysfunctions within the P53 pathway have long been associated with ovarian cancer[62]. P53 mutations in tumours have also been linked with drug resistant ovarian cancer and a shortened survival of patients with advanced resistant disease[63]. However, although common, P53 mutations are not required to cause resistance in high grade serous ovarian cancer (HGSOC). Hartwitch et al.[64] have demonstrated that P53 protein aggregation can occur as a resistance mechanism to chemotherapy in serous ovarian cancer. The aggregation of p53 protein has been discovered in different types of cancers and may be responsible for impairing the

normal transcriptional activation and pro-apoptotic functions of p53. Hartwitch demonstrated that in a unique population of HGSOC cancer cells with cancer stem cell properties, p53 protein aggregation is associated with p53 inactivation and platinum resistance. A novel peptide inhibitor of P53 aggregation has even been shown to rescue P53 function to promote tumour suppressive properties[65].

Lastly, another reported mechanism of resistance to taxanes has been identified that involves increased expression of enzymes capable of metabolizing taxanes. Cytochrome P450 enzymes, although typically expressed in the liver to metabolize a wide variety of substrates, are involved in the metabolism of several anticancer agents, including taxanes[56]. CYP2C8, a member of the Cytochrome P450 superfamily of proteins, has been shown to detoxify paclitaxel to a metabolite that is approximately 30 fold less cytotoxic [66]. CYP1B1 has been identified in many malignant tumours, and it has been shown that its increased expression is associated with metastatic disease. A study investigating *CYP1B1*expression *in vitro* and *in vivo* in epithelial ovarian cancer has found an association between increased expression of this P450 cytochrome and lower response rate to paclitaxel treatment[67]. Although there is evidence for a link between cytochrome enzymes and ovarian cancer drug resistance, the literature seems to suggest that the connection is rather minor.

An important and rather overlooked aspect of cancer drug research is the fact that *in vitro* research does not always model what occurs *in vivo*. *In vivo* drug resistance to taxanes is often associated to the strongly reduced drug delivery to the tumour site due to differences in the tumour micro-environment[68]. Poor tumour vascularization, changes in tumour acidity and hypoxia along with activation of autophagic survival mechanisms in the poorly vascularized tumour are among the most prominent factors that promote tumour survival[69] *in vivo*. Recent

research is beginning to highlight that the previously mentioned characteristics of the tumour microenvironment can be manipulated to improve current therapies[69].

1.2 The Eukaryotic Ribosome, Ribosome Biogenesis and Ribosomes in a Cancer Setting

1.2.1. Ribosome composition, structure, function and link to cancer

Protein synthesis is a fundamental cell process whose proper execution is a critical function for regular and healthy cell growth – a statement that applies to all forms of life from the prokaryotic to the eukaryotic kingdom. Ribosomes, and particularly the ribosomal RNA (rRNA) that displays catalytic ribozymal activity, are the primary and sole effectors of protein synthesis. Once a nascent mRNA chain is synthesized in the nucleus from its DNA sequence in the genome, it undergoes several possible posttranslational modifications (which include capping, cleavage, splicing and polyadenylation). It is then exported from the nucleus into the cytosol[70]. Following final modification in the cytoplasm, the ribosomal machinery utilizes mature mRNA molecules as templates (recognizing their start and stop codons) to produce new polymers of amino acids (proteins), a process termed translation. Although it has been accepted as dogma that the cytoplasm (along with mitochondria) is the only site of protein synthesis, accumulated evidence is beginning to make a strong argument for nuclear translation[71]. Firstly, evidence concerning the destruction of nuclear mRNAs containing premature termination codons by nonsense-mediated decay (NMD) is very convincing. NMD is a process in which ribosomes scan for mRNAs with premature stop codons and mark them for degradation. The only known way to detect termination codons is by the ribosome, and as some NMD occurs within the nuclear fraction, active nuclear ribosomes could perform the required detection[72]. There is also

the evidence that tagged amino acids are incorporated into nascent polypeptides in a nuclear process coupled to transcription as well as the fact that components involved in translation, NMD and transcription co-localize, co-immunoprecipitate and co-purify[73].

The eukaryotic ribosome is a large "80S" macromolecular complex of proteins and rRNAs, where 80S refers to its sedimentation coefficient in Svedberg units upon centrifugation in sucrose density gradients. The 80S ribosome is composed of large (60S) and small (40S) subunits, with the larger subunit being of approximately twice the size of the small[74]. Both subunits are composed of a complex, folded 3D structure of rRNAs that have ribosomal proteins (RP) bound to their exterior structure. The eukaryotic human large subunit contains the 28S, 5.8S and 5S rRNAs, which are 5025 nucleotides (nt), 160 nt and 120 nt, respectively. The small subunit contains the 18S rRNA, which is 1900nt [75]. The primary catalytic function of the ribosome is located within the 28S rRNA itself (in the peptidyl transferase center). The 18S rRNA functions as the decoding center, bringing together aminoacyl-tRNA molecules and mRNA codons that are complementary to each other. It is generally accepted that the RPs most likely help with the folding of the rRNA and certain other accessory functions in translation; some of which have been identified[74]. The various ribosomal proteins and rRNAs will be described in detail in sections to follow. The large subunit has approximately 46 RPs while the small subunit has approximately 33 RPs adhered to their respective rRNAs[76] (See Appendix Figure 17).

There are three global steps that allow for protein synthesis to occur at the ribosome: *initiation* (with the help of initiation factors, the mRNA binds to the small subunit of the ribosome), e*longation* (the GTP-dependent process of recruiting amino-acyl tRNA to shuttle the new peptide through the aminoacyl, peptidyl and exit (APE) sites (See Appendix Figure 15) of

the ribosome with the help of elongation factors) and *termination* (the release of the nascent polypeptide chain with the aid of release factors at UAA or UAG stop codons)[77]. There are about 20,000 – 25,000 protein-coding genes in the human genome, with recent evidence suggesting the number may be as low as 19 000[78]. Protein products for about 18,000 of these genes have been detected in at least one human tissue. About 10,000 of these proteins are present in all cells and between 1500 and 2000 proteins are derived from genes that are essential for cell function[79]. Every single one of these proteins is produced, in a regulated manner by the sub-cellular machinery that we call the ribosome. Therefore, the generation of mRNA molecules and proteins occurs in a coordinated and regulated manner to allow the expression of specific amounts of proteins at specific times in the cell cycle to allow for the coordinated process we call life.

Evidence is starting to highlight the fundamental differences in ribosomes between different organisms and also the ribosome variability within a species[75,80]. However, most striking is that we are now beginning to shed light on ribosome structural heterogeneity within different tissues of the same organism[81]. Historically, the ribosome was viewed as an unchangeable entity, constantly equipped with the entire complement of RNAs and proteins to translate all proteins in an unbiased manner. Conversely, several lines of evidence indicate the presence of functional selective ribosomal subpopulations in bacteria that exhibit variations in the RNA or the protein components and modulate the translational program in response to environmental changes[82]. Therefore, although ribosomes were shown to be effectors of translation 40 years ago, it has only recently become apparent that they also act as regulators. During evolution, ribosomes from higher eukaryotes have selected additional RPs and rRNA segments that are not directly involved in mRNA decoding and peptide formation, but are predicted to support regulatory events[83]. As the 'relative complexity' of an organism increases,

in general, a corresponding increase in the size of the rRNAs and the numbers of associated ribosomal proteins is observed. Also, ribosomes with variable composition have been identified that support distinct translational activity depending on cell type or in response to viral infection,[84]. In addition, changes in ribosome composition (termed ribosomopathies) result in developmental defects in both animals and humans while having no, or only a weak, effect on the survival of cultured cells[85].

Ribosome heterogeneity is a fascinating field of science that is just in its beginnings and when we start to apply this theory in the presence of dysregulated cell growth, i.e. cancer, it becomes even more intriguing. The concept of differential regulation of translation at the ribosome is supported by a recent genome wide profiling study[86], that has demonstrated the heterogeneity of ribosome composition and how this affects the translated population of mRNA molecules. Recent research reviewed by Lafontaine (2015) has also shown that rRNA heterogeneity can regulate translation to generate distinct translatomes, which can promote tumorigenesis[87].

Some cancer scientists are now beginning to shift the way they view cancer as a disease[88]. Classically, cancer is thought to be a disease that is most often caused by accumulation of mutations or other alterations to nuclear DNA. However, nucleolar morphology (the site of rRNA synthesis) is used by some pathologist to predict clinical outcome of cancer[89]. There is evidence that the nucleolus is the starting point of a series of metabolic changes that characterize cancer cells. In a typical healthy cell, the nucleolus is a key cellular sensor to stress and plays a central role in P53 activation[61]. In cancer cells, cell entry into the cell cycle is always associated with up-regulation of nucleolar function, increased nucleolar size, and increased synthesis of ribosomes, which are also directly dependent on the rapidity of cell cycle progression[89]. Also,

alterations of the tumour suppressor retinoblastoma (Rb) and p53 pathways contribute to the stimulation of nucleolar function and to nucleolar enlargement, which have been attributed to greater aggressiveness of cancer tissues[89]. This accumulating evidence suggests that cancer is a disease significantly affected by the activity of the ribosomal compartment[90]. Just recently, disruption of ribosome biogenesis with an agent known as a small molecule inhibitor of RNA Polymerase I transcription, CX-5461, has shown unexpected, potent, and selective killing of tumor cells via disruption of nucleolar function leading to activation of p53, independently of DNA damage[91].

Recent studies have also begun to highlight the fundamental roles that previously identified, important oncogenes such as MYC, RAS, MTORC1 and PI3K play in driving RNA Polymerase I transcription in the nucleolus[92,93,94,95], which is a master orchestrator of ribosome biogenesis. In addition to maintaining essential levels of protein synthesis, hyper-activated ribosome biogenesis and nucleolar function play a central role in suppressing p53 activation in response to oncogenic stress[96]. It has now been shown that cells with enhanced tumour aggressivity display a marked increase in the synthesis of various rRNA precursors with activation of alternative pre-rRNA synthetic pathways, a decrease in the regulation of P53 mRNA, along with enhanced post-transcriptional methylation of specific sites located with the 28s RNA molecule[97]

1.2.2 Ribosome Biogenesis: rRNA loci, rRNA gene transcription, and rRNA processing in nucleoli

Ribosomes are necessary for the production of all proteins found within the cell. Therefore the energy and effort that a cell must dedicate to the production of these protein

factories is actually quite substantial[76]. In eukaryotic cells, ribosome biogenesis recruits all three RNA polymerases, requires the work of over 200 transiently associated ribosome assembly factors and the sequential importing of many ribosomal proteins within the nucleolus and nucleus followed by the export of ribosomal particles and pre-ribosomes to the cytosol. The process all begins within the nucleolus, which is the largest visible structure within the nucleus. The nucleolus is an amalgamation of protein and RNA which forms around specific genetic loci termed nucleolar organizer regions (NOR) which are tandem repeats of rDNA. Specifically, they contain the genetic information for the 28S, 18S and 5.8S rRNA which, in humans, are clustered on chromosomes 13, 14, 15, 21 and 22[98]. In other words, the nucleolus is like an organelle formed by the act of building a ribosome and that its structure does not need to be maintained for proper function[98].

RNA polymerase I transcribes the long 47S rRNA precursor molecule which contains the three aforementioned rRNA molecules along with spacers in the following order: 5' ETS (externally transcribed spacer), 18S rRNA, ITS1 (internally transcribed spacer), 5.8s rRNA, ITS2, 28S rRNA and the 3' ETS. The mature human rRNA transcripts are generated by a series of complex cleavage and maturation steps, many of which still remain to be understood[76] and are inferred to exist based on evidence from experiments in other organisms. It is currently known that multiple processing pathways exist during the processing of rRNA in humans, although it is not specifically known which pathways are active/utilized. The endonuclease responsible for 5' ETS cleavage still remains to be found, whereas the degradation of the 5' ETS primarily requires the cooperative action of the 5′ →3′ exoRNase XRN2 and the exosome in mammalian cells[76]. In humans, it has been shown that the exosome is necessary for the cleavage and degradation of the ITS1, which aids in the generation the mature 18S subunit along with NOB1 (processing factor)

which trims the 18S RNA in the cytoplasm[99]. The 5.8S rRNA maturation process is assisted by the RNA helicase Dob1p/Mtr4p, which functions in unwinding the secondary structures or displacing the bound proteins that may otherwise hamper progression of the function of the exosome[100]. The exosome initiates cleavage (with the help of exosome-associated factors MTR4, C1D and MPP6) and trimming of the 5.8S RNA with the Rrp6 exo/endo-nuclease subunit of the exosome in the ITS2 region to release the mature rRNA[100]. In terms of the maturation of the 28S subunit in humans, the exonuclease XRN2 ensures the trimming of the 5' end of the rest of the ITS2[101].

The 5S rRNA on the other hand is transcribed in the nucleus from chromosome 1 in an independent fashion as a 3' end-extended precursor by RNA polymerase III (Pol III)[75]. The presence of 5S rRNA is required for normal translation in most ribosomes, although its exact function within the ribosome is unclear. The 5S rRNA remains the most elusive of all rRNAs regarding its precise function and how this correlates with structure. However, it is thought to play a critical role in both protein–RNA and RNA–RNA interactions within the ribosome[102]. RPLa and RPL5 have been shown to be necessary pre-ribosomal binding proteins that facilitate the maturation of the 5s rRNA, which then allows it to be exported to the cytoplasm[102]. It is known that yeast exonucleases process the 3' section of 5S rRNa although this has not been extensively studied in humans. The 5S rRNA can be polyadenylated and subsequently degraded by the exosome. Interestingly, nucleotides in eukaryotic 5S rRNA are rarely pseudouridylated and methylated by H/ACA and C/D Box snoRNAs[102].

During the various cleavage and processing steps mentioned above, it has been shown that various snoRNAs (small nucleolar RNAs) are active in the form of snoRNPs (small nucleolar ribonucleoparticles) that play important roles in the generation of rRNA transcripts.

However, we are just beginning to elucidate their implications. Lafontaine recently reviewed the current knowledge of over 200 snoRNAs involved in ribosome biogenesis[87]. SnoRNAs are small, abundant and stable RNAs of ancient origin that localize to the nucleolus at a steady state and are found in all eukaryotes. snoRNAs act in pre-rRNA modification, processing and folding through typical Watson-Crick base pairing with their substrate RNA sequences. All three classes of snoRNAs (box C/D, box H/ACA and MRP) are all active as snoRNPs in tight association with conserved core proteins[87]. It is mostly C/D and H/ACA snoRNPs that drive RNA modification. Box MRP is mainly involved in rRNA processing (ITS1 removal)[87]. BOX C/D and H/ACA snoRNAs range in size from 60-250nt and are associated with four core proteins; among which are the enzymes that mediate rRNA modification[103]. Box C/D snoRNPs methylate the 2'-hydroxyl moiety to form a 2'-O-methylated nucleotide of rRNA with the help of the methyltransferase Fibrillarin, while box H/ACA snoRNPs mediate the pseudouridylation of specific uridine residues in rRNA using the pseudouridine synthase Dyskerin[104],[103]. Considering that each human ribosome contains 200 total modifications (around 100 ribose methylations and 100 pseudouridines), and considering that each position is subject to individual regulation through specific snoRNA guides, the combinatorial potential is immense. Therefore, it can be argued that snoRNA-mediated rRNA modification, is one of the most prominent sources of ribosome heterogeneity, as discussed in the previous section[87]. Interestingly, the biogenesis of certain snoRNAs (along with Fibrillarin) was found to be essential for the development and progression of breast cancer *in vitro* and *in vivo*[105]. This highlights the molecular involvement and implications of P53, the nucleolus, and the ribosome in tumorigenesis.

Clusters of human ribosomal DNA (rDNA), which code for rRNAs, exhibit great variability in length (50kb to >6Mb) and composition, manifest complete heterozygosity, and

provide each person with their own unique rDNA electrophoretic karyotype[75]. By analyzing multigenerational families, Stults et al. discovered that the rDNA clusters are subject to meiotic re-arrangement at a frequency >10% per cluster, per meiosis. This suggests that rDNA clusters themselves demonstrate a very high level of genomic plasticity, and when combined with the snoRNA mediated rRNA combinatorial modifications and diversity in RPs, there can be no doubt of a very substantial ribosome heterogeneity.

1.2.3 Ribosomal proteins, function, localization and connection to apoptosis

Ribosomal proteins are synthesized by the translating macromolecular machine itself (the ribosome). This tends to raise the typical "who came first" story: the chicken or the egg? It is quite evident, but somehow confusing that functional ribosomes translate their own proteins that will be then integrated into the next generation of synthesized ribosomes. These newly synthesized RPs are then imported into the nucleus/nucleolus and have been implicated in the maturation of pre-rRNA molecules[74]. Most RPs are small enough to passively enter the nucleus (7-70kDa); however, their import is facilitated by nuclear transporters that recognize their nuclear localization signals along with several chaperones specific to certain RPs[74]. The precise functions of RPs in pre-rRNA processing along with ribosome biogenesis remain elusive. X-ray crystallography and cryo-electron microscopy (EM) structures of mature ribosomes have shown that most RPs share common structural features, in particular globular domains interspersed by poorly structured loops that bind to rRNA or other RPs[106] (See Appendix Figure 17). In eukaryotes, we especially observe that RPs contain tails extending from their globular domains. Several of these extensions protrude far into the rRNA, while most pass across the surface of the ribosomal subunits contacting multiple secondary structures within the rRNA sequence[74]. This suggests the strongly basic RPs play a crucial role in bringing and/or keeping rRNA domains

together[74]. Studies in prokaryotes and eukaryotes indicate that the interaction network between proteins and RNA commences loosely and dynamically, gradually tightens as subunit assembly occurs, and eventually forms translating cytoplasmic ribosomal subunits[107]. It is generally thought that during subunit assembly RPs function as chaperones assisting the proper folding of the nascent pre-rRNA molecules. Only recently have the implications of RPs in ribosome biogenesis been investigated, because typical efforts to study ribosome biogenesis were focused on the processing of pre-rRNAs, ribosome structure and assembly co-factors with most of the studies performed in yeast and bacteria.

Indeed, *in vitro* assembly of bacterial ribosomes have shown that RPs are required in a hierarchical order[108]. RPs that are necessary for the early steps of 28S pre-rRNA processing are located on the exposed surface of the large subunit of the ribosome, mainly bound to domains I and II of the 28S rRNA[109]. The group of RPs required for the intermediate steps of 28s rRNA processing tend to be located near the polypeptide exit tunnel of the mature ribosome, on domains I and III of both the 28s rRNA as well as the 5.8S rRNA. RPs involved in early processing of the 5.8S rRNA are located on the large and small subunit interface and those required for late steps of maturation cluster around the central protuberance of ribosomes[109] (See Appendix Figure 16).

As was discussed briefly, the nucleolus and therefore ribosome biogenesis is a strong sensor of cellular stress. Ribosomal proteins are known to interact with the P53 pathway to mediate this stress signal. It is important to note that MDM2 regulates p53 in two ways. MDM2 binds directly to p53, preventing its transactivation domain from accessing the transcriptional machinery. MDM2 also acts as an E3 ubiquitin ligase for its conjugate p53, mediating the ligation of ubiquitin to p53 and its subsequent degradation by the proteasome[61]. A plethora of

events imparting instability to the ribosomal biogenesis process can cause nucleolar stress. As a response to this stress, the increase in free ribosomal proteins can bind to MDM2 and block MDM2-mediated p53 ubiquitination and degradation, resulting in p53-dependent cell cycle arrest[110]. By enabling the arrest of the cell cycle, the ribosomal proteins play a crucial role in connecting deregulated cell growth with inhibition of cell division; a process which becomes dysregulated in cancer. A variety of settings and agents (serum deprivation, chemical agents, oxidative stress, and ribosome malfunction) have been shown to generate nucleolar stress that signals to p53[61]. This allows cells to halt proliferation under unhealthy and poor ribosomal biogenesis conditions, a function necessary to ensure healthy growth of the organism and tissues. To date, several RPs, including RPL11[111], RPL23[112] and RPL5[113], have been found to activate p53 through their interactions with MDM2.

By inhibiting ribosome assembly in a stressed cell setting, there is less ribosomal protein binding to the rRNA and there is an increased binding of RPL5, RPL11, and RPL23 to MDM2. This binding inhibits MDM2 function, resulting in p53 accumulation and activation. In addition to the three aforementioned RPs, RPS7 and RPL26 have also been shown to interact with MDM2[114,115]. The consequence of the RPS7-MDM2 interaction resembles that of the aforementioned three RPs in terms of their mechanism of action in binding MDM2 and activation of p53. This stress induced loss of RPs from ribosomes would also expose the underlying rRNA to degradation, as discussed in the next sub-section.

1.3 Ability of Chemical Agents to Inhibit Ribosome Biogenesis and Affect Ribosome Integrity

1.3.1 Cell death inducing agents: rRNA disruption and ribosome biogenesis disruption

It has been known for several decades that cell death inducing agents, specifically apoptosis inducers, often result in the ordered laddering and degradation of DNA through the cleavage and activation of caspases that in turn activate caspase-activated DNases (CADs). The link of chemical and apoptotic inducing agents with the cleavage of rRNA was initially observed after many studies had established the link between DNA cleavage and apoptosis. Early work on apoptosis-inducing agents and RNA cleavage was performed by Houge et al., who demonstrated that several cytotoxic agents (okadaic acid, prednisolone, cycloheximide, and camptothecin, among others) could induce specific 28S and 18S degradation fragments in a variety of eukaryotic cell types [116,117]. These agents induce 28S rRNA cleavages in regions known as variable or divergent domains[118]. Also known as expansion segments[119], these regions have greater sequence variability than highly conserved regions. In mice thymoma cell lines treated with a calcium ionophore, rRNA degradation was observed in the absence of caspase activation and in a Bcl-2 independent manner, suggesting that apoptosis induction may not be necessary for rRNA degradation to occur[120]. Since these earlier studies, various other cell death inducing agents, including a variety of mycotoxins, have been shown to elicit the response of ordered disruption of the 28s rRNA[121,122]. Regardless of the type of cell death, rRNA has been shown to be an early cellular target affected by various cell death-inducing agents in a variety of eukaryotic cell types. Unfortunately, the molecular mechanisms mediating the cleavage of the 28S rRNA remain elusive.

DNA damage has long been known to activate p53 through a variety of mechanisms. However, studies by Rubbi and Milner suggests a connection between DNA damage and activation of p53 through rRNA-related pathways. In an experiment in which directed DNA damage was generated using localized UV irradiation, p53 was not activated when the nucleolus remained unaffected. The investigators concluded that DNA damage alone cannot activate p53 and that nucleolar disruption is a prerequisite for p53 activation[123]. Therefore, to effectively initiate apoptotic cell death through P53 and nucleolar disruption, ribosome biogenesis disruption may be necessary[124]. Agents such 5-Fluorouracil and bleomycin have been shown to interrupt ribosome biogenesis and cause P53 activation[123]. A survey study of various chemotherapy agents that were previously unknown to interfere with ribosome biogenesis, has demonstrated that many chemotherapeutic/cytotoxic agents also cause ribosome biogenesis disruption at various levels within rRNA biogenesis[125]. This evidence points to the nucleolus as being an early sensor of cytotoxic onslaught, with the rRNA and ribosomes being regulated by cleavage, as just discussed. However, the mechanisms involved in regulating the interplay between ribosome biogenesis disruption and rRNA cleavage are unknown, as is the timeline that occurs between the two, if any.

1.3.2 Ribosomal Integrity as an Indicator of Response to Several Chemotherapy Agents

Quite recently, Narendrula et al.[126] have determined that several ovarian and breast cancer cell lines (A2780, CAOV-3, MCF-7, SKBR-3, MDA-MB-231) reproducibly demonstrate significant rRNA disruption when treated with a variety of chemotherapy agents with succinctly distinct mechanisms (DXL, paclitaxel, carboplatin, cisplatin, vincristine, irinotecan and etoposide). The authors also report that there is an absence of rRNA cleavage products when cells are treated with a drug to which they are resistant. DXL was shown to be one of the most

reproducible and robust agents to induce rRNA degradation in this study[126]. This demonstrates that chemotherapy triggered cell death involves the degradation of rRNA, and that this appears to be a measure of the sensitivity of the cell line to the administered drug.

Since the discovery of taxanes as microtubule disruption agents, it has since been assumed that they elicit their cytotoxic activity through the induction of apoptosis subsequent to the stabilization of β-tubulin subunits by the drug[34]. However, as Burger et al. have shown, many other chemotherapy agents with different mechanisms also inhibit ribosome biogenesis at various levels[125]. DXL is used to treat a variety of cancers[41] and it is therefore of great importance to determine whether other pathways induced by the drug contribute to cell death.

1.4 Reviewing Possible Mechanisms Involved in rRNA Degradation

1.4.1 Early research and links to apoptosis

RNA degradation, in particular degradation of the 28S rRNA into distinct fragments, had been observed earlier by Houge et al. and was found to coincide with DNA fragmentation, a hallmark of apoptosis[116,127]. The association between RNA degradation and apoptosis was also observed in oat cells, undergoing cell death as a result of exposure to a host-specific toxin, victorin, produced by the fungus *Cochliobolus victoriae*[128]. As a result of apoptosis induction in developing rat cerebellum, degradation of both the 28S rRNA and 18S rRNA was observed with DNA fragmentation, demonstrating yet again that rRNA degradation often occurs with apoptosis induction[129]. A strong piece of evidence that linked apoptosis with rRNA degradation were the findings of Nadano *et al.* which showed that activating Fas receptor with an anti-Fas antibody

could produce rRNA degradation patterns[130]. Quite recently He et al. have demonstrated that the mycotoxins deoxynivalenol as well as satratoxin, anisomycin and ricin selectively cleave the 28S rRNA, and is related to apoptosis. This cleavage can be abrogated by inhibiting P53[131].

1.4.2. RNase L and other RNases as candidates of rRNA disruption

Cellular RNA is highly stable, and its transcription and degradation are under many levels of control. RNA-degrading enzymes called ribonucleases (RNases) interact with co-factors such as helicases, polymerases and chaperone proteins, to promote the degradation of messenger RNA (mRNA), transfer RNA (tRNA) and rRNA, through highly controlled processes[132]. Approximately 80% of the total RNA content of eukaryotic cells consists of rRNA[133], and although to date there has been little evidence to demonstrate rRNA cleavage by RNases in human cells, one can postulate that several degradation processes and therefore several RNases would be in place to cleave ribosomes that are dysfunctional and/or in a cell stress setting.

One RNase that has been implicated in the cleavage of rRNA is RNase L. RNase L was initially discovered as an RNase implicated in an interferon-mediated antiviral response mechanism involving the activation of 2′,5′-oligoadenylate (2-5A) synthetase (OAS). Once the host is infected with an RNA virus, interferon gamma (IFNγ) is produced. IFNγ induces RNase L production and activates OAS, which, in turn, activates the induced RNase by promoting 2-5A production. This cleaves both the viral and host cellular RNAs[134]. RNase L is one of the key enzymes involved in the function of interferons (IFNs), a family of cytokines participating in innate immunity against viruses and other microbial pathogens. Upon binding with its activator, 2-5A, RNase L degrades single-stranded viral and cellular RNAs and thus plays an important

role in the anti-viral and anti-proliferative functions of IFNs[134]. Zhou et al. have shown a 2-fold decrease in apoptosis *in vivo* in the thymuses and spleens of RNase $L^{-/-}$ mice[135]. Furthermore, apoptosis was substantially suppressed in RNase $L^{-/-}$ thymocytes and fibroblasts treated with different apoptotic agents. These results suggest that both interferon action and apoptosis can be controlled by the activity of RNase L. Additionally, RNase L induction was shown by Han *et al.* to cause cleavage of mature rRNA products in Hela cells due to the 2-5A response, which was similar to virally induced cleavage[136]. Very recently, a doxifluridine conjugated 2-5A analog of 2-5A was shown to have even greater activation ability than 2-5A itself for RNase L and has demonstrated potent anticancer activity against cervical cancer cells[137]. This research was critical at demonstrating a link between RNase L induction and suppression of cancer using an endogenously activated RNase, although its mechanism of tumour suppression is unknown.

Malathi et al. have also demonstrated that small dsRNAs produced by RNase L promote a switch from autophagy to apoptosis by caspase-mediated cleavage of Beclin-1, terminating autophagy[138]. Cleavage of Beclin-1 inhibits autophagy and the C-terminal fragment translocates to the mitochondria along with the pro-apoptotic protein, Bax, promoting the release of cytochrome C to the cytosol and inducing apoptosis. This demonstrated a clear link between RNase L decay products and apoptosis and demonstrates the importance of trying to identify decay products of endogenous RNases.

Another possible RNase candidate to explain RNA disruption previously observed by Narendrula et al.[126] and others is IRE1. The serine/threonine protein kinase/endoribonuclease inositol-requiring enzyme 1 (IRE1) is an ER transmembrane sensor that activates the unfolded protein response to maintain the ER and cellular function. Although mammalian IRE1 promotes cell survival, it can initiate apoptosis via decay of anti-apoptotic miRNAs[139]. IRE1 has been

shown to induce translational repression through 28S ribosomal RNA cleavage in response to ER stress[140]. Specifically IRE1β mediates the site-specific cleavage of 28S rRNA and translational attenuation of protein synthesis through its endonuclease function. Although there has not been a link between chemotherapy induced RNA degradation and IRE1 activation, it remains a possibility.

1.4.3 The exosome or NRD as potential mechanisms involved in rRNA disruption

To ensure that ribosomes are accurately synthesized and carry out their function properly, an active surveillance system exists that recognizes aberrant or stalled pre-ribosomes and targets them for degradation. Research by Allmang et al.[141] and Mitchell et al.[142] has demonstrated that pre-ribosomes which accumulate in the nucleus are degraded by the exosome. The exosome or exosome complex (sometimes abbreviated PM/Scl) is a multiprotein complex capable of degrading a variety of RNA substrates. The core of the exosome contains an inactive six-membered ring structure to which other RNases and proteins are attached[141]. Eukaryotes also contain an additional three core subunits, which form a structural cap that bridges the ring structure. Dis3 and Rrp6 constitute the associated RNases[143]. In eukaryotic cells, the exosome complex is present in the cytoplasm, nucleus and especially the nucleolus where nuclear pre-rRNAs (by the addition of a 3' oligo-A tail) can be degraded. *In vivo* exosome activity is regulated by associated enzymatic cofactors and RNA-binding adapters, which facilitate exosome access and recruitment to a multitude of substrates. The most characterized cofactor which aids the exosome is the Trf4p/5p-Air1p/2pMtr4p polyadenylation or TRAMP complex[144]. The exosome has been shown to demonstrate exoribonucleolytic function as well as endoribonucleolytic function in humans[145,146]. The most recent research is beginning to show that the human nuclear exosome is necessary for the proper cleavage and maturation of the rRNA

precursor molecule at site A2, which is necessary for removal of the internally transcribed spacer 1 or ITS1[99]. Quite recently Thoms et al. have also shown that the exosome plays a key role in the cleavage and removal of the ITS2 sequence from the end of 5.8S rRNA[100]. Although it is not clear how the exosome may play a role in chemotherapy induced RNA degradation, it is conceivable that some of these pathways may be involved due to their tight knight involvement in human ribosome biogenesis.

Non-functional RNA decay, abbreviated NRD, has been shown to degrade rRNA in ribosomes with a non-functional 28S subunit (mutated Peptidyl Transferase Center) by Lariviere et al[147]. These experiments indicate that the non-functional rRNAs are produced and incorporated into ribosomes similarly to wild-type rRNAs, but are then degraded faster by NRD following the completion of rRNA processing and ribosome assembly. Studies involving large subunit ribosomal NRD have shown that ubiquitylation levels are strongly increased and that this may play a strong role in the activation of NRD[148]. Fuji et al. have also demonstrated that this specifically requires the proteins Mms1 and Rtt101, which seem to localize to specific perinuclear locations[148]. The mechanism of RNA degradation in NRD is not known, although it is speculated that the exosome may play a role. rRNA is the most abundant nucleic acid in cells and although it is quite stable, is susceptible to damage from chemicals, ROS and stress. Furthermore, toxins like sarcin, ricin, and other ribosome-inactivating proteins depurinate rRNA, rendering the ribosomes nonfunctional[149]. Thus, NRD likely exists to clear the cell of rRNAs that have been damaged in a variety of manners.

One thing that remains clear is that although the rRNA of defective ribosomal particles has been extensively studied and shown to be submitted to regulation by distinct mechanisms, the fate of the ribosomal proteins from the defective ribosomes remains unclear. It also remains

unknown what mechanism is being employed by a variety of mechanistically distinct anti-cancer agents to induce rRNA degradation

1.5 Monitoring the Ribosome to Predict Chemotherapy Outcome

1.5.1 The Ribosome as an early sensor to chemotherapy

Typically, chemotherapeutic agents were selected on the basis of certain rudimentary properties that were initially identified as crucial to kill rapidly dividing cancer cells by damaging or stressing cells to initiate apoptosis: interference with DNA metabolism, drug-induced DNA crosslinking or production of ROS. Classically, cancer is thought to be a genetic disease that is most often caused by accumulation of mutations and damage wrought on DNA within the nucleus of cells. However, as was previously mentioned, evidence is now beginning to be shed that demonstrates that disruption of normal ribosomal function can contribute to the development of cancer as a disease as well[88]. When it comes to chemotherapy treatment, Burger et al. demonstrate that multiple chemotherapeutic drugs inhibit ribosome biogenesis at various levels, which rather contradicts our current understanding of the mechanisms of action of certain chemotherapeutic agents[125]. The authors of this study evaluated the synergism of drugs inhibiting rRNA synthesis at different levels. Drugs inhibited rRNA synthesis at several levels, including: rRNA transcription (*e.g.* oxaliplatin, doxorubicin, mitoxantrone, and methotrexate), early rRNA processing (*e.g.* camptothecin, flavopiridol, roscovitine) and late rRNA processing (*e.g.* 5-fluorouracil, MG-132, homoharringtonine). It was reported that inhibiting rRNA transcription or early rRNA processing steps caused nucleolar disintegration, whereas blockage of latter rRNA processing steps did not affect nucleolar integrity. There has even been recent research interest in blocking eukaryotic initiation factor 4F (EIF4F), which is responsible for recruiting mRNA to

the ribosome during protein production[150]. Cencic et al reports that an EIF4F inhibitor greatly sensitizes cancer cells to chemotherapy agents in several settings[150]. With this emerging evidence, many are starting to now understand that inhibition of ribosome biogenesis by chemotherapeutic drugs potentially may contribute to the efficacy of therapeutic regimens. Because of the ability of chemotherapy agents to induce damage to the ribosome and ribosome biogenesis intermediates, the ribosome therefore has promising potential to become a new way to measure the efficacy of chemotherapeutic agents, as well screening for potential new drug candidates. With this in mind, it would also enable the ribosome and its integrity as an early sensor/monitor to chemotherapy treatment.

1.5.2 RDA; a tool using rRNA integrity to predict patient response

Recently, a Toronto based company, RNA Diagnostics was founded based on a study (the CAN-NCIC-MA.22 clinical trial) which monitored rRNA integrity in women with locally advanced or inflammatory breast cancer treated with epirubicin and DXL at 2 or 3 weekly intervals in sequential cohorts[151]. Breast biopsy cores were obtained from 50 patients pre-, mid-, and post-treatment and the relationship between various biomarkers and treatment response was assessed. It was determined that a low mid-treatment tumour RNA Integrity Number (RIN) of samples correlated with pathological complete response (pCR) post-treatment, suggesting that tumor RIN may represent an important new biomarker for measuring response to chemotherapy in breast cancer patients. Rna Diagnostics, Inc. have since developed the RNA Disruption Assay (RDA), which uses a proprietary algorithm to quantify the creation of high molecular weight rRNA degradation products in tumours (RNA disruption) early in chemotherapy treatment[152]. A biopsy is taken during chemotherapy treatment and the amount of RNA disruption expressed as an RNA disruption index. When rRNA is sufficiently disrupted, tumour cells can no longer make

proteins and other substances necessary for cell division. When rRNA disruption is more extensive, cells can no longer maintain basic functions and die. Thus, it appears that tumour cells can only tolerate a small level of RNA disruption, above which they become non-viable[152].

This could be very useful as a "chemoresponse" assessment tool. If chemotherapy is working (as measured by RDA), the physician and patient can continue chemotherapy with confidence. However, if chemotherapy is not working well enough, physicians may consider alternate therapies. For the cancer patient, this allows for the avoidance of harmful side effects from ineffective chemotherapy regimens and an opportunity for improved survival outcomes. This tool would allow physicians to identify non responding patients, typically those that develop chemo-resistance within the cancer, and ultimately help guide cancer care. Thus, rRNA degradation may now be a useful new tool to monitor the progress of chemotherapy treatment and predict patient outcome. However, there is a still a great lack of knowledge of how chemotherapeutic agents affect ribosomes structure and promote the degradation of rRNA.

1.5.3 Implications of ribosomal proteins and their facilitation of rRNA degradation: monitoring ribosomal proteins following chemotherapy administration

As it has been previously stated, chemotherapeutic agents cause the ordered degradation of rRNA in cancer cells[126]. The degradation of rRNA can be monitored to evaluate tumour response to specific chemotherapy regimens and to predict patient outcome after treatment[152]. However, it is also known that the ribosome is a macromolecular complex composed of several rRNAs and multiple ribosomal proteins. In previous investigations of ribosomal proteins, there have been several independent research projects that have demonstrated the implication of ribosomal proteins in the maintenance and regulation of the cell cycle as well as the progression

to apoptosis. Repression of a large portion of 60S and 40S ribosomal proteins in a yeast model induced cell cycle arrest in either the G1 or G2/M phase of the cell cycle[153]. Interestingly, Thapa et al. also found that the ribosomal proteins whose repression generates similar effects on cell cycle progression, cluster in the same area of ribosome physical structure, allowing the authors to infer that different topological areas of the precursor and/or mature ribosome are mechanistically connected to separate aspects of the cell cycle. This could mean that to induce specific cell cycles changes (i.e. cell death through a defined pathway/mechanism), a specific ribosomal protein (or a specific subset of ribosomal proteins) may need to have an altered expression level or be degraded. Therefore, it is likely that changing the expression or activity of specific ribosomal proteins would be expected to have significant effects on the cell.

There have been several ribosomal proteins that have been shown to regulate the cell cycle and apoptosis through their expression levels. Abnormal expression levels of ribosomal protein L7 in Jurkat T-lymphoma cells has been shown to arrest the cell cycle in G1[154] and to induce apoptosis. Expression of L13a in humans was shown to interfere with cell cycle progression by arresting the cell cycle in G2/M phase and inducing apoptosis, while inhibition caused apoptosis as well[155]. Naora et al. have also shown that human ribosomal protein S3a (RPS3a) plays important roles in cell transformation and death. Constitutive or transiently enhanced RPS3a expression primes a cell for apoptosis, whilst the suppression of enhanced expression acts as the execution signal of the cell[156]. Knockdown of ribosomal protein S15a was shown to induce apoptosis in a human glioblastoma cell model[157]. The examples of ribosomal protein expression changes resulting in apoptotic cell death in the literature are numerous, although it is difficult to correlate the levels of expression of the ribosomal proteins to those seen at a physiological level. The involvement of ribosomal proteins in apoptosis is further evident in

their interaction with Mdm2, an ubiquitin ligase that maintains P53 levels under normal cellular conditions by binding and inactivating P53 (as discussed in section 1.2.3). To date, several RPs, including RPL11[111], RPL23[112] and RPL5[113], have been found to activate p53 through their interactions with MDM2.

Although cellular events associated with changes in ribosomal protein expression have been identified, it is not known what occurs to the ribosomal proteins following chemotherapeutic treatment. Earlier research involving doxorubicin treatment of Jurkat cells showed that ribosomes are structurally altered in apoptotic cells following the inactivation of protein synthesis[158]. Nishisda *et al*. have also shown that degradation of 3 ribosomal proteins following treatment was partially abrogated using a Z-VAD FMK caspase inhibitor.

Based on preliminary research involving ribosomal proteins, there is reason to believe that chemotherapeutic induction of apoptosis/cell death of cancer cells would alter the expression of ribosomal proteins. It is unknown whether changes in ribosomal protein composition occur upon chemotherapy treatment that would contribute to cell death, possibly by apoptosis. There is a lack of evidence in the literature exploring the effects of chemotherapy agents on ribosome composition and structure, which may in turn, activate apoptotic and other cell death pathways. Of particular interest as well, given the implications of rRNA disruption to chemotherapy action[126], is the effect of chemotherapy and ribosomal protein expression changes on rRNA cleavage. If there are any changes in the expression of ribosomal protein and/or it association with the ribosome, this could lead to changes in the ribosome structure and/or accessibility of certain RNases to the backbone rRNA. Further investigations into ribosomal protein changes following chemotherapeutic treatment could potentially shed light on: a) rRNA disruption and

the underlying mechanisms, b) links to apoptotic cell death and c) determine whether changes in ribosome protein composition temporally precede rRNA integrity changes

1.6 Hypothesis and research aims

Based on previous findings, investigating the alteration of ribosome structure following chemotherapeutic treatment may provide insight into the mechanism of rRNA disruption and/or the cell death pathways elicited shortly after drug exposure. Here, we hypothesize that chemotherapeutic treatment (DXL) of A2780 ovarian carcinoma cells will result in changes in ribosome composition, both rRNA and ribosomal protein; while we expect a lack of change in resistant cells. We further hypothesize that chemotherapy treatment results in the loss of ribosomal proteins, which precedes RNA disruption, possibly by permitting access to the underlying rRNAs by RNA-degrading RNases. Finally, chemotherapy-dependent rRNA degradation will be lower in assembled ribosomes than in nuclei containing rRNAs that have yet to be assembled into ribosomes (greater access to RNases) To investigate this hypothesis, 5 aims have been proposed.

- Aim A) To purify ribosomes from control and DXL-treated ovarian tumour cells
- Aim b) To identify differences in the composition of purified ribosomes between control and DXL-treated cells (rRNA and protein) at various times after DXL administration.
- Aim c) To assess whether ribosome composition is unaltered in ovarian tumour cells resistant to DXL.

- Aim d) To assess whether ribosomal proteins are lost from ribosomes prior to rRNA degradation (RNA disruption)
- Aim e) To determine whether rRNA degradation (RNA disruption) is lower in assembled ribosomes than in nuclei containing fresh rRNA transcripts that have not yet been assembled into ribosomes

2.0 Materials and Methods

2.1 Cell lines and cell culture

The A2780 ovarian carcinoma epithelial cell line was used as an *in vitro* ovarian cancer model in this study. The A2780 cell line was purchased from the European Collection of Cell Cultures (ECACC, Salisbury, UK) and maintained in RPMI-1640 medium with 2mM Glutamine, which contained 10% fetal bovine serum (FBS) (Gibco, ThermoFisher, Canada), and 1% Penicillin (10,000 U/ml)/Streptomycin (10,000 μg/ml) solution (HyClone, South Logan, Utah, US) to a final concentration of 100 U/mL penicillin and 100 μg/ml streptomycin. The A2780 ovarian cancer cell line is likely of the endometrioid subtype[159]. During this study the DXL resistant A2780 cell line (A2780DXL) was used as an in vitro model of DXL-resistant ovarian cancer. The A2780DXL cell line was generated by selecting A2780 cells for survival in increasing doses of DXL as described by Armstrong et al.[12], using the method of Guo et al.[160]. Briefly, the selection began at a dose 1000x below the IC_{50} for DXL and doses were repeatedly increased 3-fold, 1.5-fold and 1.25-fold, with retention of the culture of cell surviving the maximum of these dose escalations. This process was continued until a culture of cells was obtained containing the maximally tolerated dose of DXL. For the A2780DXL cells used in this study, resistance to DXL was maintained by adding 4.05×10^{-7} M DXL to the medium weekly. All cell lines, including drug resistant cell lines, were cultured in Corning T75 cm^2 vented tissue culture flasks (Corning, New York, United States) and incubated in a water jacketed CO_2 incubator set at 37ºC with 5% CO_2. Cell lines were allowed to reach 70-90% confluency, as determined by microscopy before undergoing sub-culturing.

2.2 Chemotherapy agents and drug treatment

DXL (Hospira Healthcare Corporation, Saint-Laurent, Québec) was used to induce RNA disruption in the A2780 cell line, as was previously described by Narendrula et al.[126]. The drug was diluted to the desired concentration in complete media and cells were treated for time periods ranging from 12 to 72 hours. The DXL concentration used was based on previous drug treatment experiments using the A2780 cell line, during which RNA disruption was observed. A concentration of 0.2μM DXL was found to induce maximal RNA disruption[126]. Unused DXL not administered to patients was graciously donated by the pharmacy services at the Northeast Cancer Centre at Health Sciences North (Sudbury, Ontario) to Dr. Amadeo Parissenti`s research group. DXL was stored in 1mL glass vials at 4ºC and was used within 1 month, as recommended by the supplier. For drug dilutions, drug was serially diluted in 15 mL centrifuge tubes in pre-calculated molar concentrations according to the cell line and its degree of resistance.

2.3 Ribosomal purification – differential centrifugation

To purify ribosomes, a differential centrifugation technique along with sucrose cushion centrifugation to sediment undesired cellular organelles and preferentially pellet intact ribosomal species was used[161]. All solutions used were made with diethylpyrocarbonate (DEPC) treated ultra-pure deionized water in order to prevent RNA degradation. Cells were plated in T75 tissue culture flasks and allowed to grow to approximately 90% confluence. After 3 washes with 15mL of cold phosphate-buffered saline (PBS) (pH 7.4), cells were scraped into 10 mL of cold PBS and harvested by centrifugation at 4^{o}C for 5 min at 500 x g; the supernatant was aspirated and discarded. Cells were re-suspended in cold Buffer A (250 mM sucrose, 250 mM KCl, 5 mM

$MgCl_2$, 50 mM Tris·HCl, pH 7.4) in such a fashion that the volume of Buffer A was 3 times the volume of the cell pellet. Cells were lysed by adding a gentle detergent solution of 10% octylphenoxypolyethoxyethanol (also known as IGEPAL CA-630), at 4°C to a final concentration of 0.7% (v/v). HALT protease and phosphatase inhibitor (Thermo Scientific, Rockford, IL, USA) with sodium fluoride (50 mM), sodium orthovanadate (0.2 mM) was added at this point to prevent further modification of proteins along with RNAseOUT (Thermo Scientific, Rockford, IL, USA), a recombinant ribonuclease inhibitor. After a 15 minute incubation period on ice (pipetting the solution twice during the incubation time to ensure proper homogenization of cells) the cell lysate was centrifuged for 10 min at 750 x g, 4°C to pellet nuclei. The remaining cytoplasmic fraction, i.e. the supernatant, was then decanted and further centrifuged for 10 min at 12,500 x g, at 4°C, to pellet the mitochondria. After decanting and separating the mitochondrial pellet, the remaining post-mitochondrial fraction was retained as it contains the ribosomes. Next, a 4 M KCl solution was slowly added to the post-mitochondrial fraction to ensure a final concentration of 0.5 M KCl. This concentration of KCl is necessary to ensure the stringent purification of ribosomes devoid of unnecessary contaminating organelles and proteins.

One mL of sucrose cushion (1 M sucrose, 0.5 M KCl, 5 mM $MgCl_2$, 50 mM Tris·HCl pH 7.4) was then layered into the bottom of a 3 ml polycarbonate centrifuge tube. The KCl-adjusted post-mitochondrial fraction was carefully layered above the sucrose cushion and the centrifuge tubes accurately balanced to within 0.01 g using Buffer B (250 mM sucrose, 0.5 M KCl, 5mM $MgCl_2$, 50 mM Tris·HCl, pH 7.4). The tubes were centrifuged for 2 hours at 250,000 x g, 4°C. Following centrifugation, the supernatant was discarded and the dense ribosomal pellet was very gently rinsed, twice, by adding 200 µL of cold RNase free water and removing it immediately

without disturbing the pellet. After washing, the ribosomes were re-suspended with three subsequent additions of 100 µL of Buffer C (25 mM KCl, 5 mM $MgCl_2$, 50 mM Tris·HCl, pH 7.4) and stored at -80°C.

2.4 Ribosomal Protein purification and quantification

The ribosomal purification protocol was followed by the addition of 0.7 volumes of absolute ethanol to the purified ribosomes in aqueous suspension. The ribosomes precipitated immediately, and the suspension was centrifuged at 8,000 x g for 10 minutes to pellet the ribosomal subunits. The supernatant was removed and the ribosomes were re-suspended in 250 µL of homogenization buffer with no sucrose, followed by the addition of 25 µL of 1 M $MgCl_2$ and 550 µL of glacial acetic acid with gentle mixing. Following a 45 minute incubation period, the precipitated RNA from the ribosomes was removed by centrifugation at 10,000 x g for 10 minutes. The supernatant was removed and placed in another tube containing 4 volumes of acetone. The ribosomal proteins immediately precipitated, but the suspension was placed in the freezer at –20°C for 2 hours to facilitate complete precipitation of the proteins. The mixture was centrifuged at 10,000 x g for 10 minutes to pellet the proteins. The proteins were washed by the addition of 1 mL of acetone and centrifuged again. This wash step was repeated once. Proteins were solubilized in distilled Millipore water. The protein concentration for the ribosomal protein solution and the different organelle fractions (monitored as a measure of quality control) were determined using the Pierce BCA Protein Assay Kit (Pierce, Rockford, IL, USA).

2.5 1D SDS-PAGE gels

For each ribosomal protein and cellular fraction preparation, 10 μg of proteins in 2× electrophoretic sample buffer (containing 1% DTT, 1M Tris·HCl and .025% Bromophenol blue) were heated at 100°C for 5 mins and resolved on 12.5% SDS-PAGE gels for 1.5-2 hours at 35 mV using the BioRad Protein Mini II cell (Hercules, California, United States). Following electrophoresis, gels were fixed using a 25% Isopropanol and 10% acetic acid solution for 1.5 hours. After fixing, gels were stained overnight in a 10% acetic acid and .0006% Coomassie Blue G-250 solution and de-stained as necessary with 10% acetic acid.

2.6 Immunoblotting

Protein samples were first loaded and run onto a 12.5% polyacrylamide gel as described in the ‘‘1D SDS PAGE’’ section above; however, the fixing and staining steps were left out. Proteins from the gel were transferred onto BioTrace PVDF membranes (Life Sciences, Pensacola, FL, USA) using a BioRad electrophoretic transfer unit. Following electrophoretic transfer, the membranes were blocked with a 5% milk solution in 1× TNE buffer (50mM Tris, 140mM NaCl and 5mM EDTA) containing 0.1% Tween-20 (FisherBiotech, Thermo Fisher Scientific Inc., Waltham, MA, USA) for 1 hour. The primary antibody was diluted in a 5% milk solution in 1x TNE buffer and incubated with the membrane on a rocker overnight at 4°C. After washing the membrane for 3× 20 min in 1× TNE, the membrane was incubated with secondary antibody diluted in 5% milk solution in 1x TNE for 1 hour at room temperature. Following treatment with the secondary antibody, membranes were washed for 3× 20 min in 1× TNE

before the proteins were visualized using the enhanced chemiluminescence (ECL) method using peroxidase[162].

In order to assess the purity of the ribosome preparations and other organelle fractions, all preparations and fractions were examined in immunoblotting experiments for expression of specific proteins known to reside in specific organelles. Antibodies to proteins in the endoplasmic reticulum, mitochondria, nucleus, and ribosomes were used in this assessment (ERP72, VDAC, H2AX, and RPL7a, respectively). The same membrane was reblotted with primary antibodies against RPL7a, RPL3, RPL4 and RPSA during ribosomal protein experiments. The antibodies for VDAC (4866) and RPL7a (E109) were obtained from Cell Signaling Technology, Inc. (New England Biolabs, Ltd., Whitby, ON, CA). Primary antibody for RPL3 (sc-86828) was obtained from Santa Cruz Biotechnology, Inc. (Santa Cruz, CA, USA). The goat anti-rabbit (sc-2030) IgG-HRP and goat anti-mouse (sc-2005) IgG-HRP secondary antibodies were obtained from Santa Cruz Biotechnology, Inc. (Santa Cruz, CA, USA). The primary antibodies for H2AX (pS139) and ERP72 (610970) were obtained from BD Biosciences (Franklin Lakes, New Jersey, USA) whilst the primary antibodies for RPL4 (11302-1-AP) and RPSA (14533-1-AP) were purchased from Proteintech Group Inc. (VWR International, Mississauga, Ontario, Canada).

2.7 Two dimensional gel electrophoresis

Ribosomal proteins were further separated and analyzed by 2D gel electrophoresis (2DGE). A dried ribosomal protein pellet (dried using a Savant SpeedVac Concentrator, Thermo Scientific, Rockford, IL, USA) containing 50-100μg of ribosomal protein was re-suspended in 100 μL Isoelectric-focusing (IEF) rehydration buffer containing 7 M Urea, 2 M Thiourea, 4%

CHAPS, 1% ampholyte (IPG Buffer pH 7-11 NL, GE Healthcare Life Sciences, Mississauga, ON, Canada), 0.001% Bromophenol blue, and 1.5% De-streaking agent (2-hydroxyethyl-disulfide) (Sigma Aldrich, Oakville, ON, Canada). After 2 hours at room temperature to allow full dissolution of the proteins, the protein solution was placed on a paper bridge (3 cm x 0.4 cm) and was actively loaded at 500V for 16 hours into a previously hydrated 18cm Immobiline isoelectric focusing dry strip (pH 6-11; GE Healthcare Life Sciences, Mississauga, ON, Canada) using anodic paper bridge loading[163]. Next, the IEF strip was focused for a total of 35 kVh using water-soaked paper wicks on both anodic and cathodic sides of the focusing tray. Following focusing, the strips were equilibrated using an equilibration buffer (6 M Urea, 0.375 M Tris HCl pH 8.8, 2% SDS, 20% glycerol) in two washing steps. The first wash step consisted of a 20 min wash with the equilibration buffer containing 130 mM DTT to reduce the proteins while the second wash step consisted of a 20 min wash with a buffer containing 135 mM Iodoacetamide to alkylate the proteins. The strip was then trimmed to a length of 11 cm to accommodate an 11 cm wide well in an 8-16% gradient acrylamide gel, buffered with Tris-HCl to pH 8.6. The gel also contained a single lane beside the 11 cm well, for loading size markers (Biorad, Hercules, California, United States). After insertion into the 11 cm IEF strip well, the IEF strip was overlaid with overlay agarose consisting of 0.75% agarose and 0.003% Bromophenol blue with 1x TGS (25mM Tris, 192mM glycine and 0.1% SDS) buffer before being run at 200v for 1 hour. Before being imaged, the 2D gel was stained with Flamingo fluorescent stain (BioRad, Hercules, California, United States) according to the manufacturer`s protocol.

2.8 RNA extraction

RNA was extracted from cells, purified ribosomes, and subcellular organelle fractions using the miRNeasy^{TM} Micro Kit from Qiagen Laboratories (Mississauga, ON, Canada). Briefly, A2780 cells, purified ribosomes and the subcellular fractions were lysed using 700µL of QIAzol lysis buffer, a monophasic solution of phenol and guanidine thiocyanate, designed to lyse tissues and inhibit RNases. The lysed cells were scraped and collected from the cell wells using sterile cell scrapers (Fisher Scientific, Ottawa, ON) and all samples were handled using sterile-RNase free centrifuge tubes (Fisher Scientific, Ottawa, ON). Samples were then disrupted and homogenized in the QIAzol Lysis Reagent by passing the homogenate through a 20 gauge needle 5-10 times. After addition of chloroform, the homogenate was separated into aqueous and organic phases by centrifugation. The RNA partitions to the upper, aqueous phase while DNA and proteins partition to the interphase or the lower, organic phase[164]. RNA was precipitated from the aqueous phase by addition of anhydrous ethanol. The RNA was then bound to a silica-based RNeasy spin column and washed with proprietary buffers (RPE and RWT buffers) before being eluted in 50 µL of RNase-free water. Samples were aliquoted in 5 µL volumes before being stored at -80ºC until further analysis was performed.

2.9 RNA quality analysis in purified ribosomes and nuclei

The integrity of extracted total RNA samples was analyzed using capillary gel electrophoresis. Specifically, RNA samples were loaded onto an RNA Nano Chip (Agilent Technologies, Santa Clara, CA) as directed by the manufacturer's protocol and analyzed with Agilent 2100 Bioanalyzer (2100 Expert software, Agilent Technologies, Santa Clara, CA). This

technology utilizes microfluidics coupled with capillary electrophoresis to generate an electropherogram. This electropherogram displays/plots the migration time in seconds of the extracted RNAs and RNA fragments, which the software converts to nucleotide (Nt) size using a set algorithm and specific masses of RNA reference standards. The fluorescence intensity of the various RNA peaks in fluorescence units (FU), can then be used to quantify the total mass of RNA present. The electropherogram displays two distinctive peaks that correspond to the 28S and 18S eukaryotic rRNA subunits. The software includes an algorithm that also calculates and analyzes all significant electrophoretic traces of RNA fragments other than the 28S and 18S ribosomal subunits. Therefore, the integrity of the RNA sample can be measured using a proprietary RIN or ‘‘RNA Integrity Number’’ value.

2.10 Statistical Analyses

During this study, the significance of differences in data sets was assessed using a Student t-test, after application of the F-test to determine if the samples within an experiment contained significantly different amounts of variation. A P value of < 0.05 was considered to be statistically significant. Statistical analyses were performed using Microsoft Excel or GraphPad Prism 5 software.

3.0 Results

3.1 1D SDS-PAGE of Protein fractions obtained during ribosomal purification

3.1.1 1D SDS-PAGE of Protein fractions obtained during Purification of Monosomes

There are different sub-populations of mature ribosomes found within the cytoplasm of eukaryotic cells. These include monosomes (a single ribosome translating a single mRNA strand) and polysomes (several actively translating ribosomes per a single mRNA strand). Both the monosomal and polysomal populations of ribosomes were investigated in this study. In order to assess the efficacy of the differential centrifugation protocol used to purify intact ribosomes (monosomes) from confluent A2780 cells (see Figure 1), a one dimensional SDS-PAGE gel of the subcellular protein fractions obtained during the purification of ribosomes was run. By observing the profile obtained from each protein fraction, we were able to assess whether or not the outlined protocol facilitates purification of intact ribosomal subunits. The total cell extract of A2780 cells had a large amount of protein that spanned a wide range of molecular sizes, as seen in Figure 2. As we would expect, the nuclear protein fraction contained a variety of proteins, with the histones being quite evident at approximately 15 kDa. The ribosomal protein fraction was indicative of purified ribosomes, since the protein banding pattern compared nicely to that obtained by Belin et al[161]. We also saw a sudden and drastic change in the quantity and variety of molecular weights present in the purified ribosomal proteins in comparison to the other lanes in the gel in Figure 2. The sharp, high intensities and distinct grouping of the proteins identified that there were fewer proteins compared to the other purification fractions, yet of a higher yield. The 79 ribosomal proteins in human cell lines display molecular weights ranging from approximately 5-50 kDa[165]. The range of molecular weights of the proteins in the ribosomal fraction that can be

seen in Figure 2 were as expected for a human ribosomal fraction. The protocol established by Bélin et al.[161], from which this protocol was adapted, used a 1D SDS-PAGE banding pattern as the sole criteria for measuring purity of the ribosomal fraction. The ribosomal protein profile presented in the original protocol bears high similarity to the Coomassie stained ribosomal profile we obtained (Figure 2), particularly the range of the molecular weights of the proteins.

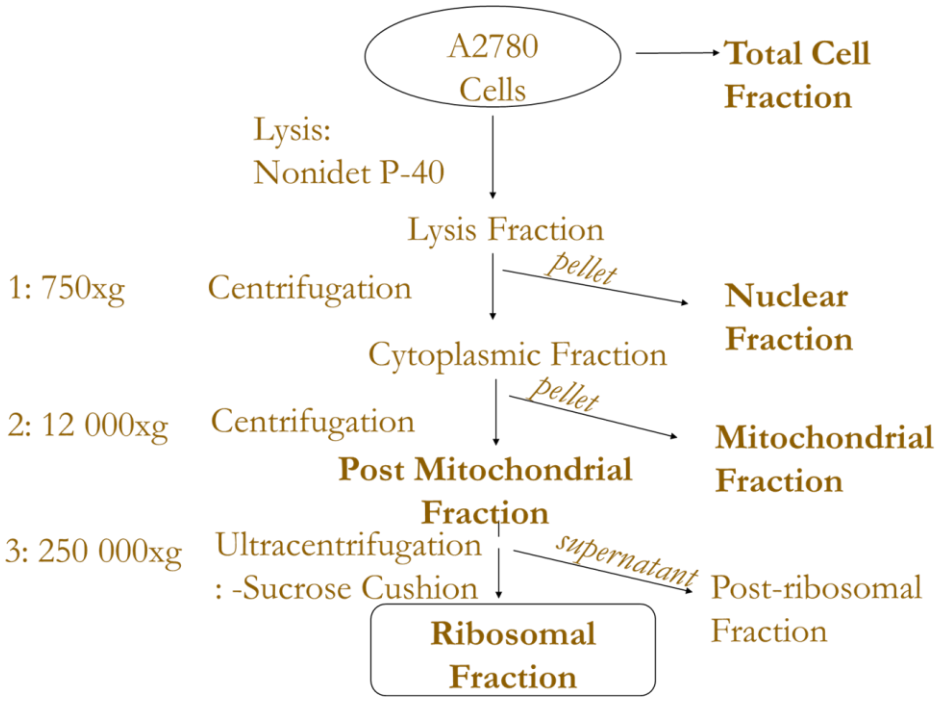

Figure 1 - Workflow of the differential centrifugation protocol for purification of intact ribosomes, based on the protocol established by S. Bélin et al.

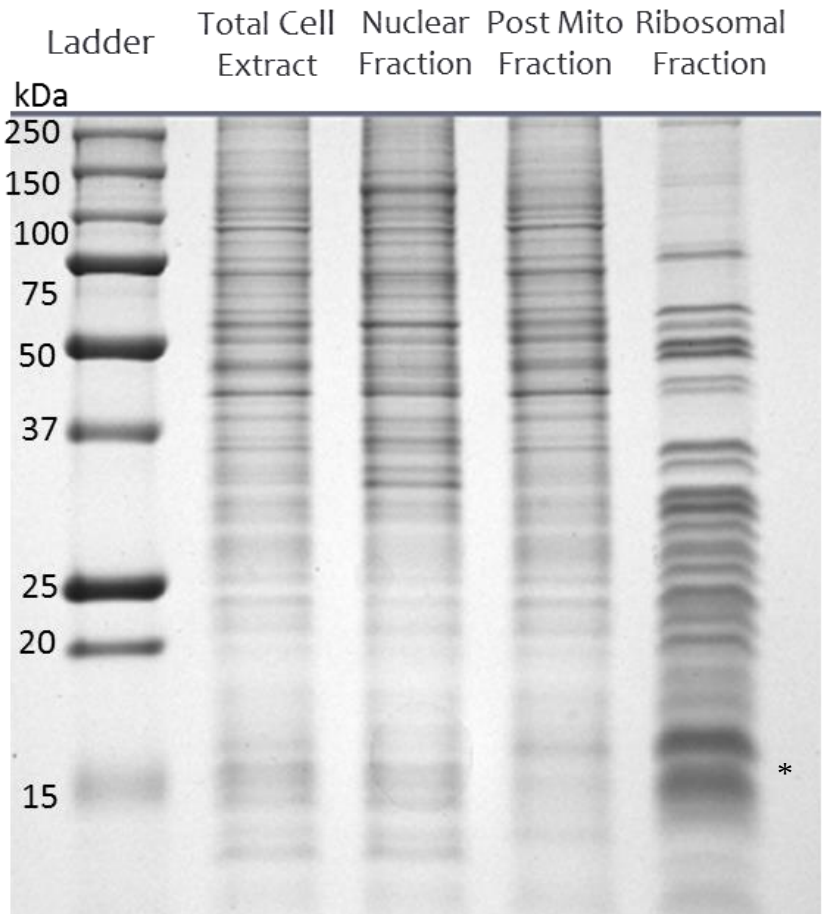

Figure 2 – Protein profiles of fractions obtained during ribosome purification. Samples were run in a 12.5% acrylamide gel and stained with Coomassie blue. 10 μg of protein were loaded per lane, as determined using the BCA assay. The profile observed above for the ribosomal fraction was indicative of pure ribosomes, as ribosomal proteins have reported molecular weights spanning from 5-50 KDa. The asterisk denotes histone proteins at 15kDa. The gel image is representative of three independently conducted experiments.

3.1.2 1D SDS-PAGE of protein fractions obtained during purification of polysomes

As shown in Figure 3, the overall pattern obtained for the protein fractions during the purification of polysomes was similar to the monosomal pattern in Figure 2. However, upon scrutiny, there was some evident discrepancies. In Figure 3, the total cell extract for the preparation of polysomes appeared to have an enrichment in the histones, which can be found around 15 kDa. However, it is probable that it is also profilin, an actin-binding protein involved in the dynamic turnover and restructuring of the actin cytoskeleton[166]. Moreover, the polysome preparations contained a large amount of protein with molecular weights above 70 kDa, which is out of the molecular weight range of human ribosomal proteins. Due to the fact that the KCl concentration must be altered (lowered to 0.025 M) for all solutions in the isolation of polysomes, this changes the stringency of the purification protocol and allows for a larger amount of protein to be co-sedimented with the ribosomal pellet during centrifugation[161]. Due to this fact, further analyses with DXL treatment will use the monosomal fractionation of ribosomes because the monosomal fractions have reduced levels of higher molecular weight proteins.

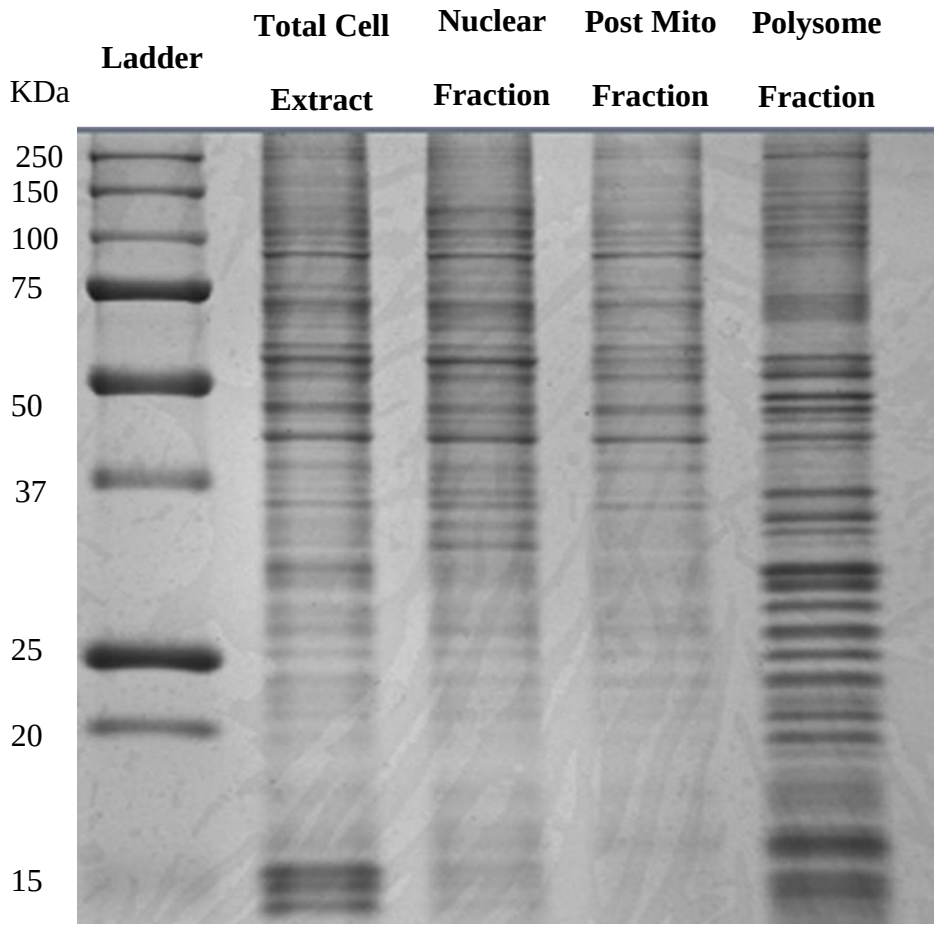

Figure 3 – Protein profiles of fractions obtained during polysome purification. Samples were run on a 12.5% acrylamide gel and stained with Coomassie blue. 10μg of protein were loaded per lane, as determined by the BCA assay. The profile observed above for the ribosomal fraction is indicative of pure ribosomes (ribosomal proteins have molecular weights spanning from 7- 67 kDa). Due to a decrease in the KCl concentration to 0.025M in buffers to accommodate for polysome purification, there is more noticeable contamination of higher molecular weight species. The gel image is representative of three independently conducted experiments.

3.2 Western blot analysis of protein fractions obtained during purification of ribosomes

As the results of Figure 2 indicate, the ribosomal protein fraction obtained after purification of intact ribosomes from A2780 cells demonstrated significant enrichment of ribosomal proteins. To ensure that there was no appreciable contamination of the ribosomal protein fraction with proteins from other cellular organelles, a series of western blots were conducted using antibodies to proteins known to be expressed abundantly in the ribosome, nucleus, mitochondria and endoplasmic reticulum. Antibodies for RPL7a (ribosomal protein 7 of the eukaryotic 60S ribosome subunit), H2Ax (nuclear histone protein), VDAC (mitochondrial-specific voltage dependent anion channel) and ERP72 (endoplasmic reticulum protein disulfide isomerase) were used in this assessment. In Figure 4, 10 μg of proteins from each cellular fraction were run on a SDS-PAGE denaturing gel, transferred to a PVDF membrane and blotted with above antibodies. We observed a clear enrichment for RPL7a in the ribosomal fraction (RB) in comparison to all other fractions. H2Ax, VDAC and ERP72 were not present in the ribosomal fraction, indicating the efficacy of the protocol for obtaining ribosomal particles devoid of contaminating organelles.

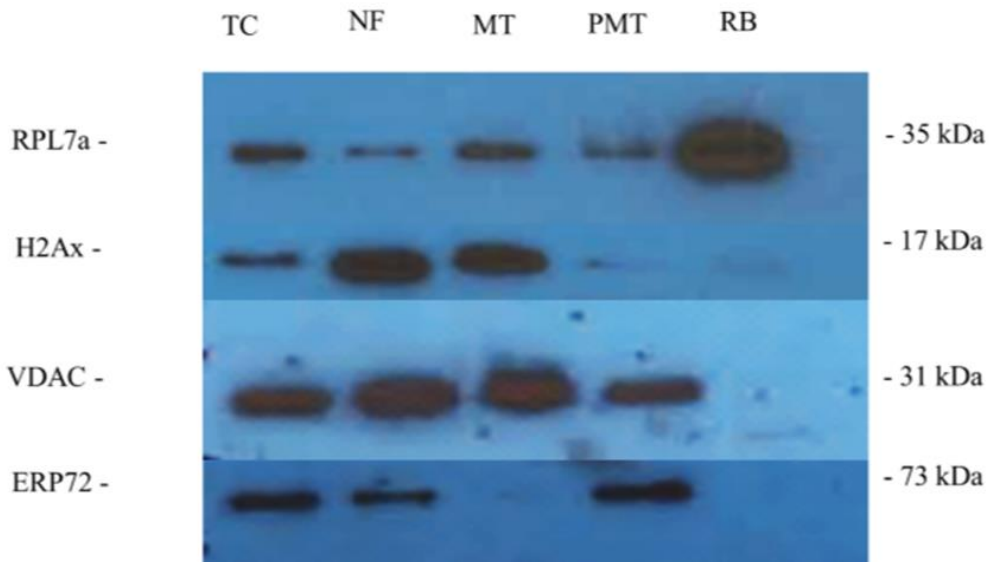

Figure 4 -Western blots of organelle fractions obtained during the differential centrifugation protocol for isolation of ribosomes. TC- Total cell extract, NF- Nuclear fraction, MT- mitochondrial fraction, PMT- Post mitochondrial fraction, RB- Ribosomal fraction. RPL7a- ribosomal protein of the eukaryotic 60s ribosome subunit, H2Ax- nuclear histone protein, VDAC- voltage dependent anion channel (mitochondrial specific), ERP72- endoplasmic reticulum protein disulfide isomerase. Samples were run on a 12.5% acrylamide gel with 10 μg of protein loaded per lane, as determined per BCA assay. The gel image is representative of three independently conducted experiments.

3.3 Capillary electrophoresis of rRNA isolated from monosomal purification

To ensure that intact ribosomes were being pelleted during the differential centrifugation protocol, rRNA isolated from the ribosomal fraction was also monitored by capillary electrophoresis on an Agilent 2100 bioanalyzer. Following the ribosomal purification, RNA was extracted from the various fractions using a Qiagen miRNeasy purification column and kit. The total cellular RNA obtained from confluent A2780 cells, is shown in Figure 5. The RNA displayed the typical strong 28S and 18S rRNA bands seen in high quality total cellular RNA. The nuclear fraction contained a variety of other RNA species above the typical 28S and 18S rRNA bands, which could speculatively be the primary rRNA transcripts prior to or partially through splicing. The monosomal fraction displayed strong 28S and 18S rRNA bands; however, there were distinct and reproducible bands that appeared with the isolation of rRNA from purified ribosomes. We believe these bands are indicative of rRNA fragments that occurring during regular ribosomal turnover, most likely ribophagy[167]. Although precautions were taken to prevent RNase contamination, it is possible the bands mentioned are due to RNase degradation All solutions used in the extraction process were DEPC treated and RNAseOUT (Thermo Scientific, Rockford, IL, USA), a recombinant ribonuclease inhibitor, was also added to the ribosomal preparations. The analysis of total cellular RNA by capillary electrophoresis informs us that intact rRNA was purified from monosomes, along with the purified proteins.

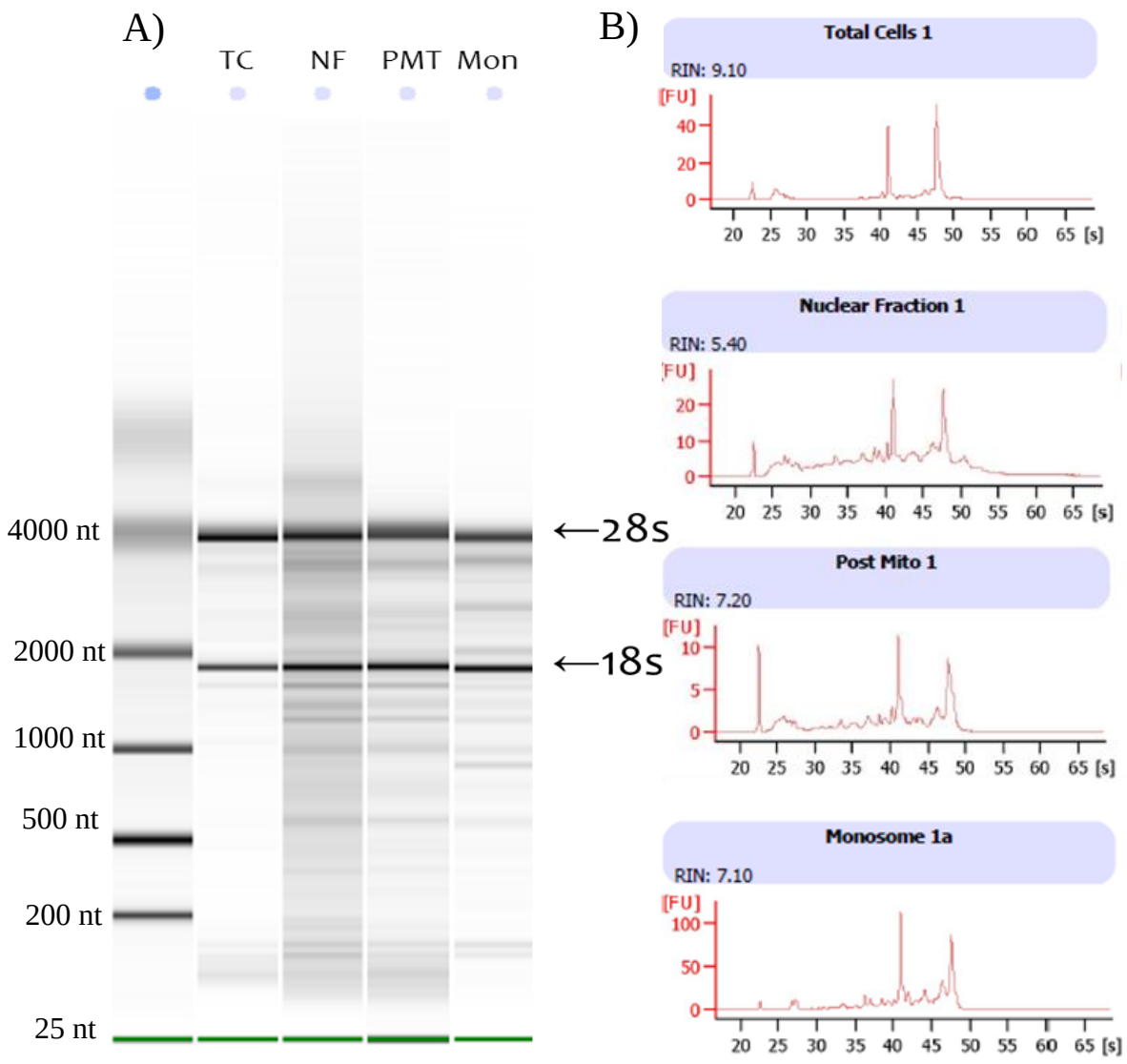

Figure 5 – Capillary gel electrophoresis of fractions obtained during the purification of monosomes. A2780 cells were grown to confluence and the monosomal population of ribosomes was purified as described previously. RNA was extracted from various fractions during monosome purification using Qiagen miRNeasy kits and the RNA in the fractions was resolved using capillary gel electrophoresis. RNA was isolated from the following fractions: TC (Total Cell Fraction), NF (Nuclear Fraction), PMT (Post Mitochondrial Fraction) and Mon (Monosomal Fraction). A) Virtual gel B) Corresponding electropherograms. The gel image is representative of three independently performed experiments.

3.4 Capillary electrophoresis of rRNA isolated from polysomes

As described previously, isolation of polysomes requires the lowering of the KCl concentration in various buffers to preferentially pellet polysomes[168]. To ensure that intact ribosomes were being pelleted during the isolation of polysomes, RNA from the various fractions were isolated using Qiagen miRNeasy kits and component RNAs monitored by capillary electrophoresis on an Agilent 2100 bioanalyzer. The total cellular RNA fraction obtained from confluent A2780 cells is shown in Figure 6 and displayed the typical strong 28S and 18S rRNA bands seen in high quality total cell RNA. Purified polysomes displayed strong 28S and 18S rRNA bands, but there was an absence of the distinct atypical bands that appeared in purified monosome preparations, which may represent rRNA turnover products. The integrity of RNA in the isolation of polysomes was facilitated by treating all solutions used in the extraction process with DEPC and by adding a recombinant ribonuclease inhibitor, RNAseOUT (Thermo Scientific, Rockford, IL, USA), to polysomal preparations. Our data suggests that intact rRNA could be purified from isolated monosomes or polysomes, along with their associated proteins.

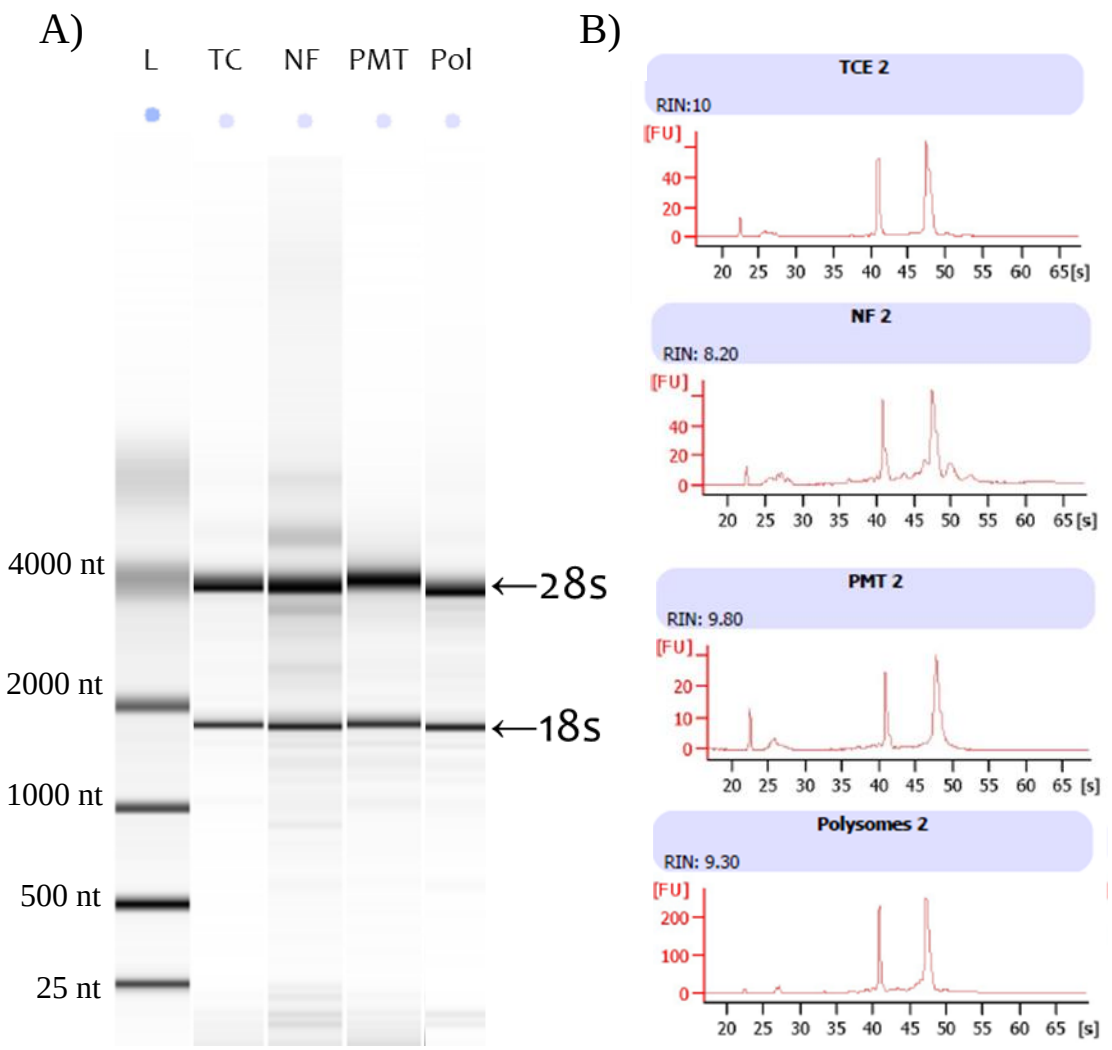

Figure 6 - Capillary gel electrophoresis of fractions during the purification of polysomes. A2780 cells were grown to confluence and polysomes purified as described previously. RNA was then extracted from the various fractions during polysome purification using Qiagen miRNeasy kits and the various component RNAs in the fractions resolved by capillary gel electrophoresis: TC (Total Cell Fraction), NF (Nuclear Fraction), PMT (Post Mitochondrial Fraction) and Pol (Polysomal Fraction). A) Virtual gel B) Corresponding electropherograms. The gel image is representative of three independently conducted experiments.

3.5 Effect of DXL treatment on rRNA from isolated ribosomes

3.5.1 Effect of 12 hour 0.2 μM DXL exposure on ribosome content and rRNA integrity in the various fractions during purification

After adequate purification of ribosomes from control (untreated) A2780 cells, the effect of DXL treatment for various lengths of time on ribosome content and quality was assessed in A2780 cells. Previously, our research group had demonstrated, using total cell RNA extracts, that RNA disruption bands can be detected as early as 24 hours, with the intensity of cleavage products relative to the parent 28S and 18S bands being most significant at 72h[126]. However, when RNA was extracted from purified ribosomes, rRNA cleavage products could be detected after only 12h of treatment (Figures 7A and 7B). When compared to the A2780 total cell fraction that was also exposed to the same treatment conditions, there was a noticeable distinct degradation product directly below the 28S rRNA band. This can be seen more clearly in the electropherograms present in Figure 7B. Of particular interest, other than this degradation band seen in isolated monosomes, the nuclear fraction displayed a striking amount of degradation after only 12h of DXL treatment, as seen by the clear absence of any noticeable intact 28S and 18S rRNA bands in this fraction. It is likely that the extensive degradation of the nuclear rRNA can be attributed to the fact that the nucleus (more specifically the nucleolus) is an early sensor of chemotherapeutic treatment[125]. It is also possible that there may be more abundant and/or more active RNases in the nuclear fraction upon DXL treatment.

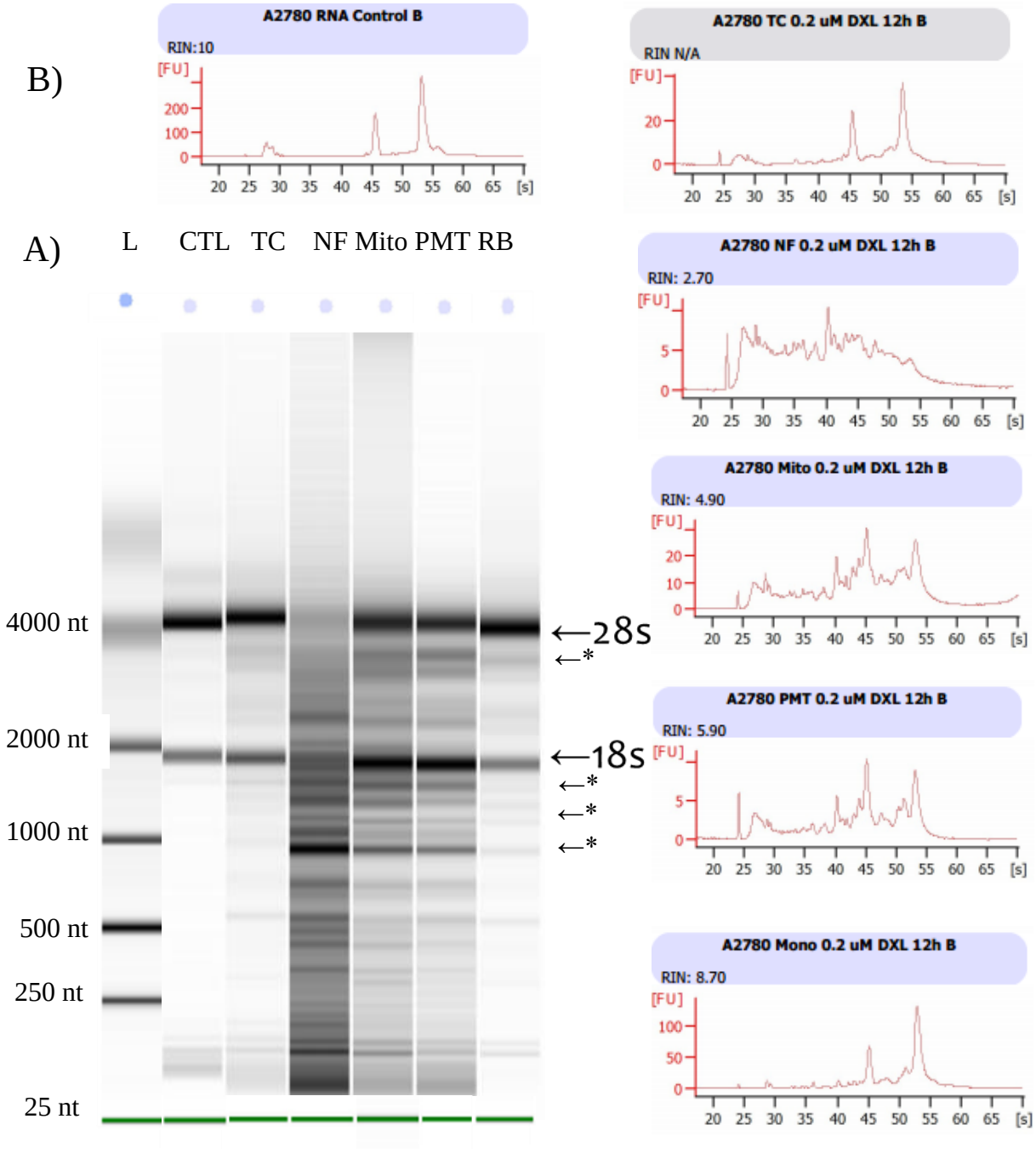

Figure 7 - Capillary gel electrophoresis of RNAs from fractions during the purification of monosomes from cells treated with 0.2 μM docetaxel for 12 h. A2780 cells were grown to confluence and monosomes purified from these cells as described previously, following a 12h

0.2μM DXL treatment. RNA was extracted from various fractions during the purifications of monosomes using Qiagen miRNeasy kits and the component RNAs resolved using capillary gel electrophoresis. The following samples were assessed: CTL (A2780 cell control), TC (12h DXL treated Total Cell Fraction), NF (12h DXL treated Nuclear Fraction), Mito (12h DXL treated mitochondrial fraction), PMT (12h DXL treated Post Mitochondrial Fraction) and 12h-RB (12h DXL treated Ribosomal Fraction). A) Virtual gel B) Corresponding electropherograms. The asterisk denotes rRNA disruption products. The gel image is representative of a three independent experiments.

3.5.2 Effect of 24 hour 0.2 μM DXL exposure on ribosomes and fractions during purification

By 24h of DXL treatment, it became evident that rRNA was cleaved in an orderly fashion, in the monosomal (mon), total cell (TC) and ribosomal (RB) fractions (Figure 8A). In Figure 8B, in the electropherogram of RNA isolated from monosomes taken from A2780 cells treated with 0.2 μM DXL for 24 h, it can be seen that there is 1 strong degradation band below the 28S rRNA, along with several slightly weaker degradation bands below the 18S rRNA. As has been previously reported by Narendrula et al.[126], the total cell fraction also began to show distinct RNA disruption bands after 24h DXL treatment. In agreement with the observation made for cells treated with DXL for 12h, the nuclear fraction (NF) was extensively degraded (Figure 8A and B), even more so than that at the 12h time point; there was only a very weak 28S rRNA band.

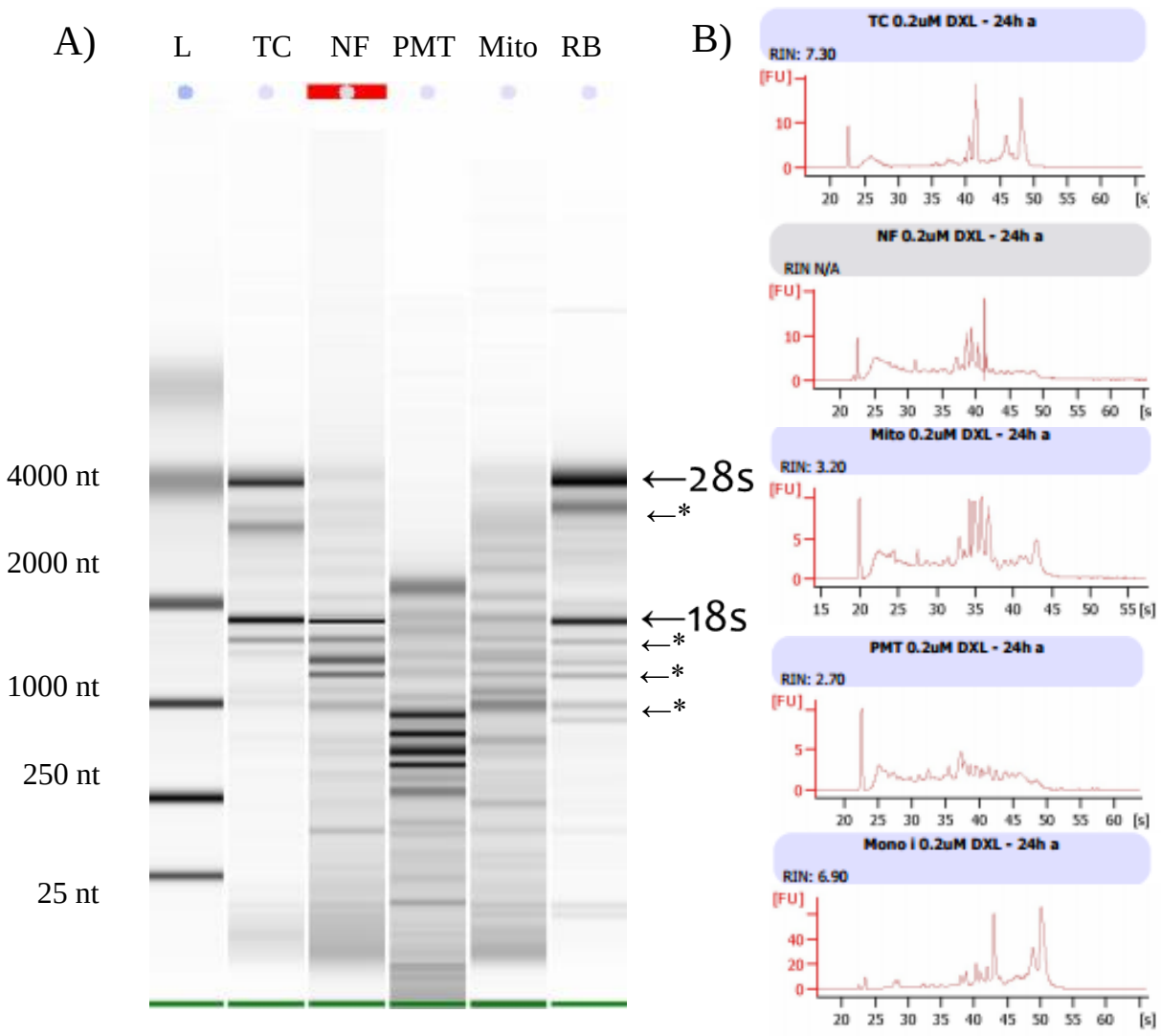

Figure 8 - RNA profiles for fractions taken from A2780 cells after treatment with 0.2µM docetaxel for 24 h. RNA was extracted using Qiagen miRNeasy kits and subsequently assessed by capillary gel electrophoresis on an Agilent 2100 bioanalyzer. The following fractions were assessed: TC (Total Cell Fraction), NF (Nuclear Fraction), Mito (mitochondrial fraction), PMT (Post Mitochondrial Fraction) and 24h-RB (Ribosomal Fraction). A) Virtual gel B) Corresponding electropherograms. Asterisk denotes degradation rRNA disruption products. The gel image is representative of three independently conducted experiments. *Note: the shifted PMT fraction is due to an error in the bioanalyzer software due to the degraded nature of the drug treated sample.

3.5.3 Effect of 48 hour 0.2 µM DXL exposure on ribosomes and fractions during purification

In Figure 9, treatment of A2780 with DXL for 48 h resulted in extensive RNA degradation in all of the fractions examined. Although the total cell extract displayed distinct degradation bands that were greater in intensity that the 28S and 18S rRNAs, the amount of degradation was greater in the purified monosomes. The 48h monosomal fraction also displayed elevated amounts of distinct reproducible rRNA degradation bands. Compared to the results in Figures 7 and 8, the nuclear fraction demonstrated very striking rRNA degradation, including a complete absence of both the 28S and 18S rRNA bands.

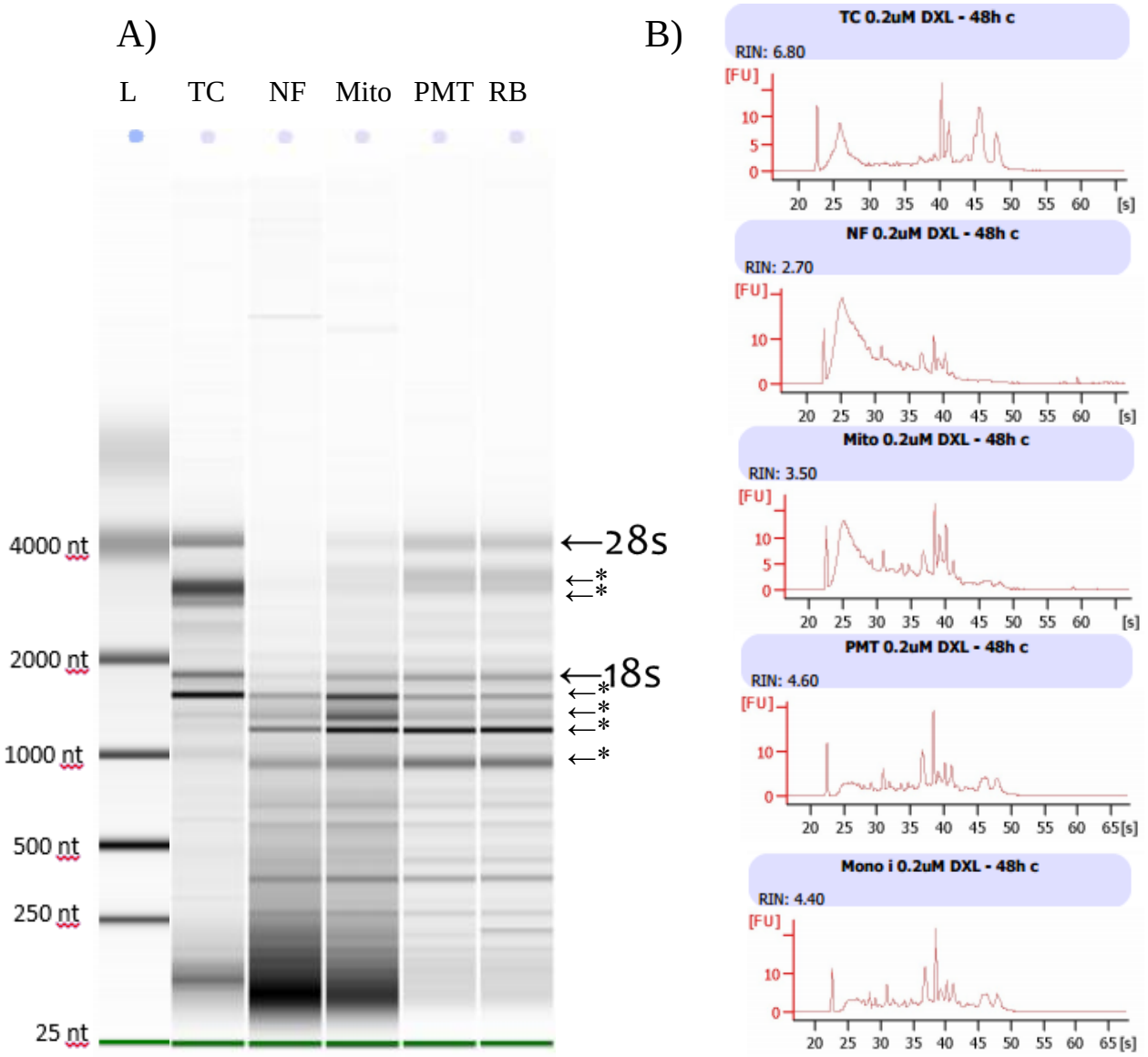

Figure 9 - Capillary gel electrophoresis of RNA isolated from cellular fractions during the isolation of monosomes from A2780 cells following treatment with 0.2 µM docetaxel for 48 h. RNA was then extracted using Qiagen miRNeasy kits and subsequently assessed by capillary gel electrophoresis. The following fractions were assessed: TC (Total Cell Fraction), NF (Nuclear Fraction), Mito (mitochondrial fraction), PMT (Post Mitochondrial Fraction) and 48h-RB (Ribosomal Fraction). A) Virtual gel B) Corresponding electropherograms. Asterisk denotes rRNA disruption products. Images are representative of three independently conducted experiments.

3.6 Effect of DXL treatment on proteins associated with isolated ribosomes over time

Once the effect of DXL treatment on rRNA associated with the cellular fractions involved in monosome or polysome isolation, the effect of DXL treatment on the protein composition of monosomes and polysomes was assessed. Figure 10 displays the protein staining pattern for control (untreated) monosomes and polysomes. The protein staining patterns were very similar, which was expected. After 12 hours of drug exposure, a global drop in the amount of ribosomal protein was observed (noted by the decrease in intensity of staining of proteins in the region of 10-70 kDa), with an increase in higher molecular weight proteins. By 24 and 48 hrs of drug exposure (Figure 10), there was a significant reduction in ribosomal protein content and the results suggest that by 24h of DXL treatment, the majority of ribosomal proteins had been "stripped" off of the rRNA backbone of the ribosomes. However, there was a cluster of higher molecular weight (40-70kDa) ribosomal proteins that appears to linger, even after 24h or 48h of DXL treatment. Although 1 dimensional SDS-PAGE does not allow us to differentiate or identify the proteins present, it provides a good starting point for further experimentation. It also provides evidence to strongly suggest that during DXL treatment of A2780 cells, a decrease in the ribosomal protein component temporally precedes the degradation of rRNA (RNA disruption).

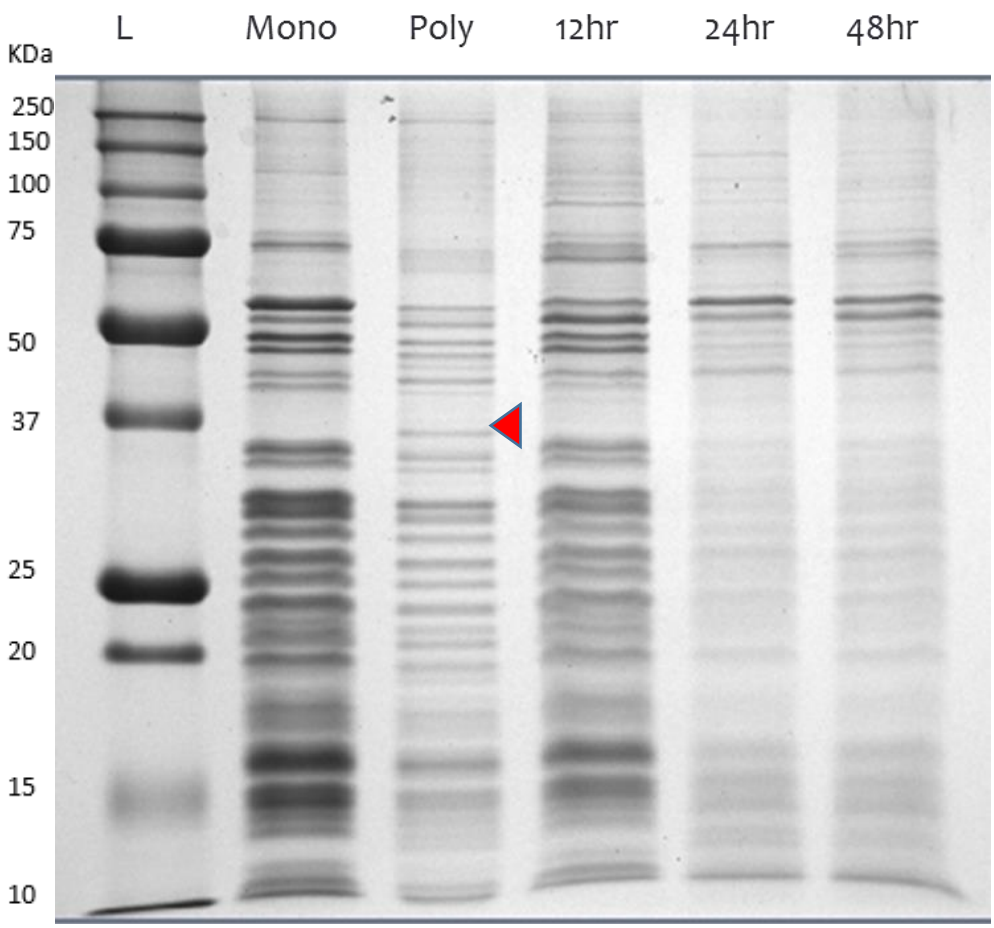

Figure 10 – Effects of DXL treatment of ribosomal protein content. A2780 cells were treated with docetaxel for various time points, after which monosomes were isolated as described above. Proteins from the various cellular fractions during monosome preparation were run on 12.5% acrylamide gels and stained with Coomassie Blue. 10 μg of protein were loaded per lane as determined per BCA assay. Mono (monosomal protein control) , Poly (polysomal protein control), 12h (monosomes isolated after 12h DXL treatment), 24h (monosomes isolated after 24h DXL treatment), 48h (monosomes isolated after 48h DXL treatment). Red arrows denote differences in the polysomal lane. The gel images are representative of three independently conducted experiments.

3.7 2D gel electrophoresis of ribosomal proteins

With the 1D SDS-PAGE of ribosomal proteins from DXL-treated A2780 cells completed, a two dimensional SDS-PAGE (2DGE) would provide the needed resolution to identify which, if any, ribosomal proteins had altered expression with DXL treatment. 2DGE separates proteins in the first dimension on an isoelectric focusing strip that separates proteins based on their isoelectric point (pI), the pH at which the respective protein's charge becomes neutral due to the nature of the R groups of the amino acids. The second dimension involves standard acrylamide gel electrophoresis. In Figure 11, an optimized resolution of ribosomal proteins from control (untreated) A2780 cells is depicted, with a pH gradient from 8.5-11. There are numerous proteins that can be seen, with some of them having good resolution. However, due to difficulties in the basic range of isoelectric focusing strips, the resolution of a large portion of basic proteins in the ribosomal protein preparations was not sufficiently adequate for spot-identification software and subsequent mass spectrometric analysis. As well, discontinuation of the aforementioned strips (pH range above 10) discontinued this avenue of research.

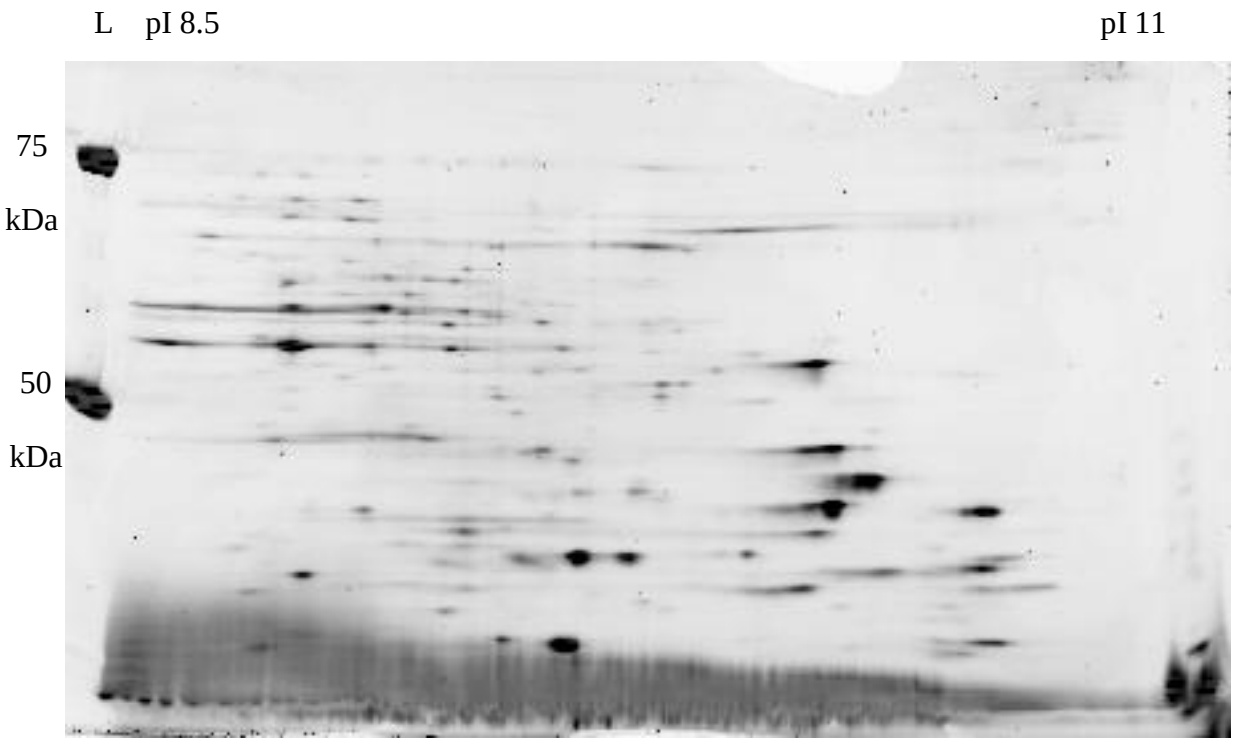

Figure 11 - 2D Gel Electrophoresis of purified ribosomal proteins; a superior resolution is required for mass-spectrometry. A 6-11 GE Healthcare IPG strip with 1% 6-11 GE ampholytes was used. The first dimension was run using de-streak reagent (hydroxyethyl disulfide) and CHAPS as a detergent with a total of 40kvhr focusing time. A paper bridge loading technique was utilized, as described in Materials and Methods. For the second dimension, 8-16% Tris-HCl SDS-PAGE pre-cast gels were used and the IPG strip was run at 200v for 55min. A total of 100µg of ribosomal proteins were loaded. Gels were fixed and stained with flamingo fluorescent protein stain before being imaged.

3.8 2D gel electrophoresis of ribosomal proteins taken from A2780 cells after treatment for 24h with 0.2uM DXL

An attempt was made to resolve by 2DGE ribosomal proteins from A2780 cells before and after DXL treatment for 24h. A 2D gel of ribosomal proteins from untreated and treated A2780 under the most optimal conditions are depicted with Figures 11 and 12, respectively. The findings suggest an overall loss of ribosomal proteins, although there are several proteins around 50 kDa that seem to remain. This supports the results seen in Figure 10, although resolution is not sufficient for conclusions to be drawn by mass-spectrometry.

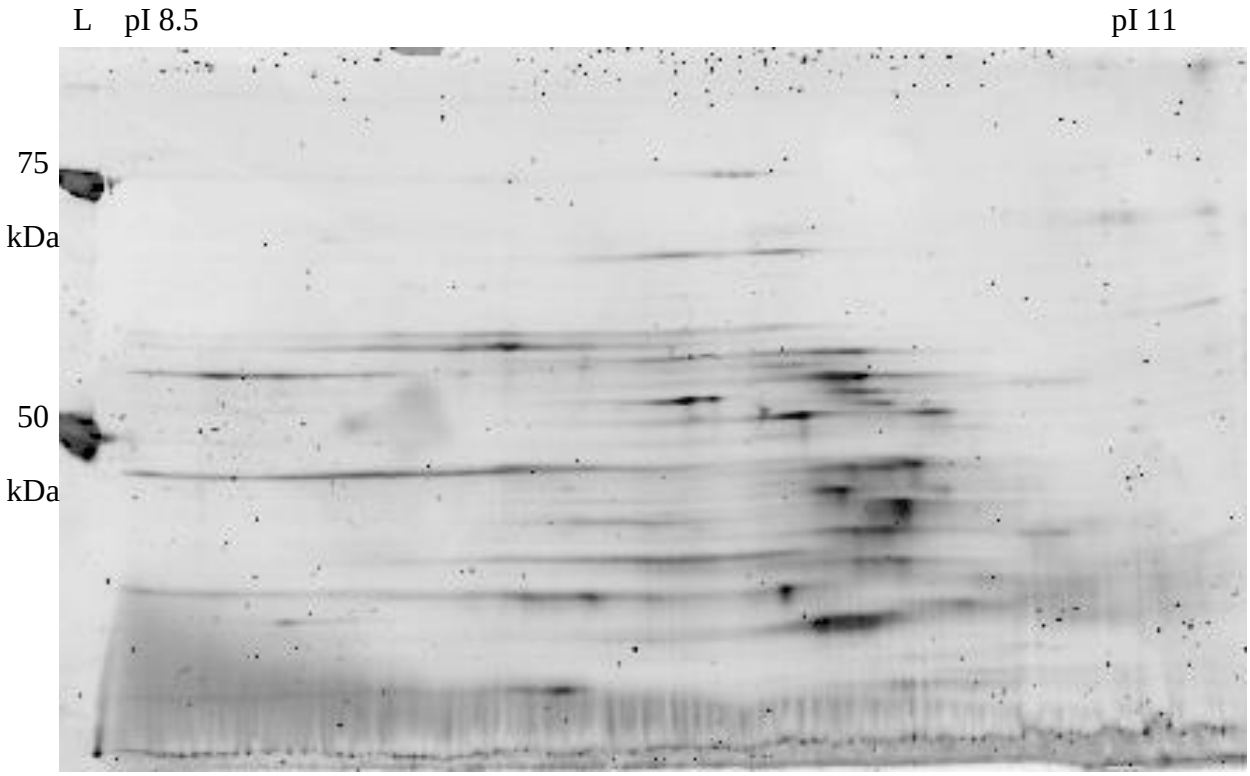

Figure 12 - 2D Gel Electrophoresis of purified ribosomal proteins from A2780 cells after treatment with 0.2µM docetaxel for 24h. 6-11 GE Healthcare IPG strips with 1% 6-11 GE ampholytes were used. The first dimension was run using de-streak reagent (hydroxyethyl disulfide) and CHAPS as a detergent, with a total of 40 kVh focusing time. A paper bridge loading technique was utilized, as described in Materials and Methods. For the second dimension, 8-16% Tris-HCl SDS-PAGE pre-cast gels were used and the IPG strip was run at 200v for 55min. A total of 100µg of ribosomal proteins were loaded. Gels were fixed and stained with flamingo fluorescent protein stain before being imaged.

3.9 The effect of DXL treatment on expression levels of select ribosomal proteins in A2780 cells

The lack of consistent, high resolution of ribosomal proteins by 2D gel electrophoresis required the use of immunoblotting experiments with antibodies for specific high molecular weight ribosomal proteins as the means to evaluate changes in ribosomal protein content upon DXL treatment. Figure 13A demonstrates changes in the amount of RPL4, RPSA, RPL3 and RPL7a in cellular fractions of A2780 cells upon treatment with DXL for 24h. Our findings suggested that there were treatment-induced changes in the expression of some of these proteins. It was further noted that RPL3 separates into 2 distinguishable isoforms during the glacial acetic acid purification step (see section 2.4 for reference). Figure 13B is a bar graph of the expression ratio for various ribosomal proteins between treated to untreated A2780 cells. Because different subcellular organelle fractions were analyzed, the bands could not be normalized to a standard housekeeping gene (GAPH, Actin, etc.). Instead, a ratio of the ribosomal proteins was generated by comparing the densitometry values of a specific ribosomal protein in the ribosomal fraction versus the total cell fraction, which was then compared between the untreated control and 24h DXL treated sample to determine if a significant fold change was observed. This allows us to analyze how specific ribosomal proteins in the isolated ribosomal fraction change in response to DXL treatment. RPL3 showed a significantly reduced expression upon treatment compared to the untreated sample, while RPL7a exhibited a significant increase in expression levels. The expression of RPL4 and RPSA did not appear to change significantly in response to DXL treatment.

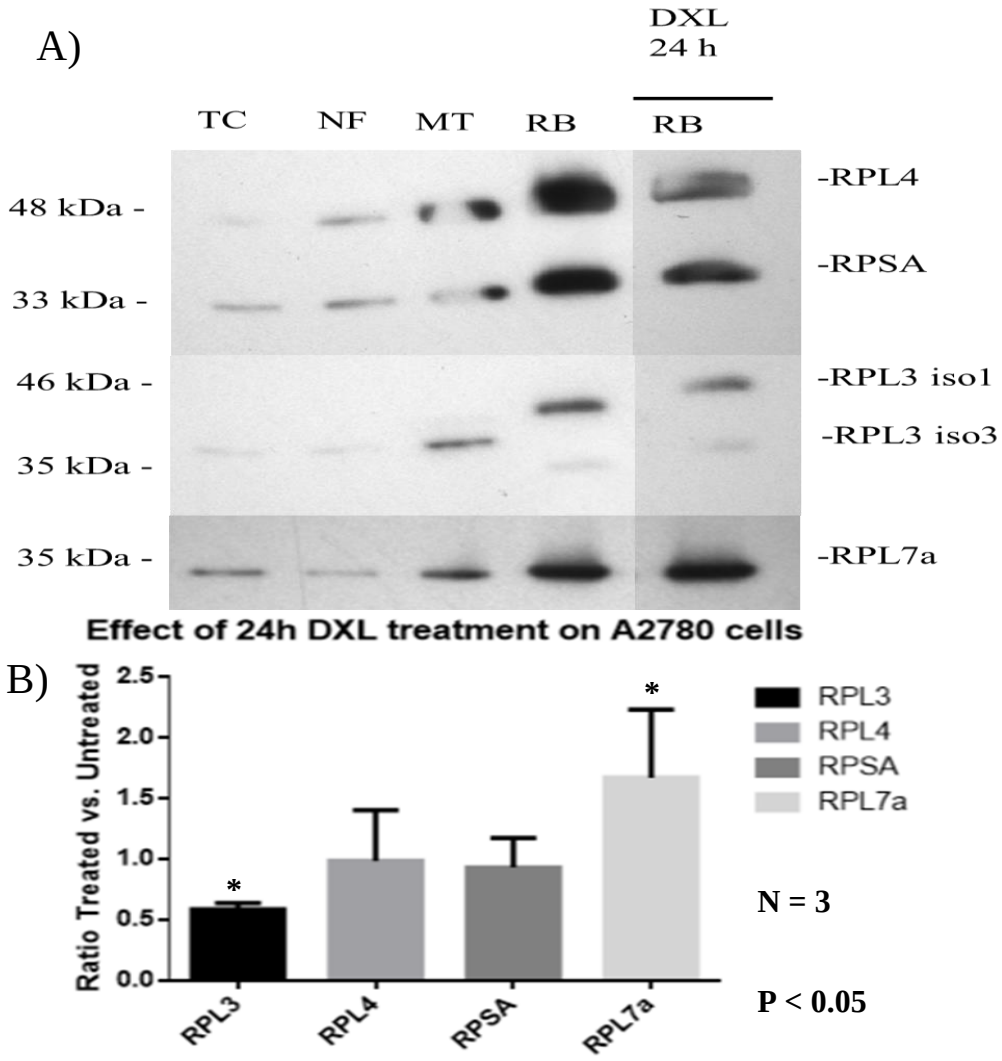

Figure 13 – A) Immunoblots documenting the effect of DXL expression on levels of various proteins in cellular fractions obtained upon isolation of ribosomes from A2780 cells. RPL4, RPL3 iso1, RPL3 iso3, and RPL7a are proteins from the larger 60S ribosomal subunit and RPSA is a protein from the smaller 40S ribosomal subunit. These are representative of some the highest molecular weight ribosomal proteins and show changes in relative expression after drug treatment (TC-total cell, NF-nuclear fraction, MT-mitochondrial, RB-ribosomal) B) Densitometry values for the ribosomal proteins were plotted using GraphPad Prism and differences with a $p < 0.05$ were considered statistically significant (*indicated by an asterisk) using a two-tailed t-test.

3.10 The effect of DXL treatment on the levels of select ribosomal proteins in ribosome preparations from the A2780DXL cell line

To investigate if DXL affected ribosomal protein composition in A2780 cells that had been selected for DXL resistance, A2780DXL cells were treated with 0.2uM DXL for 24 hours, in the same fashion as A2780 cells depicted in Figure 13. The immunoblot results of RPL3, RPSA, RPL7a and RPL4 for this experiment are shown in Figure 14A. As mentioned, different subcellular organelle fractions were analyzed, which meant that the bands could not be normalized to a standard housekeeping gene (GAPH, Actin, etc.). Instead, a ratio of the ribosomal proteins was generated by comparing the densitometry values of a specific ribosomal protein in the ribosomal fraction versus the total cell fraction, which was then compared between the untreated control and 24h DXL treated sample to determine if a significant fold change was observed. This allows us to analyze how specific ribosomal proteins in the isolated ribosomal fraction change in response to DXL treatment. There were no apparent differences in the level of these proteins between DXL-treated and untreated A2780DXL cells. Interestingly, the immunoblot for RPL3 did not produce two distinct isoforms as was observed in Figure 13.

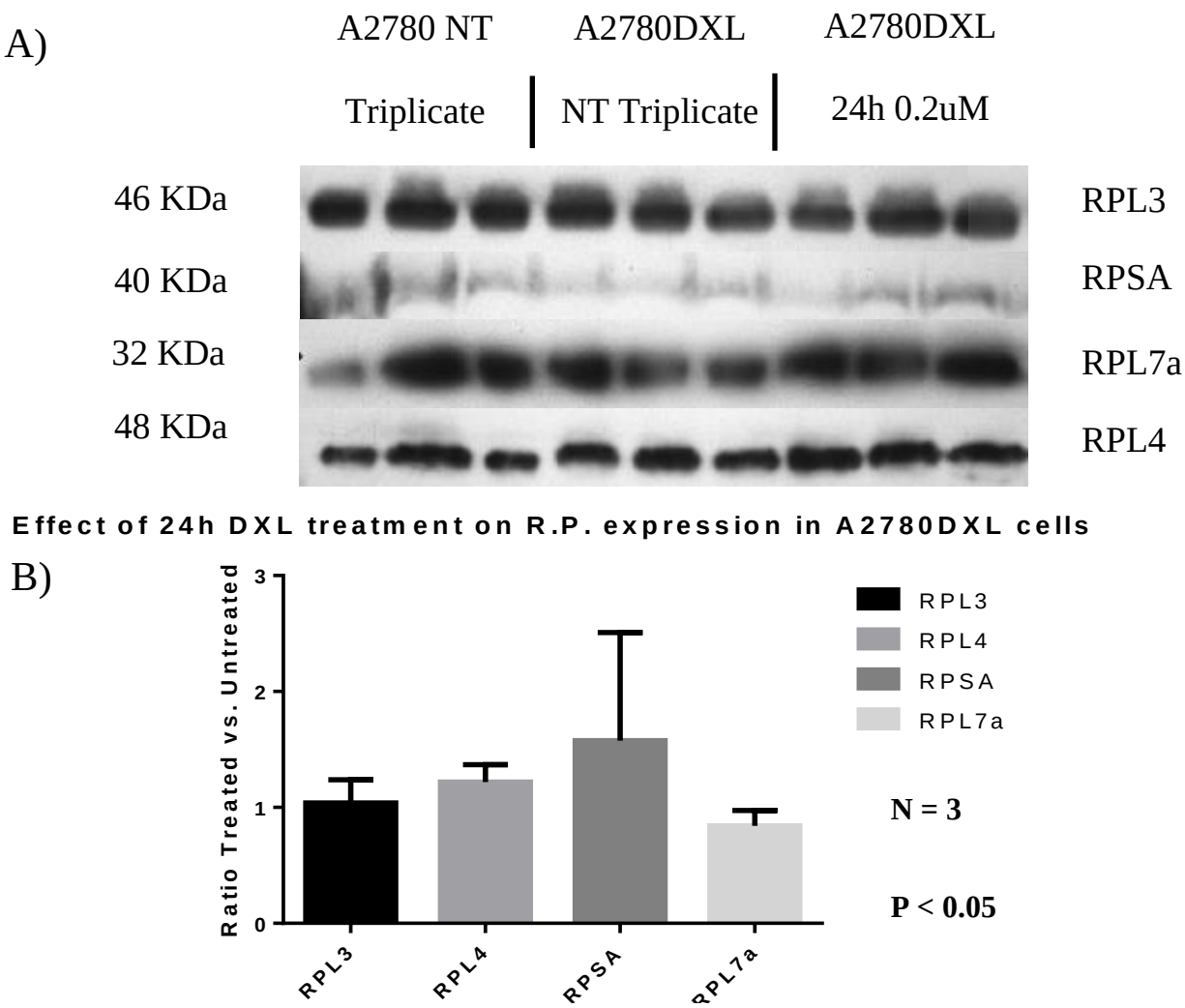

Figure 14 – A) Immunoblots of ribosomal proteins in ribosomal fractions of: untreated A2780 cells, untreated A2780DXL cells and A2780DXLcells after treatment with 0.2 µM DXL for 24 h. RPL4, RPL3 iso1, RPL3 iso3, and RPL7a are proteins from the larger 60S ribosomal subunit and RPSA is a protein from the smaller 40S ribosomal subunit. These are representative of some of the highest molecular weight ribosomal proteins and show few changes in relative protein levels after drug treatment. B) Densitometry values of the ribosomal proteins were plotted using GraphPad Prism and differences with $p < 0.05$ were considered statistically significant using a two-tailed t-test.

4.0 Discussion

The NCIC-CTG-MA.22 clinical trial assessed tumours of patients pre-, mid-, and post treatment in order to identify potential biomarkers of response to chemotherapy[151]. Since only a very small percentage of patients with the most abundant subtype of breast cancer (ER+/Her2- tumours) receive a survival benefit from chemotherapy [169], there is an urgent, unmet need for a robust biomarker of response to chemotherapy. This need is particularly urgent, because the vast majority of patients receive significant short and long-term toxicities from treatment, including cardiotoxicity, thromboemboli, neuropathies, neutropenia, fatigue, and secondary neoplasms[169]. Thus, a robust chemoresponse biomarker could possibly enable physicians to identify non-responders early in treatment, in order to avoid these toxicities and move patients to other downstream treatments.

Although earlier studies had shown that chemotherapy agents interfered with ribosome biogenesis[125], the clinical trial reported by Parissenti et al., was the first study to show that treatment with cytotoxic chemotherapy agents such as epirubicin and DXL can induce RNA degradation in patient tumors. It has been recently shown by Narendrula et al.[126] that several ovarian and breast cancer cell lines (A2780, CAOV-3, MCF-7, SKBR-3, MDA-MB-231) reproducibly demonstrate significant RNA disruption following the application of a variety of chemotherapy agents with contrasting mechanisms (DXL, paclitaxel, carboplatin, cisplatin, vincristine, irinotecan and etoposide). As was previously stated, DXL was shown to be one of the most reproducible and robust agents to induce rRNA degradation in this study[126]. This suggests that many chemotherapy agents, despite their distinct mechanisms, ultimately promote the degradation of rRNA. If so, then this could reliably be used as a measure of response to chemotherapy in cancer cells.

However, the mechanism(s) by which these chemotherapy agents induce RNA disruption *in vitro* and *in vivo* is unknown. We thus decided to investigate how chemotherapy treatment affects ribosome composition, including ribosomal protein content. We hoped that this would provide beneficial and new insight into the process and mechanisms of chemotherapy-induced RNA disruption. The study of ribosomal proteins following chemotherapy treatment required the purification of intact ribosomes from the cytoplasm of tumour cells. This would also allow us to monitor the integrity of RNA in ribosomes only, along with the associated ribosomal proteins.

Consequently, the objectives of this study were to: a) assess the feasibility of purifying ribosomes from control and chemotherapy treated A2780 ovarian cancer cells; b) identify differences in the composition of purified ribosomes between control and chemotherapy-treated cells (rRNA and protein); c) to determine whether any protein composition changes that are present in the drug-sensitive A2780 cells would be absent in the DXL resistant A2780DXL cell line; d) to assess whether ribosomal proteins are lost from ribosomes prior to rRNA degradation (RNA disruption); and e) to determine whether rRNA degradation (RNA disruption) is lower in assembled ribosomes than in nuclei containing fresh rRNA transcripts that have not yet been assembled into ribosomes

4.1 Evaluation of the purification of ribosomes from A2780 cells using differential centrifugation: 1D SDS PAGE and immunoblotting of organelle markers

In order to evaluate the effectiveness of the differential centrifugation protocol employed to purify intact translating ribosomes from the cytoplasm of A2780 ovarian cancer cells, 1D acrylamide gel was used to monitor the expression of proteins in the fractions obtained during

ribosome purification. The expression of the resolved proteins on the acrylamide gel was assessed by staining with Coomassie blue[161]. Figure 2 demonstrates the typical protein profiles that were obtained during the purification of ribosomes. Fractions included a total cell extract, the nuclear fraction, the post mitochondrial fraction and the ribosome fraction, respectively. It is important to remember that although this protocol does create a nuclear and mitochondrial fraction, these fractions are not free of other contaminating organelles. The goal of the process was to isolate ribosomes devoid of contaminating organelles.

The gel in Figure 2, shows that there was a clear enrichment of proteins in the 10-70 kDa when going from left to right. The total cell extract, nuclear fraction and post mitochondrial fraction contain many different proteins of vastly different molecular sizes. However, the ribosomal fraction of protein contains a reduced number of protein bands that increase in intensity in the 10-70 kDa range[161]. The banding pattern in the 10-70 kDa range is indicative of a clear enrichment of ribosomal proteins. Although previous studies have used this as an endpoint to determine purity of their ribosomal samples, we determined it was necessary to evaluate the purity of the ribosomal sample using markers for contamination by subcellular fractions other than the ribosome.

4.2 Changes in ribosome protein content in response to DXL

Ribosomal proteins are not simply participants in the function of protein synthesis, several ribosomal proteins have 'second lives', displaying extra-ribosomal functions that are not dependent on the ribosome[170]. This tendency of ribosomal proteins to have other functions, can be explained by theories postulating the pre-existence of the ribosomal proteins as independent

molecules before forming the various sub-units of the ribosome[171]. These proteins are also known to affect development, apoptosis and aging when their expression levels have been altered[156]. Specifically, it is known that ribosomal protein S3a (RPS3a) plays important roles in cell transformation and death. Constitutively or transiently enhanced RPS3a expression can be regarded as 'priming' a cell for apoptosis[172]. Therefore, monitoring changes in ribosomal protein expression following chemotherapeutic treatment is of interest to investigate the mechanism of cell death and ribosomal disruption.

Figure 10 displays the effect of DXL treatment over time on the protein composition of ribosomes in A2780 cells. At 12h of treatment, there was a relative reduction in the ribosomal protein content (10-70 kDa) compared to the untreated ribosome fraction and there appeared to be some changes in the expression of higher molecular weight proteins. By 24h, the bulk of the effect of DXL on ribosomal protein content appeared to take effect. There was a cluster of ribosomal proteins around 30-50 kDa that appeared to retain their expression, even with prolonged treatment (up to 48h). It is possible that the retention of these proteins in the ribosome structure following drug treatment may provide some mechanistic or functional link to drug related cellular effects. However it is also just as likely that the increased amount of positive charges in the longer polypeptide chains allows for them to be retained to a greater extent by the negative backbone of rRNA.

The altered ribosomal protein content could very well have a direct effect on a cancer cell's translatome (translated array of proteins by the ribosomes present in a cell); although speculative, blocked translational capacity could be a part of the cell death mechanism. Iwawaki et al. have shown a direct connection between ER stress, the cessation of translational capacity and the induction of rRNA degradation by IRE1[140]. The evidence in this study suggests that ER

transmembrane kinase/ribonuclease IRE1beta induces translational repression through 28S rRNA cleavage in response to an ER stress response. If the stress persists, there may be sufficient degradation of rRNAs to render cells non-viable. It is possible that a similar process may be occurring here, explaining the RNA disruption observed.

Some may argue, however, that as the catalytic peptidyl transferase function is located within the 28s rRNA, that this would not affect the 'translatome', because ribosomes are just blind protein producing machines. Refuting this argument is the fact that RPs are extremely basic. The inherent capability of the extremely basic ribosomal proteins (pIs typically above a pH of 9 or 10)[165] is to bind RNA molecules, such that they play a major role in ribosome structure. The primary function of RPs, if not to participate directly in translation, is to modulate the affinity of the rRNA for an mRNA substrate or to aid in the discrete folding of the rRNA in the ribosome to achieve a certain 3D catalytic structure to achieve catalytic activity [173]. It can therefore be argued that differential expression of RPs can alter the translatome by altering the fine structure of the ribosome; the same can be said for rRNA modifications. It is also important to note that the loss of certain ribosomal proteins would likely expose certain sites in the rRNA to cleavage by endogenous RNases, including IRE1 and RNase L as previously mentioned. This would explain the RNA disruption observed.

4.3 rRNA content of A2780 Ribosomes

Figure 5 displays the capillary gel electrophoresis results for cellular fractions during the purification of ribosomes from untreated A2780 cells. All fractions displayed strong, intact 28S and 18S rRNAs. Interestingly, what was not expected is that the purified ribosomal fraction

(even when DEPC treated solutions and RNAse inhibitors were used) contained reproducible 'turnover bands' in the electropherograms. These rRNA bands most likely had once been part of a functioning ribosome or are in the process of being degraded in a mature ribosome. This can most likely be attributed to regular cellular turnover of ribosomes, as they are highly monitored within the cell even during regular growth[167]. Although these turnover products may seem to confuse detection of chemotherapy –induced degradation, they are not very intense and do not affect the interpretation of the effects of drug treatment as treatment bands are of a distinctly different molecular size and intensity.

As shown in Figure 6, we observed that purified polysomes demonstrated much fewer rRNA turnover products than purified monosomes. However, as it had already been determined that the polysome purification (changes in KCl concentration) allowed for a higher amount of contamination by other organelle fractions, the monosomal extracts were used for further experiments during drug treatment.

4.4 Changes in rRNA integrity in response to DXL

While DXL-induced degradation of rRNA has previously been observed by our research group in A2780 cells, it was unclear whether these rRNA degradation bands stemmed from a cytoplasmic population of mature ribosomes or from freshly synthesized ribosomes, rRNA and/or rRNA pre-cursors in the nucleus. To address this question, the integrity of the rRNA present in various cellular fractions during monosome purification was assessed using the Agilent 2100 bioanalyzer. This was achieved by differential centrifugation; ensuring that only the high molecular weight ribosomes were pelleted followed by preparation of RNA from

monosomes. Figure 7 displays the effect of a 12 hour 0.2 µM DXL treatment on the integrity of rRNA in cellular fractions obtained during the purification of monosomes. The nuclear fraction demonstrated significantly aberrant rRNA profiles compared to the untreated control. There were degradation bands present in the mitochondrial and post mitochondrial fractions as well, with a variety of other RNA bands not usually seen in the total cell extracts. These additional RNA species most likely arise from the enrichment of various rRNA fragments not readily apparent in the total cellular RNA preparation. Although these fractions have been included to monitor the ribosome purification process, no conclusions could be drawn from them because these fractions still contained a mixture of cellular organelles. The purified monosomes displayed discrete bands appearing below the 28S and 18S rRNAs. Although not as intense as the parental rRNA bands, the degradation bands were noticeable in monosomal RNA preparations after 12 hours of drug exposure. This was particularly noticeable in the electropherogram of Figure 7B, a phenomenon not readily observable in total cell extracts. By 24h of treatment, there were significant disruption bands present in the ribosomal fraction, and by 48h of DXL treatment, the intact rRNA bands were almost completely absent (Figure 9). Several attempts at purifying ribosomes from 72h treated cells were made, but the ribosome degradation was so severe that no intact ribosomes could be pelleted upon centrifugation. However, it is noteworthy that in comparison to total cell extracts, the disruption products from purified ribosomes: a) can be detected earlier than in total cell extracts (as early as 12 hours); and b) are representative of translating cytoplasmic ribosomal particles and therefore cannot be detected post 48h of treatment (greater sensitivity).

Other than the ribosomal fraction undergoing degradation, it is quite important to note that the rRNA fraction extracted from the pelleted nuclei of DXL-treated A2780 cells underwent extensive degradation. The degradation of the nuclear fraction of rRNA was very extensive even

after only 12 hours of DXL treatment (Figure 7). By 24h and especially at 48h of DXL treatment, there was no recognizable 28S or 18S in the isolated RNA from the nuclear fraction, in Figures 8 and 9 respectively. This quick degradation of rRNA after drug exposure can be interpreted as the nuclear, and most likely the nucleolar, fractions undergoing extensive degradation/regulation to prevent the further production of ribosomes. Before large disruption bands appear in the cytoplasmic (monosomal) fraction of ribosomes, the nascent ribosomes (rRNA and pre-rRNA) in the nucleus are extensively degraded after 12h of drug exposure. This is added evidence to suggest effective chemotherapeutic treatment of cancer cells targets the ribosomes as part of, or as a by-product of the mechanism of cell death[125]. Further research needs to be conducted in evaluating how chemotherapy agents may interfere with ribosome biogenesis and structure. This avenue shows much promise for advances in treatment, patient care and potential cures for specific cancers.

The most likely candidate to explain the loss of 28S and 18S rRNA and the presence of specific rRNA cleavage products is an endogenous RNase. As mentioned, RNAse L and IRE1 form likely candidates as they have already been implicated with degradation of the 28S rRNA following situations of cell stress (IRE1 is activated in situations of ER stress while RNase L is activated in a situation of viral infection or detection of dsRNA). Although no mechanism has been delineated, we propose that the treatment of cancer cells with chemotherapeutic agents elicits similar or identical responses of cell stress (ER stress, nuclear stress, production of foreign dsRNA molecules) that activate stress induced RNases, allowing to cleave unprotected regions of rRNA.

4.5 2DGE: evaluating the effect of DXL treatment on ribosome protein content

In order to evaluate the changes in expression of a relatively large and complex set of proteins, two dimensional gel electrophoresis is an unrivaled molecular biology technique to accomplish this task. Mammalian ribosomal proteins have an average molecular weight of 18,500 Da (the range is 47,280 for L4 to 3,454 for L41). They have an average of 164 amino acids (the range is 421 to 25) [165]. The proteins are very basic; they have an average pI of 11.05 (the range for pI is 4.07 to 13.46) and contain 22% arginine and lysine amino acid residues[165]. The proteins are likely to contain a number of clusters of basic residues. Unfortunately, these characteristics of ribosomal proteins make them some of the most difficult to analyze by commercially available 2D electrophoresis systems using strip gels or IPG (immobilized pH gradients) for the 1st dimension (isoelectric focusing). The pH gradients of IPGs are generated by means of buffers that are covalently bound into porous, polyacrylamide gels[174]. While 2-D PAGE is an ideal tool for discovery-phase research, not all expressed proteins can be displayed in a single gel. Low-abundance proteins, very large and very small proteins, basic, acidic proteins, and hydrophobic proteins present their own special challenges for 2-D PAGE. Of noted difficulty, IPGs for very basic proteins, with pIs in the pH 8-11 range, may require matrices other than polyacrylamide[175]. For reasons that are not clear, proteins with pIs greater than about pH 10.5 are extremely difficult to focus in IPGs[174].

Figures 11 and 12 display the results of optimized 2D gels for proteins extracted from ribosomes isolated from untreated and DXL-treatedA2780 cells, respectively. Although a clear reduction in ribosome protein content was observed upon DXL treatment, the resolution of the 2D gels was not sufficient enough to allow for mass spectrometric analysis. A year was devoted to optimizing 2D gels for mass spectrometric analysis. The addition of several agents, utilization

of several sets of detergents, reducing agents, IPG strips, loading techniques, voltage times and intensities, etc. were explored. However, the difficulties in resolving strongly basic proteins in 2D gels, along with the discontinuation of certain IPG products, lead to inconsistent quality of gels, prompting us to abandon the 2DGE approach for evaluating the effects of DXL treatment on ribosome protein content. The 2DGE results presented in Figures 11 and 12 cannot identify changes in the levels of specific ribosomal proteins in response to DXL treatment. But, they did document a large drop in the levels of specific ribosomal proteins, while other proteins exhibited increased or little change expression with DXL treatment. This interesting finding corroborates the 1D gel results obtained in Figure 10, and warranted subsequent western blotting experiments to identify which specific ribosomal proteins were increased/decreased.

4.6 Altered composition of high molecular weight ribosomal proteins in response to DXL treatment

A subset of 4 high molecular weight proteins stemming from both the large and the small subunit of the ribosome (RPL3, RPL4, RPL7a and RPSA) were queried for possible changes in their levels following DXL treatment. These proteins were chosen as their molecular weights matched a series of ribosomal proteins that seemed to have and increased/altered levels. In Figure 13B, it is evident that RPL3 showed significantly lower levels in ribosomes isolated for DXL-treated cells compared to the untreated cells, while RPL7a exhibited increased levels. Although there were some changes in RPL7a and RPL3 levels, the ratios of RPL4 and RPSA seem to remain unchanged. This tells us that there is an altered levels of ribosomal proteins following DXL treatment. As discussed in section 4.2 of the discussion, it is possible that these

changes in ribosomal protein content are part of a cell death mechanism that changes the translatome of cancer cells, promoting apoptotic death[156].

It is interesting that, of the ribosomal proteins investigated, RPL7a was found to be the only protein to increase in content after DXL treatment. Previously, changes in RPL7 expression have been linked to changes in the cell cycle and progression to cell death[154]. RPL7 was found to contain a basic region leucine zipper (BZIP), characteristic of eukaryotic transcription factors, which can bind to and interact with cognate sites on mRNA to inhibit cell free translation of distinct mRNAs[176]. Corroborative with previously discussed implication with ribosomal proteins and apoptosis, constitutive expression of human ribosomal protein L7 arrests the cell cycle in G1 and induces apoptosis in Jurkat T-lymphoma cells[154]. Based on this observation in Jurkat cells, it is possible that the increase in RPL7a could be a contributing factor to cell death in A2780 cells following DXL treatment. Further studies would need to be conducted to explore this potential link.

At this time it is unknown what causes the change in RP levels, as a number of causes could provide a valid explanation: selective degradation, loss from the rRNA backbone of the ribosome or even cleavage. Because there was a removal/degradation/loss of ribosomal proteins from the intact cytoplasmic ribosomes following 24 hour DXL treatment in A2780 cells, it is possible that the loss of specific ribosomal proteins could allow or facilitate subsequent selective cleavage of the underlying rRNA sequences (as presented in Figures 7-9). At this time it is difficult to delineate a definite mechanism, or point to specific ribosomal proteins that may be involved. Wen et al. have shown that eIF3f promotes rRNA degradation through direct interaction with heterogeneous nuclear ribonucleoprotein (hnRNP) K. Specifically, hnRNP K is required for maintaining rRNA stability: under stress conditions, eIF3f dissociates hnRNP K

from rRNA, thereby preventing it from protecting rRNA from degradation[177]. It is very likely that that the ribosomal proteins protect the RNA in a similar fashion from RNase cleavage.

We have previously shown that the rRNA of cancer cells was selectively cleaved following chemotherapeutic treatment. The results in figure 13 are the first to demonstrate that the ribosomal proteins of A2780 ovarian cancer cells also undergo a process of degradation. When both of these results are taken into consideration, the hypothesis that ribosomes are a target and/or sensor of chemotherapeutic treatment appears compelling. Results of 1D gels of ribosomal proteins following treatment (see Figure 10) also tend to suggest that the loss of the protein fraction of ribosomes tend to occur at an earlier rate that that of the rRNA. By 12h, very noticeable changes with ribosomal protein can be noted in Figure 10; the same of which cannot be stated for the rRNA at this time. Our data and the above findings thus suggest that RP loss precedes and facilitates RNA disruption

rRNA and the disruption products produced following chemotherapy treatment are currently being evaluated as a biomarker to monitor the efficacy and predict outcome of the chemotherapeutic regimen being utilized, as mentioned in the introduction section. A company formed to develop RNA disruption as a biomarker of response to chemotherapy, RNA Diagnostics, Inc., and they have developed a proprietary algorithm based diagnostic tool termed RDA (RNA Disruption Assay), which is a diagnostic test measuring breast tumor response early in chemotherapy treatment[152]. It does so by analyzing the extent of rRNA disruption in patient samples. As the research above demonstrates, there is also the possibility that ribosomal proteins and their expression/presence within translating ribosomes following chemotherapeutic treatment could be used to monitor treatment efficacy of screen for new agents. Human ribosomal proteins and their expression and regulation within human tissues are relatively newly studied subjects

(especially when it comes to their relation with cancer). There is a lack of research in the field of ribosomal proteins and the implication of ribosomes and cancer; and especially how this plays a role in the treatment of cancer.

5.0 Summary and Future Perspectives

Although it was known from previous studies in our laboratory that chemotherapeutic treatment of cancer cells *in vitro* caused cleavage of the 28S and 18S rRNAs[126], it was not known whether this occurred in the translating population of cytoplasmic ribosomes and if similar changes also occurred in the composition of translating ribosomes, including levels of RPs. We have used a highly efficient protocol for the purification of intact ribosomes (monosomes), devoid of contamination, as assessed by one dimensional gel electrophoresis, with subsequent western blotting for assessment of expression for proteins associated with other cellular organelles. RNA and protein preparations from the purified ribosomes were then obtained for further analysis.

We were able to demonstrate that for DXL-treated ovarian tumour cells, the creation of cellular fractions for ribosome purification appeared to allow for more sensitive detection of rRNA disruption by capillary electrophoresis than a total cellular RNA preparation. Following DXL treatment, the rRNA within cytoplasmic ribosomes underwent significant degradation in cytoplasmic ribosomes - first noticeable after 12h, but with even greater degradation as time progressed to 24 and 48 hours. Interestingly, by 72h of DXL treatment, there were no intact ribosomes remaining in the cytosol of A2780 cells. Of particular interest was the nuclear fraction of rRNA, which reproducibly showed extensive degradation after only 12 hours of DXL exposure. This was interpreted as the rRNA primary transcript and nascent rRNA molecules (yet to be incorporated into mature ribosomes with their associated proteins) undergoing extensive degradation by RNAses following drug exposure.

The number and amount of ribosomal proteins from purified ribosomes, as assessed by 1DGE, decreased after DXL treatment, as early as 12h. By 24h, there was a greater drop in the

total ribosomal protein content of purified ribosomes. In contrast, there appeared to be elevated levels of other ribosomal protein, the majority of which had higher molecular weights in comparison to the average ribosomal protein. It is difficult to say if the retention of these basic proteins was due to their inherent longer length and the resulting increased points of contact with the acidic rRNA, or due to other reasons. Further experimentation would need to be conducted to determine how the loss of some ribosomal proteins could allow for the cleavage of the underlying rRNA sequences by endogenous RNases, which would explain the rRNA cleavage patterns observed.

2D gels of human ribosomal proteins using IPG strips are not advised as means of evaluating differences in ribosome content between control and chemotherapy-treated tumour cells, as the inherent basic nature of human ribosomal proteins (average pI of 11) causes much difficulty in the isoelectric focusing of the proteins. With an insufficient resolution in the 1st dimension, mass spectrometric analysis becomes impossible due to streaky and unresolved gels in the 2D gel. Although it is possible to use this technique to achieve greater resolution of ribosomal proteins, these technical issues provide no advantage over classical 1D SDS-PAGE

The levels of certain proteins in isolated ribosomes were assessed by western blotting using untreated and DXL-treated A2780 cells. Of particular interest was RPL7a. While RPL7a was shown to increase in relative quantity, some ribosomal proteins had the same relative expression to the untreated control and RPS3 decreased significantly. It is possible that these changes in ribosomal protein (e.g. RPL7a) could initiate apoptotic cell death, or that these decreases in ribosomal protein e.g. (RPS3) could allow for subsequent accessibility of RNases to the rRNA structure, producing the rRNA disruption bands observed following chemotherapeutic treatment.

There is an absence of changes in ribosomal protein content following treatment of the resistant cell line with DXL. This can be correlated with an absence of DXL-induced RNA disruption in these cells, as reported previously[126]. This strengthens the utility of RNA disruption as a chemoresponse biomarker. The rRNA degradation products following chemotherapeutic treatment are already being evaluated as a biomarker for positive response to treatment as reviewed in Section 1.5.2. It may be possible to also detect changes in ribosomal protein content in samples, as a measure of response to chemotherapy treatment. If an alteration in ribosome structure (rRNA + protein) is a consequence of cellular exposure to many structurally distinct chemotherapy drugs, then it would be extremely beneficial to use agents that demonstrate a higher selectivity for cancer cell ribosomes, potentially avoiding unwanted side effects and improving patient care. This would also strengthen the argument to monitor ribosome decay products as a screen for new potent anti-cancer agents, as there has not been a leap in cancer drug discovery in recent years. RNA disruption, as assessed by RDI^{TM} would prove a great means of screening chemotherapeutic agents for potential ribosome decay products. Screening for changes in ribosomal protein content would also be possible (and made easier if a specific ribosomal protein was a known target) by using mass spectrometric analysis of ribosomal protein extracts. Furthermore, by altering the levels of ribosomal proteins or targeting the ribosome structure directly, it may be possible to more effectively target cancer cells directly, although to our knowledge this has yet to be done. Just as disruption of ribosome biogenesis with an inhibitor of RNA polymerase I transcription, CX-5461, has shown unexpected, potent, and selective effects in killing tumor cells via disruption of nucleolar function[91], it may be possible to disrupt the function of mature ribosomes in the cytosol via other agents in order to render tumour cells non-viable.

Although the research herein demonstrates the potential connection between successful chemotherapy treatment and alterations in ribosome content, further research needs to be conducted to solidify these findings. Specifically, further investigation into the specific sites of rRNA cleaved and the mechanism leading to RNA disruption in cancer cells following chemotherapeutic treatment will provide a much needed base of knowledge to this field. Also, determining the alteration of the entire subset of ribosomal proteins following treatment may provide a rationale for the observed rRNA cleavage[126]. The knowledge gained from these studies could then potentially explain how some chemotherapy-induced apoptotic events are precipitated, for example through retention or increased expression of RPL7[154] in ribosomes (see section 1.5.3)

6.0 Appendix

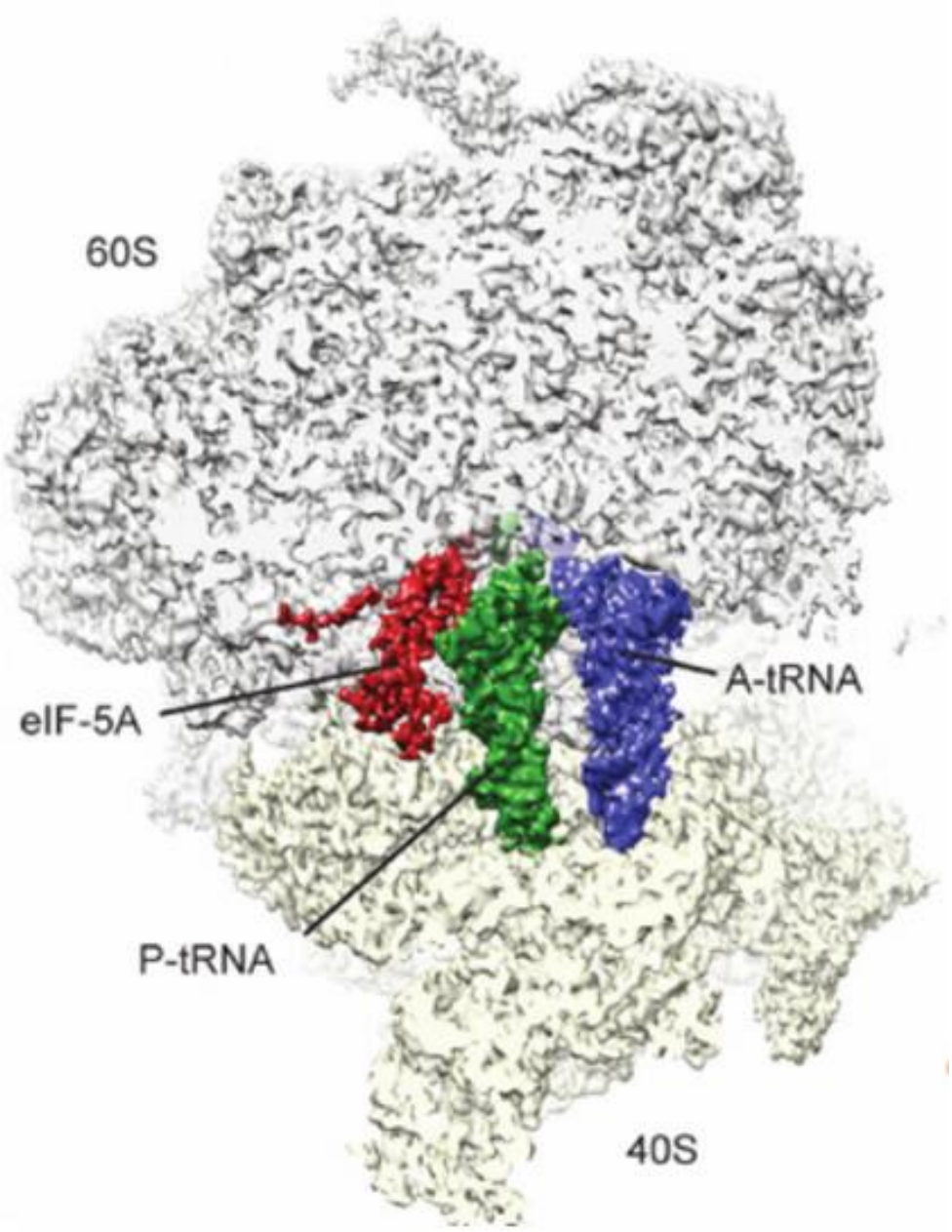

Figure 15 – Transverse Cryo-EM image of A-tRNA, P-tRNA and eIF-5A (A, P and E sites) bound to yeast 80S ribosome. Figure adapted from Schmidt et al (2015)[179], Figure 1A.

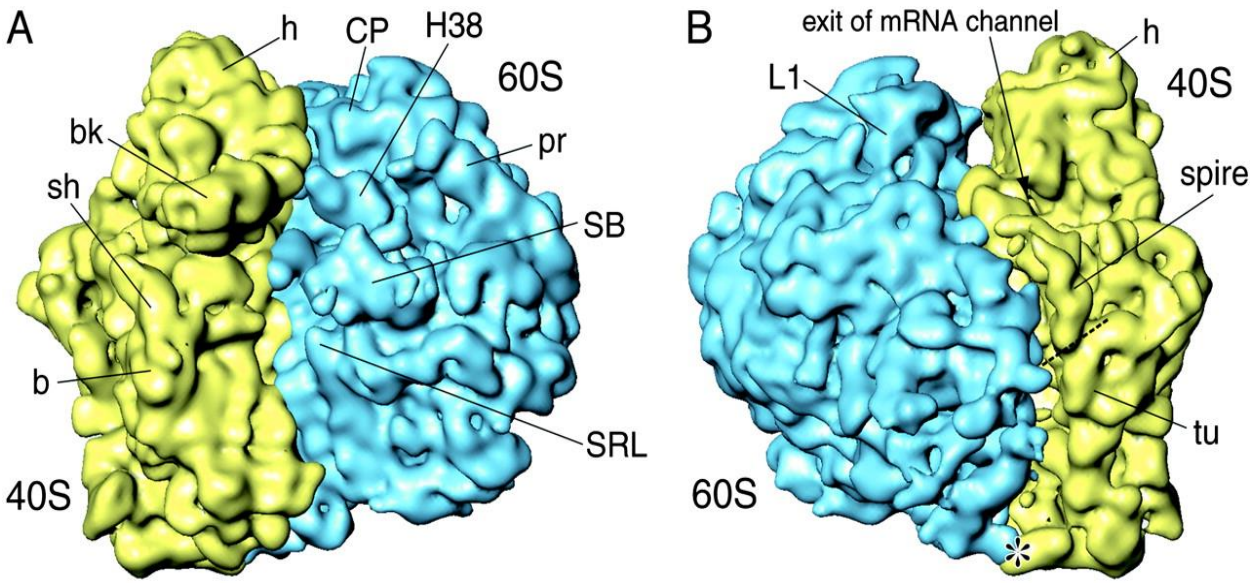

Figure 16 - The 12-Å resolution cryo-EM density map of the 80S ribosome from *Trypanosoma cruzi*. The density map is shown in two side views of the 80S ribosome. The 40S subunit is in yellow and the 60S subunit in blue. Landmarks for the 40S subunit: h, head; bk, beak; sh, shoulder; b, body; tu, turret; landmarks for the 60S subunit: CP, central protuberance; H38, helix 38; SB, stalk base; pr, prong; SRL, sarcin–ricin loop; L1, L1 stalk. This figure was adapted from figure 1 as taken from Gao et al (2005)[180]

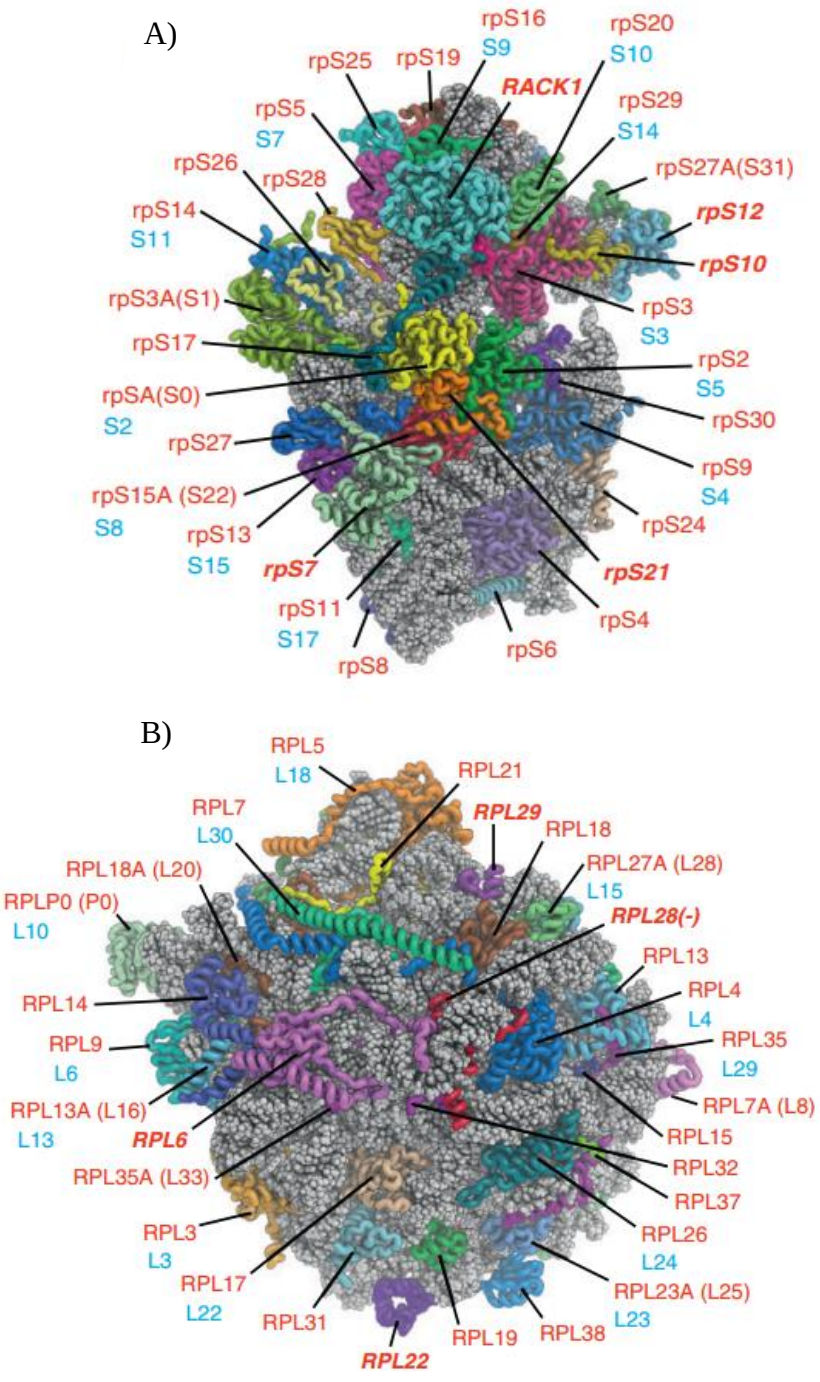

Figure 17 – Architecture of Eukaryotic ribosomal subunits along with bound ribosomal proteins. A) 40S B) 60S subunit. Proteins are labeled with eukaryotic names (red), differing yeast names in parentheses, and names of prokaryotic homologs (light blue). The figure was adapted from Figure 2 of Klinge et al. (2012)[178].

7.0 References

1. Society CC. Canadian Cancer Statistics Publication. http://www.cancer.ca/en/cancer-information/cancer-101/canadian-cancer-statistics-publication/?region=on. Published 2016.

2. Siegel R, Miller K, Jemal A. Cancer statistics , 2015 . *CA Cancer J Clin*. 2015;65(1):29. doi:10.3322/caac.21254.

3. Menon U, Griffin M, Gentry-Maharaj A. Ovarian cancer screening--current status, future directions. *Gynecol Oncol*. 2014;132(2):490-495. doi:10.1016/j.ygyno.2013.11.030.

4. Chan A, Gilks B, Kwon J, Tinker A V. New insights into the pathogenesis of ovarian carcinoma: time to rethink ovarian cancer screening. *Obstet Gynecol*. 2012;120(4):935-940. doi:10.1097/AOG.0b013e318269b8b1.

5. Goff B a, Mandel L, Muntz HG, Melancon CH. Ovarian carcinoma diagnosis. *Cancer*. 2000;89(10):2068-2075. doi:10.1002/1097-0142(20001115)89:10<2068::AID-CNCR6>3.0.CO;2-Z.

6. Yap TA, Carden CP, Kaye SB. Beyond chemotherapy: targeted therapies in ovarian cancer. *Nat Rev Cancer*. 2009;9(3):167-181. doi:10.1038/nrc2583.

7. Badgwell D, Bast RC. Early detection of ovarian cancer. *Dis Markers*. 2007;23(5-6):397-410. doi:10.1155/2007/309382.

8. Elit L, Oliver TK, Covens A, et al. Intraperitoneal chemotherapy in the first-line treatment of women with stage III epithelial ovarian cancer: A systematic review with metaanalyses. *Cancer*. 2007;109(4):692-702. doi:10.1002/cncr.22466.

9. Ledermann JA, Kristeleit RS. Optimal treatment for relapsing ovarian cancer. In: *Annals of Oncology*. Vol 21. ; 2010. doi:10.1093/annonc/mdq377.

10. Armstrong DK. Relapsed ovarian cancer: challenges and management strategies for a chronic disease. *Oncologist*. 2002;7 Suppl 5(suppl 5):20-28. doi:10.1634/theoncologist.7-suppl_5-20.

11. Agarwal R, Kaye SB. Ovarian cancer: strategies for overcoming resistance to chemotherapy. *Nat Rev Cancer*. 2003;3(7):502-516. doi:10.1038/nrc1123.

12. Armstrong SR, Narendrula R, Guo B, et al. Distinct genetic alterations occur in ovarian tumor cells selected for combined resistance to carboplatin and docetaxel. *J Ovarian Res*. 2012;5(1):40. doi:1757-2215-5-40 [pii]10.1186/1757-2215-5-40.

13. Johnson SW, Ozols RF, Hamilton TC. Mechanisms of drug resistance in ovarian cancer. *Cancer*. 1993;71(2 Suppl):644-649. http://www.ncbi.nlm.nih.gov/pubmed/17983517.

14. Prat J. New insights into ovarian cancer pathology. *Ann Oncol*. 2012;23(SUPPL. 10). doi:10.1093/annonc/mds300.

15. Bowtell DD. The genesis and evolution of high-grade serous ovarian cancer. *Nat Rev Cancer*. 2010;10(11):803-808. doi:10.1038/nrc2946.

16. Norquist BM, Garcia RL, Allison KH, et al. The molecular pathogenesis of hereditary ovarian carcinoma: alterations in the tubal epithelium of women with BRCA1 and BRCA2 mutations. *Cancer*. 2010;116(22):5261-5271. doi:10.1002/cncr.25439.

17. Vergote I, Amant F, Kristensen G, Ehlen T, Reed NS, Casado A. Primary surgery or neoadjuvant chemotherapy followed by interval debulking surgery in advanced ovarian

cancer. *Eur J Cancer*. 2011;47 Suppl 3:S88-S92. doi:10.1016/S0959-8049(11)70152-6.

18. Bristow RE, Eisenhauer EL, Santillan A, Chi DS. Delaying the primary surgical effort for advanced ovarian cancer: A systematic review of neoadjuvant chemotherapy and interval cytoreduction. *Gynecol Oncol*. 2007;104(2):480-490. doi:10.1016/j.ygyno.2006.11.002.

19. Markman M. New, expanded, and modified use of approved antineoplastic agents in ovarian cancer. *Oncologist*. 2007;12(2):186-190. doi:10.1634/theoncologist.12-2-186.

20. Alberts DS. Carboplatin versus cisplatin in ovarian cancer. *Semin Oncol*. 1995;22(5 Suppl 12):88-90. http://www.ncbi.nlm.nih.gov/pubmed/7481869.

21. Vasey PA, Jayson GC, Gordon A, et al. Phase III randomized trial of docetaxel-carboplatin versus paclitaxel-carboplatin as first-line chemotherapy for ovarian carcinoma. *J Natl Cancer Inst*. 2004;96(22):1682-1691. doi:10.1093/jnci/djh323.

22. Coward JI, Middleton K, Murphy F. IJWH-52379-new-perspectives-on-targeted-therapy-in-ovarian-cancer. *Int J Womens Health*. 2015;7:189-203. doi:10.2147/IJWH.S52379.

23. McCluggage WG. Morphological subtypes of ovarian carcinoma: a review with emphasis on new developments and pathogenesis. *Pathology*. 2011;43(5):420-432. doi:10.1097/PAT.0b013e328348a6e7.

24. Sato S, Itamochi H. Neoadjuvant chemotherapy in advanced ovarian cancer: latest results and place in therapy. *Ther Adv Med Oncol*. 2014;6(6):293-304. doi:10.1177/1758834014544891.

25. Verleye L, Vergote I, van der Zee AG. Patterns of care in surgery for ovarian cancer in Europe. *Eur J Surg Oncol*. 2010;36 Suppl 1:S108-S114. doi:10.1016/j.ejso.2010.06.006.

26. Monk BJ, Herzog TJ, Kaye SB, et al. Trabectedin plus pegylated liposomal Doxorubicin in recurrent ovarian cancer. *J Clin Oncol*. 2010;28(19):3107-3114. doi:10.1200/JCO.2009.25.4037.

27. Rose PG, Fusco N, Fluellen L, Rodriguez M. Second-line therapy with paclitaxel and carboplatin for recurrent disease following first-line therapy with paclitaxel and platinum in ovarian or peritoneal carcinoma. *J Clin Oncol*. 1998;16(4):1494-1497.

28. Vergote I, Tropé CG, Amant F, et al. Neoadjuvant chemotherapy or primary surgery in stage IIIC or IV ovarian cancer. *N Engl J Med*. 2010;363(10):943-953. doi:10.1056/NEJMoa0908806.

29. McCourt C, Dessie S, Bradley AM, Schwartz J, Brard L, Dizon DS. Is there a taxane-free interval that predicts response to taxanes as a later-line treatment of recurrent ovarian or primary peritoneal cancer? *Int J Gynecol Cancer*. 2009;19(3):343-347. doi:10.1111/IGC.0b013e3181a12eb9.

30. Fauzee NJS, Dong Z, Wang YL. Taxanes: Promising anti-cancer drugs. *Asian Pacific J Cancer Prev*. 2011;12(4):837-851.

31. Nobili S, Lippi D, Witort E, et al. Natural compounds for cancer treatment and prevention. *Pharmacol Res*. 2009;59(6):365-378. doi:10.1016/j.phrs.2009.01.017.

32. Maenpaa JU. Docetaxel: promising and novel combinations in ovarian cancer. *BrJ Cancer*. 2003;89 Suppl 3(0007-0920):S29-S34. doi:10.1038/sj.bjc.6601498.

33. Rowinsky EK. The development and clinical utility of the taxane class of antimicrotubule chemotherapy agents. *Annu Rev Med*. 1997;48:353-374.

doi:10.1146/annurev.med.48.1.353.

34. Perez E a. Microtubule inhibitors: Differentiating tubulin-inhibiting agents based on mechanisms of action, clinical activity, and resistance. *Mol Cancer Ther*. 2009;8(8):2086-2095. doi:10.1158/1535-7163.MCT-09-0366.

35. Morse DL, Gray H, Payne CM, Gillies RJ. Docetaxel induces cell death through mitotic catastrophe in human breast cancer cells. *Mol Cancer Ther*. 2005;4(10):1495-1504. doi:10.1158/1535-7163.MCT-05-0130.

36. Guéritte-Voegelein F, Guénard D, Lavelle F, Le Goff MT, Mangatal L, Potier P. Relationships between the structure of taxol analogues and their antimitotic activity. *J Med Chem*. 1991;34(3):992-998. doi:10.1021/jm00107a017.

37. Ferlini C, Distefano M, Pignatelli F, et al. Antitumour activity of novel taxanes that act at the same time as cytotoxic agents and P-glycoprotein inhibitors. *Br J Cancer*. 2000;83:1762-1768. doi:10.1054/bjoc.2000.1500.

38. Stanton RA, Gernert KM, Nettles JH, Aneja R. Drugs that target dynamic microtubules: A new molecular perspective. *Med Res Rev*. 2011;31(3):443-481. doi:10.1002/med.20242.

39. Moos PJ, Fitzpatrick F a. Taxanes propagate apoptosis via two cell populations with distinctive cytological and molecular traits. *Cell Growth Differ*. 1998;9(8):687-697.

40. Mediavilla-Varela M, Pacheco FJ, Almaguel F, et al. Docetaxel-induced prostate cancer cell death involves concomitant activation of caspase and lysosomal pathways and is attenuated by LEDGF/p75. *Mol Cancer*. 2009;8(1):68. doi:10.1186/1476-4598-8-68.

41. Muenchen HJ, Poncza PJ, Pienta KJ. Different docetaxel-induced apoptotic pathways are

present in prostate cancer cell lines LNCaP and PC-3. *Urology*. 2001;57(2):366-370. doi:10.1016/S0090-4295(00)00935-3.

42. Pickard RD, Spencer BH, McFarland AJ, et al. Paradoxical effects of the autophagy inhibitor 3-methyladenine on docetaxel-induced toxicity in PC-3 and LNCaP prostate cancer cells. *Naunyn Schmiedebergs Arch Pharmacol*. 2015;388(7):793-799. doi:10.1007/s00210-015-1104-7.

43. Mullins DW, Alleva DG, Burger CJ, Elgert KD. Taxol, a microtubule-stabilizing antineoplastic agent, differentially regulates normal and tumor-bearing host macrophage nitric oxide production. *Immunopharmacology*. 1997;37(1):63-73. doi:10.1016/S0162-3109(97)00004-0.

44. Sprowl JA, Reed K, Armstrong SR, et al. Alterations in tumor necrosis factor signaling pathways are associated with cytotoxicity and resistance to taxanes: a study in isogenic resistant tumor cells. *Breast Cancer Res*. 2012;14(1):R2. doi:10.1186/bcr3083.

45. Mhaidat NM, Thorne RF, Zhang XD, Hersey P. Regulation of docetaxel-induced apoptosis of human melanoma cells by different isoforms of protein kinase C. *Mol Cancer Res*. 2007;5(October):1073-1081. doi:10.1158/1541-7786.MCR-07-0059.

46. Yigit R, Figdor CG, Zusterzeel PLM, Pots JM, Torensma R, Massuger LFAG. Cytokine analysis as a tool to understand tumour-host interaction in ovarian cancer. *Eur J Cancer*. 2011;47(12):1883-1889. doi:10.1016/j.ejca.2011.03.026.

47. Luqmani YA. Mechanisms of drug resistance in cancer chemotherapy. *Med Princ Pract*. 2005;14 Suppl 1(SUPPL. 1):35-48. doi:10.1159/000086183.

48. Vasey PA. Resistance to chemotherapy in advanced ovarian cancer: mechanisms and current strategies. *Br J Cancer*. 2003;89 Suppl 3:S23-S28. doi:10.1038/sj.bjc.6601497.

49. Kavallaris M, Kuo DY, Burkhart CA, et al. Taxol-resistant epithelial ovarian tumors are associated with altered expression of specific beta-tubulin isotypes. *J Clin Invest*. 1997;100(5):1282-1293. doi:10.1172/JCI119642.

50. Monz?? M, Rosell R, S??nchez JJ, et al. Paclitaxel resistance in non-small-cell lung cancer associated with beta-tubulin gene mutations. *J Clin Oncol*. 1999;17(6):1786-1793.

51. Orr GA, Verdier-Pinard P, McDaid H, Horwitz SB. Mechanisms of Taxol resistance related to microtubules. *Oncogene*. 2003;22(47):7280-7295. doi:10.1038/sj.onc.1206934.

52. Wang Z, Goulet R, Stanton KJ, Sadaria M, Nakshatri H. Differential effect of anti-apoptotic genes Bcl-xL and c-FLIP on sensitivity of MCF-7 breast cancer cells to paclitaxel and docetaxel. *Anticancer Res*. 2005;25(3 C):2367-2379.

53. Zaffaroni N, Pennati M, Colella G, et al. Expression of the anti-apoptotic gene survivin correlates with taxol resistance in human ovarian cancer. *Cell Mol Life Sci*. 2002;59(8):1406-1412. doi:10.1007/s00018-002-8518-3.

54. Jiang L, Luo RY, Yang J, Cheng YX. Knockdown of survivin contributes to antitumor activity in cisplatin-resistant ovarian cancer cells. *Mol Med Rep*. 2013;7(2):425-430. doi:10.3892/mmr.2012.1216.

55. Chen L, Liang L, Yan X, et al. Survivin status affects prognosis and chemosensitivity in epithelial ovarian cancer. *Int J Gynecol Cancer*. 2013;23(2):256-263. doi:10.1097/IGC.0b013e31827ad2b8.

56. Gillet J-P, Gottesman MM. Mechanisms of multidrug resistance in cancer. *Methods Mol Biol*. 2010;596:47-76. doi:10.1007/978-1-60761-416-6_4.

57. Gottesman MM, Fojo T, Bates SE. Multidrug resistance in cancer: role of ATP-dependent transporters. *Nat Rev Cancer*. 2002;2(1):48-58. doi:10.1038/nrc706.

58. Duan Z, Brakora KA, Seiden M V. Inhibition of ABCB1 (MDR1) and ABCB4 (MDR3) expression by small interfering RNA and reversal of paclitaxel resistance in human ovarian cancer cells. *Mol Cancer Ther*. 2004;3(7):833-838. doi:3/7/833 [pii].

59. Baekelandt MM, Holm R, Nesland JM, Trop?? CG, Kristensen GB. P-glycoprotein expression is a marker for chemotherapy resistance and prognosis in advanced ovarian cancer. *Anticancer Res*. 2000;20(2 B):1061-1067.

60. Gao B, Russell A, Beesley J, et al. Paclitaxel sensitivity in relation to ABCB1 expression, efflux and single nucleotide polymorphisms in ovarian cancer. *Sci Rep*. 2014;4:4669. doi:10.1038/srep04669.

61. Golomb L, Volarevic S, Oren M. P53 and ribosome biogenesis stress: The essentials. *FEBS Lett*. 2014;588(16):2571-2579. doi:10.1016/j.febslet.2014.04.014.

62. Kupryjańczyk J, Thor a D, Beauchamp R, et al. P53 Gene Mutations and Protein Accumulation in Human Ovarian Cancer. *Proc Natl Acad Sci U S A*. 1993;90(11):4961-4965. doi:10.1073/pnas.90.11.4961.

63. Reles A, Wen WH, Schmider A, et al. Correlation of p53 mutations with resistance to platinum-based chemotherapy and shortened survival in ovarian cancer. *Clin Cancer Res*. 2001;7(10):2984-2997.

64. Yang-Hartwich Y, Soteras MG, Lin ZP, et al. P53 Protein Aggregation Promotes Platinum Resistance in Ovarian Cancer. supplimentary data. *Oncogene*. 2014;34(September):25263447. doi:10.1038/onc.2014.296.

65. Soragni A, Janzen DM, Johnson LM, et al. A Designed Inhibitor of p53 Aggregation Rescues p53 Tumor Suppression in Ovarian Carcinomas. *Cancer Cell*. 2016;29(1):90-103. doi:10.1016/j.ccell.2015.12.002.

66. Garcia-Martin E, Pizarro RM, Martinez C, et al. Acquired resistance to the anticancer drug paclitaxel is associated with induction of cytochrome P450 2C8. *Pharmacogenomics*. 2006;7(4):575-585. doi:10.2217/14622416.7.4.575.

67. Zhu Z, Mu Y, Qi C, et al. CYP1B1 enhances the resistance of epithelial ovarian cancer cells to paclitaxel in vivo and in vitro. *Int J Mol Med*. 2015;35(2):340-348. doi:10.3892/ijmm.2014.2041.

68. Minchinton AI, Tannock IF. Drug penetration in solid tumours. *Nat Rev Cancer*. 2006;6(8):583-592. doi:10.1038/nrc1893.

69. Saggar JK, Yu M, Tan Q, Tannock IF. The Tumor Microenvironment and Strategies to Improve Drug Distribution. *Front Oncol*. 2013;3(June):154. doi:10.3389/fonc.2013.00154.

70. Agirrezabala X, Frank J. From DNA to proteins via the ribosome: structural insights into the workings of the translation machinery. *Hum Genomics*. 2010;4(4):226-237. doi:10.1186/1479-7364-4-4-226.

71. Iborra FJ, Jackson D a, Cook PR. Coupled transcription and translation within nuclei of

mammalian cells. *Science*. 2001;293(August):1139-1142. doi:10.1126/science.1061216.

72. Reid DW, Nicchitta C V. The enduring enigma of nuclear translation. *J Cell Biol*. 2012;197(1):7-9. doi:10.1083/jcb.201202140.

73. Brogna S, Sato TA, Rosbash M. Ribosome components are associated with sites of transcription. *Mol Cell*. 2002;10(1):93-104. doi:10.1016/S1097-2765(02)00565-8.

74. de la Cruz J, Karbstein K, Woolford JL. Functions of ribosomal proteins in assembly of eukaryotic ribosomes in vivo. *Annu Rev Biochem*. 2015;84:93-129. doi:10.1146/annurev-biochem-060614-033917.

75. Stults DM, Killen MW, Pierce HH, Pierce AJ. Genomic architecture and inheritance of human ribosomal RNA gene clusters. *Genome Res*. 2008;18(1):13-18. doi:10.1101/gr.6858507.

76. Henras AK, Plisson-Chastang C, O'Donohue MF, Chakraborty A, Gleizes PE. An overview of pre-ribosomal RNA processing in eukaryotes. *Wiley Interdiscip Rev RNA*. 2015;6(2):225-242. doi:10.1002/wrna.1269.

77. Clancy S, Brown W. Translation : DNA to mRNA to Protein. *Nat Educ*. 2008;1(2008):101.

78. Ezkurdia I, Juan D, Rodriguez JM, et al. Multiple evidence strands suggest that theremay be as few as 19 000 human protein-coding genes. *Hum Mol Genet*. 2014;23(22):5866-5878. doi:10.1093/hmg/ddu309.

79. Wang T, Birsoy K, Hughes NW, et al. Identification and characterization of essential genes in the human genome. *Science (80-).* 2015;350(6264):1096-1101.

doi:10.1126/science.aac7041.

80. Hillis DM, Dixon MT. Ribosomal DNA - molecular evolution and phylogenetic inference. *Q Rev Biol*. 1991;66(4):411-453. doi:10.1086/417338.

81. Kondrashov N, Pusic A, Stumpf CR, et al. Ribosome-mediated specificity in Hox mRNA translation and vertebrate tissue patterning. *Cell*. 2011;145(3):383-397. doi:10.1016/j.cell.2011.03.028.

82. Byrgazov K, Vesper O, Moll I. Ribosome heterogeneity: Another level of complexity in bacterial translation regulation. *Curr Opin Microbiol*. 2013;16(2):133-139. doi:10.1016/j.mib.2013.01.009.

83. Anger AM, Armache JP, Berninghausen O, et al. Structures of the human and Drosophila 80S ribosome. *Nature*. 2013;497(7447):80-85. doi:10.1038/nature12104.

84. Xue S, Barna M. Specialized ribosomes: a new frontier in gene regulation and organismal biology. *Nat Rev Mol Cell Biol*. 2012;13(6):355-369. doi:10.1038/nrm3359.

85. Jiang T, Shi W, Natowicz R, et al. Statistical measures of transcriptional diversity capture genomic heterogeneity of cancer. *BMC Genomics*. 2014;15(1):876. doi:10.1186/1471-2164-15-876.

86. Xiao Z, Zou Q, Liu Y, Yang X. Genome-wide assessment of differential translations with ribosome profiling data. *Nat Commun*. 2016;7:11194. doi:10.1038/ncomms11194.

87. Lafontaine DLJ. Noncoding RNAs in eukaryotic ribosome biogenesis and function. *Nat Struct & Mol Biol*. 2015;22(1):11-19. doi:10.1038/nsmb.2939.

88. Ruggero D, Pandolfi PP. Does the ribosome translate cancer? *Nat Rev Cancer*. 2003;3(3):179-192. doi:10.1038/nrc1015.

89. Derenzini M, Montanaro L, Treré D. What the nucleolus says to a tumour pathologist. *Histopathology*. 2009;54(6):753-762. doi:10.1111/j.1365-2559.2008.03168.x.

90. Pelava A, Schneider C, Watkins NJ. The importance of ribosome production, and the 5S RNP–MDM2 pathway, in health and disease. *Biochem Soc Trans*. 2016;44(4):1086-1090. doi:10.1042/BST20160106.

91. Haddach M, Schwaebe MK, Michaux J, et al. Discovery of CX-5461, the first direct and selective inhibitor of RNA polymerase I, for cancer therapeutics. *ACS Med Chem Lett*. 2012;3(7):602-606. doi:10.1021/ml300110s.

92. Iadevaia V, Liu R, Proud CG. MTORC1 signaling controls multiple steps in ribosome biogenesis. *Semin Cell Dev Biol*. 2014;36:113-120. doi:10.1016/j.semcdb.2014.08.004.

93. Hsieh AL, Walton ZE, Altman BJ, Stine ZE, Dang C V. MYC and metabolism on the path to cancer. *Semin Cell Dev Biol*. 2015;43:11-21. doi:10.1016/j.semcdb.2015.08.003.

94. Mendoza MC, Er EE, Blenis J. The Ras-ERK and PI3K-mTOR pathways: Cross-talk and compensation. *Trends Biochem Sci*. 2011;36(6):320-328. doi:10.1016/j.tibs.2011.03.006.

95. Shepherd C, Banerjee L, Cheung CW, et al. PI3K/mTOR inhibition upregulates NOTCH-MYC signalling leading to an impaired cytotoxic response. *Leukemia*. 2012;27(October):1-36. doi:10.1038/leu.2012.285.

96. Woods SJ, Hannan KM, Pearson RB, Hannan RD. The nucleolus as a fundamental regulator of the p53 response and a new target for cancer therapy. *Biochim Biophys Acta*.

2015;1849(7):821-829. doi:10.1016/j.bbagrm.2014.10.007.

97. Belin S, Beghin A, Solano-Gonzàlez E, et al. Dysregulation of ribosome biogenesis and translational capacity is associated with tumor progression of human breast cancer cells. *PLoS One*. 2009;4(9):e7147. doi:10.1371/journal.pone.0007147.

98. M??l??se T, Xue Z. The nucleolus: an organelle formed by the act of building a ribosome. *Curr Opin Cell Biol*. 1995;7(3):319-324. doi:10.1016/0955-0674(95)80085-9.

99. Sloan KE, Mattijssen S, Lebaron S, Tollervey D, Pruijn GJM, Watkins NJ. Both endonucleolytic and exonucleolytic cleavage mediate ITS1 removal during human ribosomal RNA processing. *J Cell Biol*. 2013;200(5):577-588. doi:10.1083/jcb.201207131.

100. Thoms M, Thomson E, Baßler J, Gnädig M, Griesel S, Hurt E. The Exosome Is Recruited to RNA Substrates through Specific Adaptor Proteins. *Cell*. 2015;162(5):1029-1038. doi:10.1016/j.cell.2015.07.060.

101. Wang M, Pestov DG. 5???-end surveillance by Xrn2 acts as a shared mechanism for mammalian pre-rRNA maturation and decay. *Nucleic Acids Res*. 2011;39(5):1811-1822. doi:10.1093/nar/gkq1050.

102. Ciganda M, Williams N. Eukaryotic 5S rRNA biogenesis. *Wiley Interdiscip Rev RNA*. 2011;2(4):523-533. doi:10.1002/wrna.74.

103. Watkins NJ, Bohnsack MT. The box C/D and H/ACA snoRNPs: Key players in the modification, processing and the dynamic folding of ribosomal RNA. *Wiley Interdiscip Rev RNA*. 2012;3(3):397-414. doi:10.1002/wrna.117.

104. Decatur WA, Liang X hai, Piekna-Przybylska D, Fournier MJ. Identifying Effects of snoRNA-Guided Modifications on the Synthesis and Function of the Yeast Ribosome. *Methods Enzymol*. 2007;425:283-316. doi:10.1016/S0076-6879(07)25013-X.

105. Su H, Xu T, Ganapathy S, et al. Elevated snoRNA biogenesis is essential in breast cancer. *Oncogene*. 2014;33(11):1348-1358. doi:10.1038/onc.2013.89.

106. Melnikov S, Ben-Shem A, Garreau de Loubresse N, Jenner L, Yusupova G, Yusupov M. One core, two shells: bacterial and eukaryotic ribosomes. *Nat Struct Mol Biol*. 2012;19(6):560-567. doi:10.1038/nsmb.2313.

107. ClatterbuckSoper S, Dator R, Limbach P, Woodson S. InVivo X-Ray footprinting of pre-30S ribosomes reveals chaperone-dependent remodeling of late assembly intermediates. *Mol Cell*. 2013;52(4):506-516. doi:10.1016/j.molcel.2013.09.020.

108. Kim H, Abeysirigunawarden SC, Chen K, et al. Protein-guided RNA dynamics during early ribosome assembly. *Nature*. 2014;506(7488):334-338. doi:10.1038/nature13039.

109. Gamalinda M, Ohmayer U, Jakovljevic J, et al. A hierarchical model for assembly of eukaryotic 60S ribosomal subunit domains. *Genes Dev*. 2014;28(2):198-210. doi:10.1101/gad.228825.113.

110. Zhang Y, Lu H. Signaling to p53: Ribosomal Proteins Find Their Way. *Cancer Cell*. 2009;16(5):369-377. doi:10.1016/j.ccr.2009.09.024.

111. Lohrum MAE, Ludwig RL, Kubbutat MHG, Hanlon M, Vousden KH. Regulation of HDM2 activity by the ribosomal protein L11. *Cancer Cell*. 2003;3(6):577-587. doi:10.1016/S1535-6108(03)00134-X.

112. Dai M-S, Zeng SX, Jin Y, Sun X-X, David L, Lu H. Ribosomal protein L23 activates p53 by inhibiting MDM2 function in response to ribosomal perturbation but not to translation inhibition. *Mol Cell Biol*. 2004;24(17):7654-7668. doi:10.1128/MCB.24.17.7654-7668.2004.

113. Marechal V, Elenbaas B, Piette J, Nicolas JC, Levine a J. The ribosomal L5 protein is associated with mdm-2 and mdm-2-p53 complexes. *Mol Cell Biol*. 1994;14(11):7414-7420. doi:10.1128/MCB.14.11.7414.Updated.

114. Chen D, Zhang Z, Li M, et al. Ribosomal protein S7 as a novel modulator of p53-MDM2 interaction: binding to MDM2, stabilization of p53 protein, and activation of p53 function. *Oncogene*. 2007;26(35):5029-5037. doi:10.1038/sj.onc.1210327.

115. Ofir-Rosenfeld Y, Boggs K, Michael D, Kastan MB, Oren M. Mdm2 Regulates p53 mRNA Translation through Inhibitory Interactions with Ribosomal Protein L26. *Mol Cell*. 2008;32(2):180-189. doi:10.1016/j.molcel.2008.08.031.

116. Houge G, Doskeland SO, Boe R, Lanotte M. Selective cleavage of 28S rRNA variable regions V3 and V13 in myeloid leukemia cell apoptosis. *FEBS Lett*. 1993;315(1):16-20. doi:0014-5793(93)81123-H [pii].

117. Samali A, Gilje B, Doskeland SO, Cotter TG, Houge G. The ability to cleave 28S ribosomal RNA during apoptosis is a cell-type dependent trait unrelated to DNA fragmentation. *Cell Death Differ*. 1997;4(4):289-293. doi:4400246 [pii]10.1038/sj.cdd.4400246.

118. Houge G, Doskeland SO. Divergence towards a dead end? Cleavage of the divergent

domains of ribosomal RNA in apoptosis. *Experientia*. 1996;52(10-11):963-967. http://www.ncbi.nlm.nih.gov/entrez/query.fcgi?cmd=Retrieve&db=PubMed&dopt=Citation&list_uids=8917727.

119. Ramesh M, Woolford JL. Eukaryote-specific rRNA expansion segments function in ribosome biogenesis. *Rna*. 2016:1153-1162. doi:10.1261/rna.056705.116.

120. King KL, Jewell CM, Bortner CD, Cidlowski JA. 28S ribosome degradation in lymphoid cell apoptosis: evidence for caspase and Bcl-2-dependent and -independent pathways. *Cell Death Differ*. 2000;7(10):994-1001. doi:10.1038/sj.cdd.4400731.

121. He K, Zhou HR, Pestka JJ. Targets and intracellular signaling mechanisms for deoxynivalenol-induced ribosomal RNA cleavage. *Toxicol Sci*. 2012;127(2):382-390. doi:10.1093/toxsci/kfs134.

122. He K, Zhou HR, Pestka JJ. Mechanisms for ribotoxin-induced ribosomal RNA cleavage. *Toxicol Appl Pharmacol*. 2012;265(1):10-18. doi:10.1016/j.taap.2012.09.017.

123. Rubbi CP, Milner J. Disruption of the nucleolus mediates stabilization of p53 in response to DNA damage and other stresses. *EMBO J*. 2003;22(22):6068-6077. doi:10.1093/emboj/cdg579.

124. Fumagalli S, Ivanenkov V V., Teng T, Thomas G. Suprainduction of p53 by disruption of 40S and 60S ribosome biogenesis leads to the activation of a novel G2/M checkpoint. *Genes Dev*. 2012;26(10):1028-1040. doi:10.1101/gad.189951.112.

125. Burger K, Muhl B, Harasim T, et al. Chemotherapeutic drugs inhibit ribosome biogenesis at various levels. *J Biol Chem*. 2010;285(16):12416-12425. doi:M109.074211

[pii]10.1074/jbc.M109.074211.

126. Narendrula R, Mispel-Beyer K, Guo B, et al. RNA disruption is associated with response to multiple classes of chemotherapy drugs in tumor cell lines. *BMC Cancer*. 2016;16(1):146. doi:10.1186/s12885-016-2197-1.

127. Houge G, Robaye B, Eikhom TS, et al. Fine mapping of 28S rRNA sites specifically cleaved in cells undergoing apoptosis. *Mol Cell Biol*. 1995;15(4):2051-2062. http://www.ncbi.nlm.nih.gov/entrez/query.fcgi?cmd=Retrieve&db=PubMed&dopt=Citation&list_uids=7891700.

128. Hoat Nakayashiki, H., Tosa, Y., Mayama, S. TX. Specific cleavage of ribosomal RNA and mRNA during victorin-induced apoptotic cell death in oat. *Plant J*. 2006;46:922-933. doi:doi: 10.1111/j.1365-313X.2006.02752.x.

129. Lafarga M, Lerga A, Andres MA, Polanco JI, Calle E, Berciano MT. Apoptosis induced by methylazoxymethanol in developing rat cerebellum: organization of the cell nucleus and its relationship to DNA and rRNA degradation. *Cell Tissue Res*. 1997;289(1):25-38. http://www.ncbi.nlm.nih.gov/entrez/query.fcgi?cmd=Retrieve&db=PubMed&dopt=Citation&list_uids=9182598.

130. Nadano D, Sato TA. Caspase-3-dependent and -independent degradation of 28 S ribosomal RNA may be involved in the inhibition of protein synthesis during apoptosis initiated by death receptor engagement. *J Biol Chem*. 2000;275(18):13967-13973. doi:10.1074/jbc.275.18.13967.

131. He K, Zhou HR, Pestka JJ. Targets and intracellular signaling mechanisms for

deoxynivalenol-induced ribosomal RNA cleavage. *Toxicol Sci*. 2012;127(2):382-390. doi:kfs134 [pii]10.1093/toxsci/kfs134.

132. Houseley J, Tollervey D. The many pathways of RNA degradation. *Cell*. 2009;136(4):763-776. doi:S0092-8674(09)00067-1 [pii]10.1016/j.cell.2009.01.019.

133. Hansen MC, Nielsen AK, Molin S, Hammer K, Kilstrup M. Changes in rRNA levels during stress invalidates results from mRNA blotting: Fluorescence in situ rRNA hybridization permits renormalization for estimation of cellular mRNA levels. *J Bacteriol*. 2001;183(16):4747-4751. doi:10.1128/JB.183.16.4747-4751.2001.

134. Liang S-L, Quirk D, Zhou A. RNase L: its biological roles and regulation. *IUBMB Life*. 2006;58(9):508-514. doi:10.1080/15216540600838232.

135. Zhou A, Paranjape J, Brown TL, et al. Interferon action and apoptosis are defective in mice devoid of 2',5'-oligoadenylate-dependent RNase L. *EMBO J*. 1997;16(21):6355-6363. doi:10.1093/emboj/16.21.6355.

136. Han Y, Donovan J, Rath S, Whitney G, Chitrakar A, Korennykh A. Structure of human RNase L reveals the basis for regulated RNA decay in the IFN response. *Science*. 2014;343(6176):1244-1248. doi:10.1126/science.1249845.

137. Kitamura Y, Kito S, Nakashima R, Tanaka K, Nagaoka K, Kitade Y. Doxifluridine-conjugated 2-5A analog shows strong RNase L activation ability and tumor suppressive effect. *Bioorg Med Chem*. 2016. doi:10.1016/j.bmc.2016.06.033.

138. Siddiqui M, Mukherjee S, Manivannan P, Malathi K. RNase L Cleavage Products Promote Switch from Autophagy to Apoptosis by Caspase-Mediated Cleavage of Beclin-

1. *Int J Mol Sci*. 2015;16(8):17611-17636. doi:10.3390/ijms160817611.

139. Chen Y, Brandizzi F. IRE1: ER stress sensor and cell fate executor. *Trends Cell Biol*. 2013;23(11):547-555. doi:10.1016/j.tcb.2013.06.005.

140. Iwawaki T, Hosoda A, Okuda T, et al. Translational control by the ER transmembrane kinase/ribonuclease IRE1 under ER stress. *Nat Cell Biol*. 2001;3(February):158-165. doi:10.1038/35055065.

141. Allmang C, Mitchell P, Petfalski E, Tollervey D. Degradation of ribosomal RNA precursors by the exosome. *Nucleic Acids Res*. 2000;28(8):1684-1691. doi:gkd297 [pii].

142. Mitchell P, Petfalski E, Shevchenko A, Mann M, Tollervey D. The exosome: a conserved eukaryotic RNA processing complex containing multiple 3’ to 5' exoribonucleases. *Cell*. 1997;91(4):457-466. doi:S0092-8674(00)80432-8 [pii].

143. Lubas M, Andersen P, Schein A, Dziembowski A, Kudla G, Jensen TH. The human nuclear exosome targeting complex is loaded onto newly synthesized RNA to direct early ribonucleolysis. *Cell Rep*. 2015;10(2):178-192. doi:10.1016/j.celrep.2014.12.026.

144. Slomovic S, Laufer D, Geiger D, Schuster G. Polyadenylation of ribosomal RNA in human cells. *Nucleic Acids Res*. 2006;34(10):2966-2975. doi:34/10/2966 [pii]10.1093/nar/gkl357.

145. Lebreton A, Tomecki R, Dziembowski A, Seraphin B. Endonucleolytic RNA cleavage by a eukaryotic exosome. *Nature*. 2008;456(7224):993-996. doi:nature07480 [pii]10.1038/nature07480.

146. Schaeffer D, Tsanova B, Barbas A, et al. The exosome contains domains with specific

endoribonuclease, exoribonuclease and cytoplasmic mRNA decay activities. *Nat Struct Mol Biol*. 2009;16(1):56-62. doi:10.1038/nsmb.1528.

147. LaRiviere FJ, Cole SE, Ferullo DJ, Moore MJ. A late-acting quality control process for mature eukaryotic rRNAs. *Mol Cell*. 2006;24(4):619-626. doi:S1097-2765(06)00697-6 [pii]10.1016/j.molcel.2006.10.008.

148. Fujii K, Kitabatake M, Sakata T, Miyata A, Ohno M. A role for ubiquitin in the clearance of nonfunctional rRNAs. *Genes Dev*. 2009;23(8):963-974. doi:10.1101/gad.1775609.

149. Sikriwal D, Batra JK. Ribosome inactivating proteins and apoptosis. *Plant Cell Monogr*. 2010;18:167-189. doi:10.1007/978-3-642-12176-0_9.

150. Cencic R, Robert F, Galicia-Vázquez G, et al. Modifying chemotherapy response by targeted inhibition of eukaryotic initiation factor 4A. *Blood Cancer J*. 2013;3:e128. doi:10.1038/bcj.2013.25.

151. Parissenti AM, Chapman JA, Kahn HJ, et al. Association of low tumor RNA integrity with response to chemotherapy in breast cancer patients. *Breast Cancer Res Treat*. 2010;119(2):347-356. doi:10.1007/s10549-009-0531-x.

152. Pritzker K, Pritzker L, Generali D, et al. RNA Disruption and Drug Response in Breast Cancer Primary Systemic Therapy. *J Natl Cancer Inst Monogr*. 2015;2015(51):76-80. doi:10.1093/jncimonographs/lgv015.

153. Thapa M, Bommakanti A, Shamsuzzaman M, et al. Repressed synthesis of ribosomal proteins generates protein-specific cell cycle and morphological phenotypes. *Mol Biol Cell*. 2013;24(23):3620-3633. doi:10.1091/mbc.E13-02-0097.

154. Neumann F. Constitutive Expression of Human Ribosomal Protein L7 Arrests the Cell Cycle in G1and Induces Apoptosis in Jurkat T-Lymphoma Cells. *Exp Cell Res*. 1997;230(2):252-261. doi:10.1006/excr.1996.3417.

155. Chen FW, Ioannou YA. Ribosomal proteins in cell proliferation and apoptosis. *Int Rev Immunol*. 1999;18(5-6):429-448. doi:10.3109/08830189909088492.

156. Naora H, Naora H. Involvement of ribosomal proteins in regulating cell growth and apoptosis: Translational modulation or recruitment for extraribosomal activity? In: *Immunology and Cell Biology*. Vol 77. ; 1999:197-205. doi:10.1046/j.1440-1711.1999.00816.x.

157. Zhang C, Fu J, Xue F, et al. Knockdown of ribosomal protein S15A induces human glioblastoma cell apoptosis. *World J Surg Oncol*. 2016;14(1):129. doi:10.1186/s12957-016-0891-8.

158. Nishida J, Shiratsuchv A, Nadano D, Sato T-A, Nakanishi Y. Structural Change of Ribosomes during Apoptosis: Degradation and Extemalization of Ribosomal Proteins in Doxorubicin-Treated Jurkat Cells 1. *J Biochem*. 2002;131:485-493.

159. Anglesio MS, Wiegand KC, Melnyk N, et al. Type-Specific Cell Line Models for Type-Specific Ovarian Cancer Research. *PLoS One*. 2013;8(9). doi:10.1371/journal.pone.0072162.

160. Guo B, Villeneuve DJ, Hembruff SL, et al. Cross-resistance studies of isogenic drug-resistant breast tumor cell lines support recent clinical evidence suggesting that sensitivity to paclitaxel may be strongly compromised by prior doxorubicin exposure. *Breast Cancer*

Res Treat. 2004;85(1):31-51. doi:10.1023/B:BREA.0000021046.29834.12.

161. Belin S, Hacot S, Daudignon L, et al. Purification of ribosomes from human cell lines. *Curr Protoc Cell Biol*. 2010;(SUPPL.49). doi:10.1002/0471143030.cb0340s49.

162. Towbin H, Staehelin T, Gordon J. Electrophoretic transfer of proteins from polyacrylamide gels to nitrocellulose sheets: procedure and some applications. *Proc Natl Acad Sci U S A*. 1979;76(9):4350-4354. doi:10.1002/bies.950190612.

163. Lilley KS, Razzaq A, Dupree P. Two-dimensional gel electrophoresis : recent advances in sample preparation , detection and quantitation Kathryn S Lilley , Azam Razzaq and Paul Dupree. *Electrophoresis*. 2002;6(1):46-50. doi:10.1016/S1367-5931(01)00275-7.

164. Tan SC, Yiap BC. DNA, RNA, and protein extraction: The past and the present. *J Biomed Biotechnol*. 2009;2009. doi:10.1155/2009/574398.

165. Wool IG, Chan YL, Gluck A. Structure and evolution of mammalian ribosomal proteins. *Biochem Cell Biol*. 1995;73(11-12):933-947. http://www.ncbi.nlm.nih.gov/entrez/query.fcgi?cmd=Retrieve&db=PubMed&dopt=Citation&list_uids=8722009.

166. Gunning PW, Ghoshdastider U, Whitaker S, Popp D, Robinson RC. The evolution of compositionally and functionally distinct actin filaments. *J Cell Sci*. 2015;128(11):2009-2019. doi:10.1242/jcs.165563.

167. Bąkowska-Zywicka K, Tyczewska A. Ribophagy - The novel degradation system of the ribosome. *Biotechnologia*. 2009;(1):99-103.

168. Shires TK, Narurkar L, Pitot HC. The association in vitro of polyribosomes with

ribonuclease-treated derivatives of hepatic rough endoplasmic reticulum. Characteristics of the membrane binding sites and factors influencing association. *Biochem J*. 1971;125(1):67-79. http://www.pubmedcentral.nih.gov/articlerender.fcgi?artid=1178026&tool=pmcentrez&rendertype=abstract.

169. Albain KS, Barlow WE, Ravdin PM, et al. Adjuvant chemotherapy and timing of tamoxifen in postmenopausal patients with endocrine-responsive, node-positive breast cancer: a phase 3, open-label, randomised controlled trial. *Lancet*. 2009;374(9707):2055-2063. doi:10.1016/S0140-6736(09)61523-3.

170. Bhavsar RB, Makley LN, Tsonis PA. The other lives of ribosomal proteins. *Hum Genomics*. 2010;4:327-344. doi:10.1186/1479-7364-4-5-327.

171. Wool IG. Extraribosomal functions of ribosomal proteins. *Trends Biochem Sci*. 1996;21(5):164-165. doi:10.1016/0968-0004(96)20011-8.

172. Tsolakidis D, Amant F, Van Gorp T, Leunen K, Neven P, Vergote I. The role of diaphragmatic surgery during interval debulking after neoadjuvant chemotherapy: an analysis of 74 patients with advanced epithelial ovarian cancer. *Int J Gynecol Cancer*. 2010;20(4):542-551. doi:10.1111/IGC.0b013e3181d4de23.

173. Korobeinikova a V, Garber MB, Gongadze GM. Ribosomal proteins: structure, function, and evolution. *Biochem Biokhimiia*. 2012;77(6):562-574. doi:10.1134/S0006297912060028.

174. Garfin DE. Two-dimensional gel electrophoresis: An overview. *TrAC - Trends Anal*

Chem. 2003;22(5):263-272. doi:10.1016/S0165-9936(03)00506-5.

175. Molloy MP, Phadke ND, Chen H, et al. Profiling the alkaline membrane proteome of Caulobacter crescentus with two-dimensional electrophoresis and mass spectrometry. *Proteomics*. 2002;2(7):899-910. doi:10.1002/1615-9861(200207)2:7<899::AID-PROT899>3.0.CO;2-Y.

176. Hemmerich P, Mikecz A Von, Neumann F, et al. Structural and functional properties of ribosomal protein L7 from humans and rodents. *Nucleic Acids Res*. 1993;21(2):223-231. doi:10.1093/nar/21.2.223.

177. Wen F, Zhou R, Shen A, Choi A, Uribe D, Shi J. The tumor suppressive role of eIF3f and its function in translation inhibition and rRNA degradation. *PLoS One*. 2012;7(3). doi:10.1371/journal.pone.0034194.

178. Klinge S, Voigts-Hoffmann F, Leibundgut M, Ban N. Atomic structures of the eukaryotic ribosome. *Trends Biochem Sci*. 2012;37(5):189-198. doi:10.1016/j.tibs.2012.02.007.

179. Schmidt C, Becker T, Heuer A, et al. Structure of the hypusinylated eukaryotic translation factor eIF-5A bound to the ribosome. *Nucleic Acids Res*. 2015;44(4):1944-1951. doi:10.1093/nar/gkv1517.

180. Gao H, Ayub MJ, Levin MJ, Frank J. The structure of the 80S ribosome from Trypanosoma cruzi reveals unique rRNA components. *Proc Natl Acad Sci U S A*. 2005;102:10206-10211. doi:10.1073/pnas.0500926102.